# ENGINEERING APPENDIX
HYDRAULICS, HYDROLOGY, & COASTAL

NASSAU COUNTY BACK BAYS
COASTAL STORM RISK MANAGEMENT
FEASIBILITY STUDY

PHILADELPHIA, PENNSYLVANIA

APPENDIX B

August 2021

Table of Contents

List of Figures

List of Tables

1 INTRODUCTION

This appendix presents the results of the Hydraulic, Hydrology and Coastal (HH&C) engineering evaluation and analysis for the Nassau County Back Bays (NCBB) Coastal Storm Risk Management (CSRM) Study. The NCBB study area is shown in Figure 1-1. This report will discuss in detail all the existing information that was reviewed and how that information was used in the HH&C engineering evaluation and analysis to come up with the contribution of the elements to get to the Tentatively Selected Plan (TSP) Milestone and Draft Feasibility Report for the study.

Figure 1-1: NCBB Study Area

2 VERTICAL DATUM

In accordance with ER 1110-2-8160 the NCBB Feasibility Study is designed to North American Vertical Datum of 1988 (NAVD88), the current orthometric vertical reference datum within the National Spatial Reference System (NSRS) in CONUS. The study area is subject to tidal influence and is directly referenced to National Water Level Observation Network (NWLON) tidal gages and coastal hydrodynamic tidal models established and maintained by the U.S. Department of Commerce (NOAA). The current NWLON National Tidal Datum Epoch (NTDE) is 1983-2001.

There are no NWLON tidal gages inside the study area. However, there are three NWLON gages in the vicinity of the study area, Sandy Hook, The Battery, and Montauk. The location of NOAA tidal stations is shown in Figure 2-1. Datum relationships for the three NWLON tidal stations in the vicinity of the study area are as presented in Table 2-1. The local NAVD88-MSL relationship at locations inside the study area are estimated using NOAA VDatum models of the project region (EM 1110-2-6056).

Table 2-1:   NOAA Tidal Gage Datum Relationships

Datum[1]	Sandy Hook, NJ	The Battery, NY	Montauk, NY
	(Feet)	(Feet)	(Feet)
MHHW	2.41	2.28	0.96
MHW	2.09	1.96	0.67
NAVD88	0.00	0.00	0.00
MSL	-0.23	-0.20	-0.33
MLW	-2.62	-2.57	-1.40
MLLW	-2.81	-2.77	-1.57
MN[2]	4.71	4.53	2.07

Notes: [1]Tidal datums based on 1983-2001 Tidal Epoch
[2]Mean Tidal Range (MHW-MLW)

Hydrodynamic modeling completed for this study was performed in meters, MSL in the current NTDE. Water elevations are converted to feet, NAVD88 using NOAA VDatum. VDatum is a vertical datum transformation software tool, that provides conversions between various tidal datums fields and mean sea level as well as between mean sea level and North American Vertical Datum of 1988 (NAVD88). The tidal datums fields (MHHW, MHW, MSL, MLW, MLLW) are derived from hydrodynamic simulations using the hydrodynamic model, ADCIRC (Yang et al. 2010). NOAA ADCIRC model results were validated by comparing with observations water level stations maintained by the NOAA's Center for Operational Oceanographic Products and Services (CO-OPS). Figure 2-1 presents the mean tidal range (MHW - MLW) for the study area. Table 2-2 presents the NOAA VDatum results for MHHW and mean tidal range (MN) at the three NOAA tidal stations. Comparison of the values in in Table 2-1 and Table 2-2 show that the VDatum results are in agreement with the NOAA tidal stations.

Table 2-2:   NOAA VDatum Tidal Datum Relationships

Datum[1]	Sandy Hook, NJ	The Battery, NY	Montauk, NY
MHHW	2.40	2.00	0.67
MN[2]	4.66	4.60	2.05

Notes: [1]Tidal datums based on 1983-2001 Tidal Epoch
[2]Mean Tidal Range (MHW-MLW)
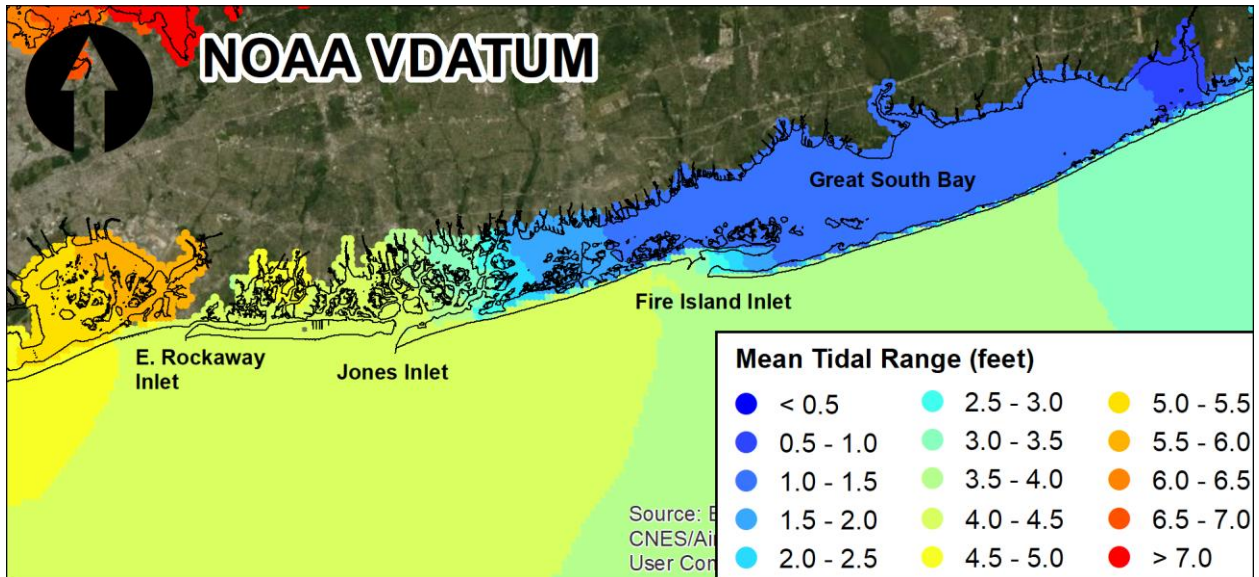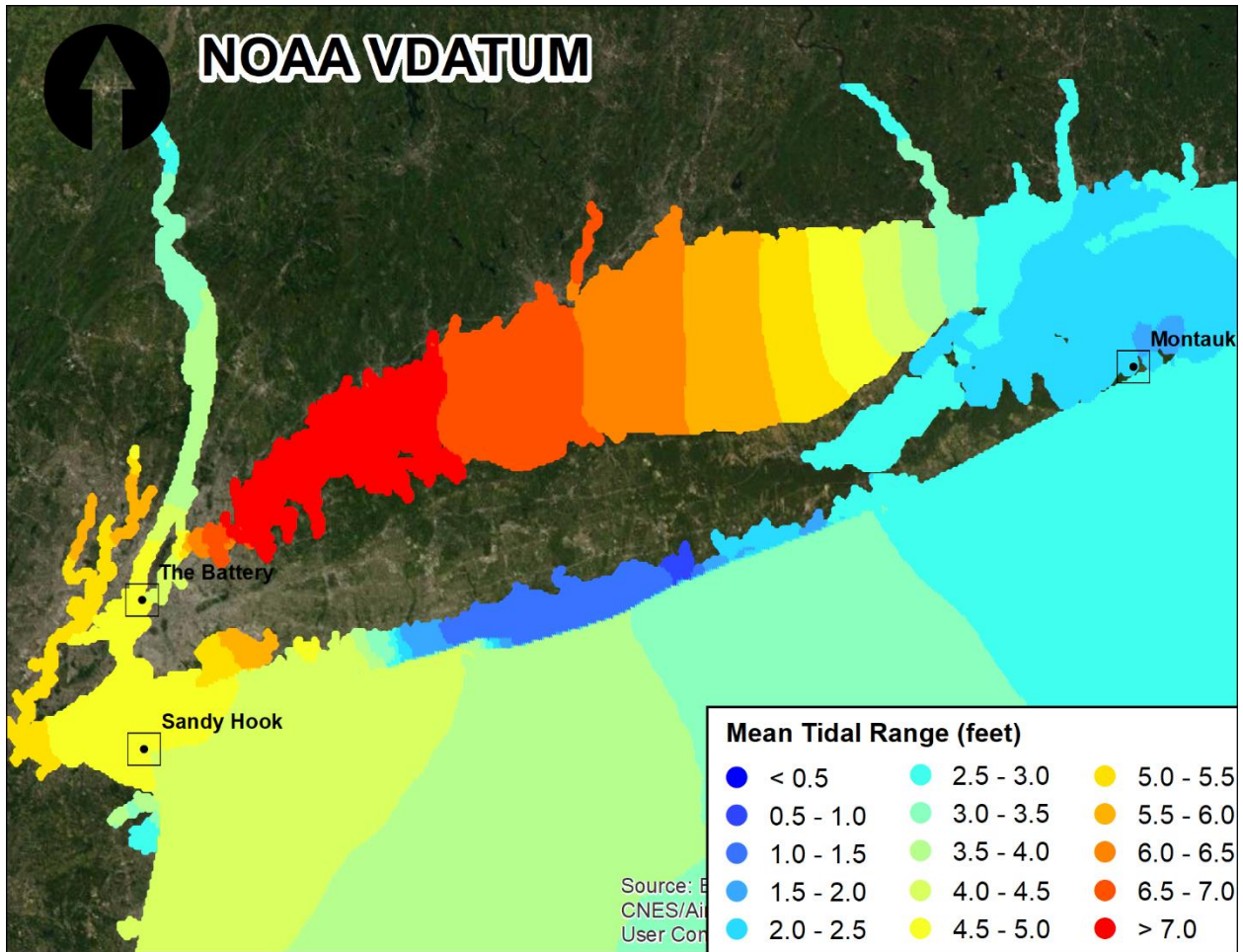
Figure 2-1: *Mean Tidal Range in the NY Bight and Study Area*

3   SEA LEVEL CHANGE

3.1   Background on SLC

Global sea level change (SLC) is often caused by the global change in the volume of water in the world's oceans in response to three climatological processes: 1) ocean mass change associated with long-term forcing of the ice ages ultimately caused by small variations in the orbit of the earth around the sun; 2) density changes from total salinity; and most recently, 3) changes in the heat content of the world's ocean, which recent literature suggests may be accelerating due to global warming. Global SLC can also be caused by basin changes through such processes as seafloor spreading. Thus, global sea level, also sometimes referred to as global mean sea level, is the average height of all the world's oceans.

Relative (local) SLC (RSLC) is the local change in sea level relative to the elevation of the land at a specific point on the coast. RSLC is a combination of both global and local SLC caused by changes in estuarine and shelf hydrodynamics, regional oceanographic circulation patterns (often caused by changes in regional atmospheric patterns), hydrologic cycles (river flow), and local and/or regional vertical land motion (subsidence or uplift).

3.2   USACE Guidance

In accordance with ER 1100-2-8162, potential effects of RSLC were analyzed over a 50-yr economic analysis period and a 100-yr planning horizon. Research by climate science experts predict continued or accelerated climate change for the 21st century and possibly beyond, which would cause a continued or accelerated rise in global mean sea level. ER 1100-2-8162 states that planning studies will formulate alternatives over a range of possible future rates of SLC and consider how sensitive and adaptable the alternatives are to SLC.

ER 1100-2-8162 requires planning studies and engineering designs consider three future sea level change scenarios: low, intermediate, and high. The historic rate of SLC represents the "low" rate. The "intermediate" rate of SLC is estimated using the modified National Research Council (NRC) Curve I. The "high" rate of SLC is estimated using the modified NRC Curve III. The "high" rate exceeds the upper bounds of IPCC estimates from both 2001 and 2007 to accommodate the potential rapid loss of ice from Antarctica and Greenland, but it is within the range of values published in peer-reviewed articles since that time.

3.3   Historical SLC

Historical RSLC for this study (3.90 mm/yr) is based on NOAA tidal records at Sandy Hook, NJ. Sandy Hook, NJ is selected to represent long-term trends in RSLC for the study area because this station best represents the regional oceanographic/atmospheric patterns and local vertical land motion. Figure 3-1 and Figure 3-2 show historical RSLC at Sandy Hook. Several metrics for sea level are presented, the monthly mean sea level (light blue), 5-year moving average (orange), and 19-year moving average (dark blue). It is apparent that over long time scales (19 years) mean sea level is steadily increasing. However, over shorter time scales mean sea level may increase or decrease.

The monthly mean sea level, light blue line in Figure 3-1, appears to go up and down every year capturing the seasonal cycle in mean sea level. The 5-year moving average, orange line in Figure 3-1 captures the interannual variation (2 or more years) of sea level.

Sea Level Rise with USACE SLC Scenarios for Sandy Hook, NJ (8531680)
Active and compliant tide gauge

USACE Sea Level Change Predictions for Sandy Hook, NJ (NOAA Tidal Gauge #8531680) for user selected datum: MSL.
Timeframe: Nov, 1932 - Jan, 2021 (88 years, 3 months)
Timeframe contains 3 missing points; the longest gap is 0 years, 3 months.
Rate of Sea Level Change: 0.013 ft/yr (Regional 2006)
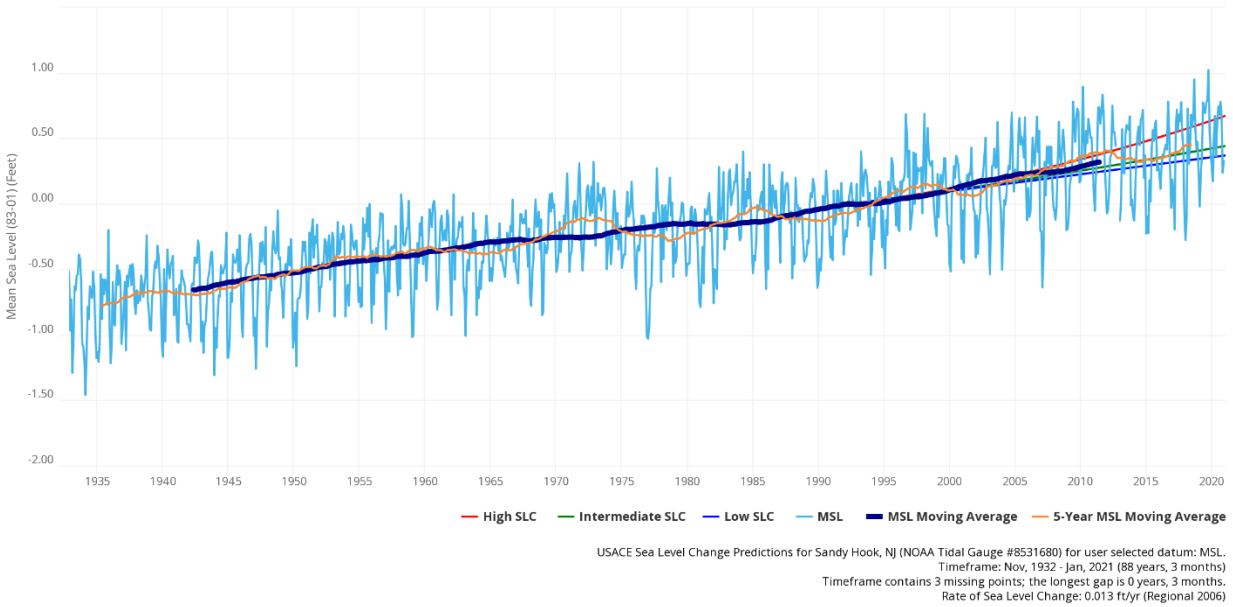
Figure 3-1   Historical (1933-2021) Relative Sea Level Change at Sandy Hook, NJ

Sea Level Rise with USACE SLC Scenarios for Sandy Hook, NJ (8531680)
Active and compliant tide gauge

USACE Sea Level Change Predictions for Sandy Hook, NJ (NOAA Tidal Gauge #8531680) for user selected datum: MSL.
Timeframe: Nov, 1932 - Jan, 2021 (88 years, 3 months)
Timeframe contains 3 missing points; the longest gap is 0 years, 3 months.
Rate of Sea Level Change: 0.013 ft/yr (Regional 2006)
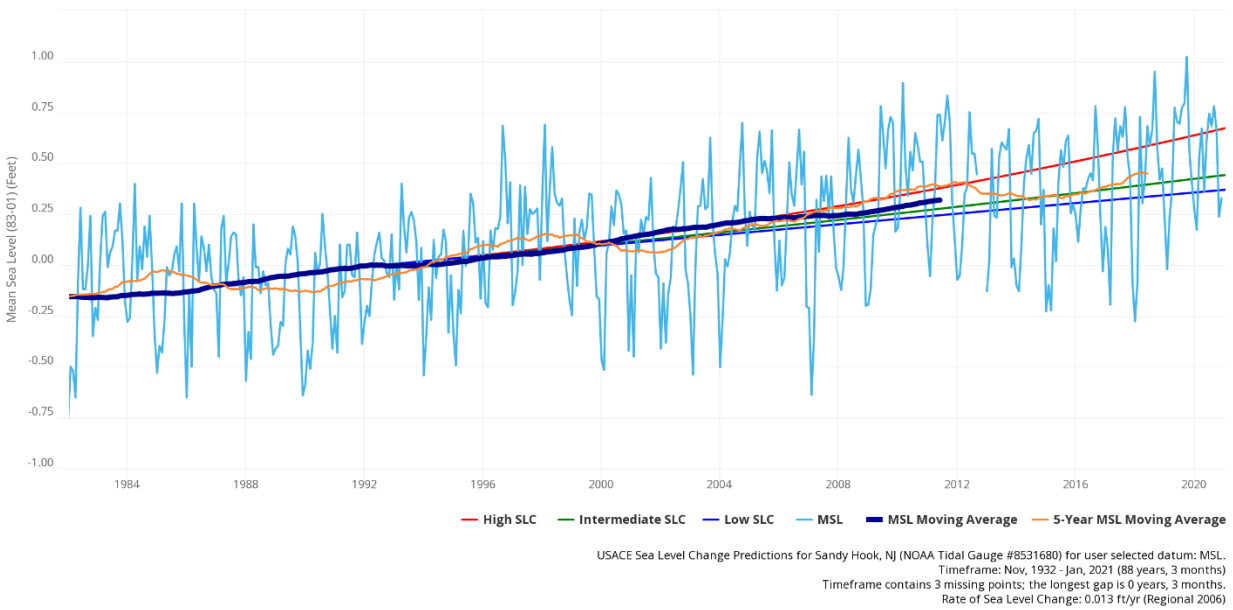
Figure 3-2   Historical (1983-2021) Relative Sea Level Change at Sandy Hook, NJ

3.4 USACE SLC Scenarios

USACE low, intermediate, and high SLC scenarios over the 100-yr planning horizon at Sandy Hook, NJ are presented in Table 3-1 and Figure 3-3. Water level elevations at year 2030 are expected to be between 0.5 and 1.0 feet higher than the current NTDE. Water elevations at year 2080 are expected to be between 1.1 and 4.0 feet higher than the current NTDE.

Hydrodynamic modeling performed for this study was completed in the current NTDE. Therefore, the modeled water levels represent MSL in 1992. Future water levels are determined by adding the SLC values in Table 3-1. For example, a water level elevation of 10 feet NAVD88 based on the current National Tidal Datum Epoch (1983-2001), will have an elevation in the year 2080 of 11.13, 11.82, and 14.0 feet NAVD88 under the USACE low, intermediate, and high SLC scenario respectively.

Table 3-1:   USACE Sea Level Change Scenarios (Derived from Sandy Hook, NJ)

Year	USACE - Low (ft, MSL[1])	USACE - Int (ft, MSL[1])	USACE - High (ft, MSL[1])
1992	0.00	0.00	0.00
2000	0.10	0.11	0.13
2021	0.37	0.45	0.68
2030	0.49	0.62	1.02
2050	0.74	1.04	1.99
2080	1.13	1.82	4.00
2100	1.38	2.42	5.71
2130	1.77	3.46	8.83

[1]Mean Sea Level based on National Tidal Datum Epoch (NTDE) of 1983-2001
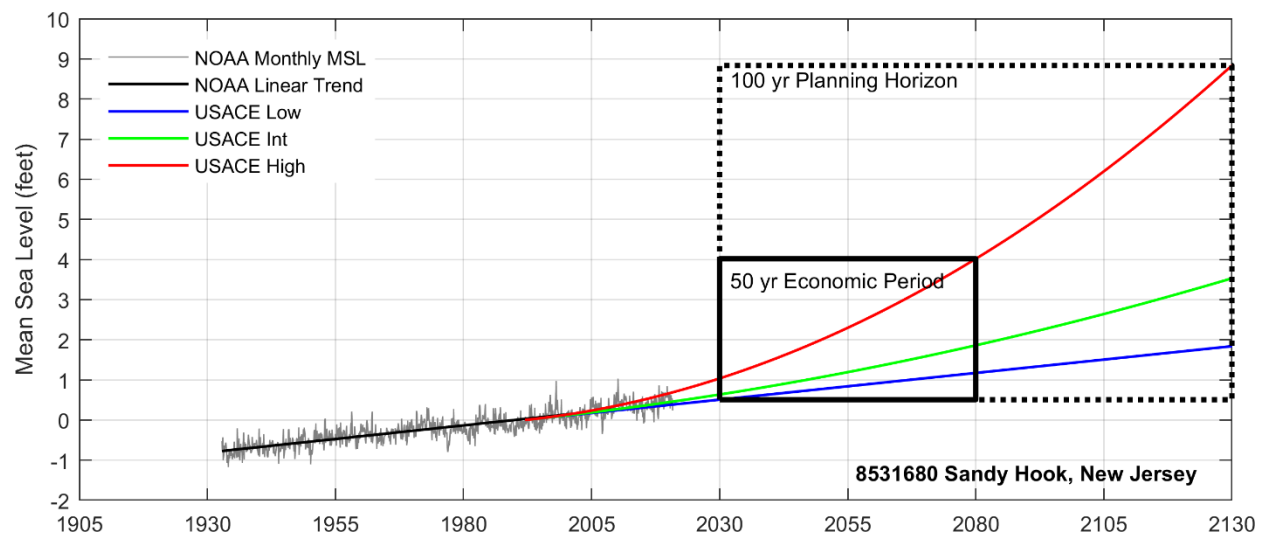
Figure 3-3:   Relative Sea Level Change Projections at Sandy Hook, NJ

4   EXISTING CONDITIONS

4.1   Astronomical Tide

Daily tidal fluctuations in the study area are semi-diurnal, with a full tidal period that averages 12 hours and 25 minutes; hence there are nearly two full tidal cycles per day. The mean tidal range in the study area ranges from 4.5 feet in the west near the City of Long Beach and 1.5 feet in east in Great South Bay. The rise and fall of the tide in the ocean leads to tidal flow through the inlets that causes a corresponding rise and fall of water levels in the back bays. Figure 2-1 shows the mean tidal range for the study area.

The western half of the study area, from East Rockaway Inlet to Jones Inlet, experiences a mean tide range that is equal to the mean range in the open ocean, typically in the 4 to 5 foot mean range. This is due to the relatively shorter distance along the coast between inlets, and the relatively short distances from the open ocean, through the inlets, to the inland extent of the bays.

East of Jones Inlet the mean tide range in the back bays gradually decreases such that at in Great South Bay, the mean range is less than 1.5 feet. The reduction in mean tide range is due to the long, narrow, and shallow geometry of Great South Bay and the relatively greater distances between inlets.

4.2   Seasonal and Interannual Fluctuations in Sea Level

The average seasonal cycle of mean sea level, shown in Figure 4-1, is caused by <u>regular fluctuations</u> in coastal temperatures, salinities, winds, atmospheric pressures, and ocean currents and on average causes a 0.5 foot (0.16 m) difference in sea level from September (highest) to January (lowest).

Interannual (2 or more years) variations in sea level, shown in Figure 4-2, are caused by <u>irregular fluctuations</u> in coastal ocean temperatures, salinities, winds, atmospheric pressures, and ocean currents (El Niño).

Seasonal and interannual fluctuations in sea level are significant in the study area and will be incorporated in design water elevations in subsequent phases of the feasibility study.
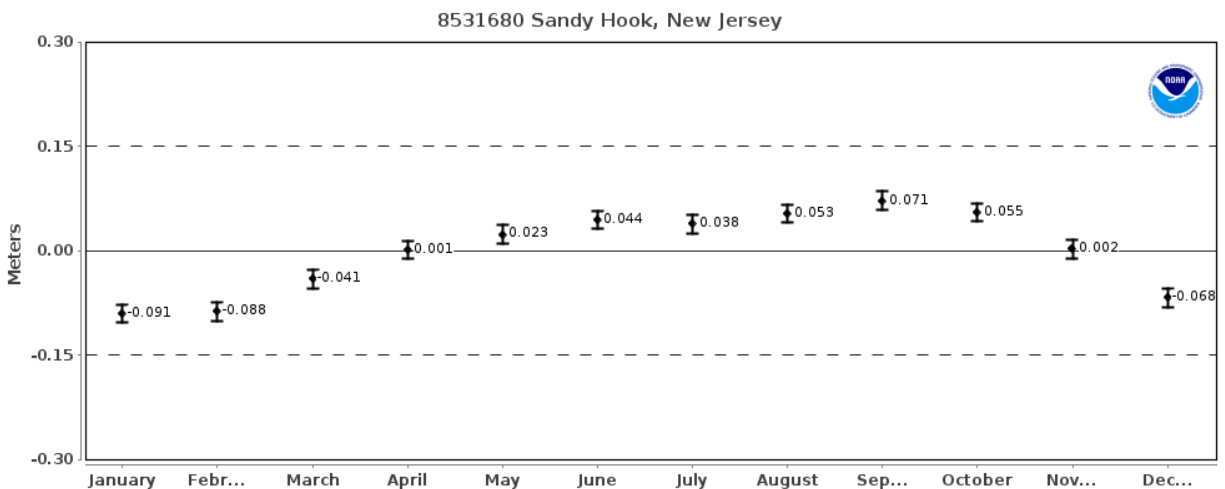
Figure 4-1:   Average Seasonal Cycle in Sea Level at Sandy Hook, NJ

8531680 Sandy Hook, New Jersey
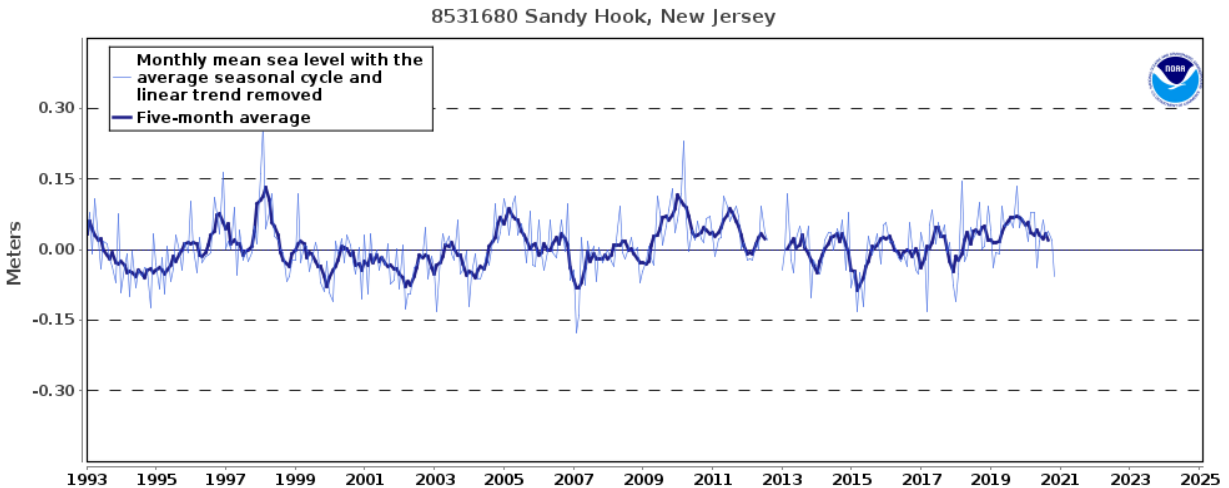
Figure 4-2:   Interannual Variation in Sea Level at Sandy Hook, NJ

4.3   Storm Surge

Storm surge is the increased water level above the predicted astronomical tide due to storm winds over the ocean and the resultant wind stress on the ocean surface. The principal factor that creates flood risk for the study area is storm surge that propagates into the back bays through the three inlets separating the barrier islands along the coast. The magnitude of the storm surge is calculated as the difference between the predicted astronomic tidal elevation and the actual water surface elevation at any time. Wind blowing over the ocean surface is capable of generating storm surge. However, the largest and most damaging storm surges develop as a result of either tropical cyclones (hurricanes and tropical storms) or extra-tropical cyclones ("nor'easters"). Although the meteorological origins of the two types of storms differ, both can generate large, low-pressure atmospheric systems with intense wind fields that rotate counter-clockwise (in the northern hemisphere). The relatively broad and shallow continental shelf along the east coast allows the generation of larger storm surge values than are typically experienced on the US Pacific coast.

Storm surge propagation into the back bays broadly mirrors the tidal propagation, with storm surge in the western portions of the study area in similar magnitude to the ocean coastline and attenuated storm surge in Great South Bay. However, storm surge in the study area is highly dependent on wind speed and direction. Strong winds are capable of "pushing" water from Great South Bay in the direction that the wind is blowing.

4.4   Waves

Wave conditions in the NCBB study area are fetch-limited and generated by local wind conditions. In fetch-limited conditions, wave heights are limited by the distance of open water in which the waves can grow. Wave conditions throughout the bay are also affected by the shallow water depths, marshes and orientation relative to the wind directions. The 100-year wave conditions in the back bays are generally between 3 and 5 feet with a peak wave period of 3 to 5 seconds. At some back bay locations wave conditions may be dominated vessel wakes.

The ocean coastline and inlets are exposed to significantly greater wave energy associated with the ocean. Wave conditions offshore may exceed 30 feet during 100-year wave conditions with peak wave periods

between 9 and 16 seconds. Wave conditions inside the inlets are affected by complex wave transformation process (wave refraction, shoaling, breaking, diffraction, reflection, and wave-current interactions) associated with the dynamic bathymetry and ebb shoals and rubble mound structures (jetties).

4.5   Historical Storms

The study area has experienced flooding from both tropical cyclones and extratropical cyclones. Table 4-1 displays the top ten historical storms at Sandy Hook, The Battery, and Montauk NOAA tidal stations. Note that the historical water levels have not been adjusted for sea level rise.

Table 4-1:   Historical Peak Water Levels at NOAA Stations

Sandy Hook, NJ (since 1932)			The Battery, NY (since 1911)			Montauk, NY (since 1932)		
Date	Type	Feet NAVD88	Date	Type	Feet NAVD88	Date	Type	Feet NAVD88
29-Oct-2012	T	11.30	30-Oct-2012	T	11.27	31-Aug-1954	T	6.87
12-Sep-1960	T	7.27	12-Sep-1960	T	7.24	29-Oct-2012	T	5.49
11-Dec-1992	E	7.26	11-Dec-1992	E	6.93	6-Feb-1978	E	5.18
28-Aug-2011	T	6.95	7-Nov-1953	E	6.74	31-Oct-1991	E	4.76
7-Nov-1953	E	6.87	28-Aug-2011	T	6.73	25-Nov-1950	E	4.67
6-Mar-1962	E	6.57	25-Nov-1950	E	6.34	7-Nov-1953	E	4.37
14-Sep-1944	T	6.57	6-Mar-1962	E	6.14	12-Nov-1968	E	4.27
13-Mar-2010	E	6.21	13-Mar-2010	E	6.03	19-Feb-1972	E	4.2
25-Nov-1950	E	6.17	31-Oct-1991	E	5.95	11-Dec-1992	E	4.17
12-Nov-1968	E	5.99	29-Mar-1984	E	5.75	27-Dec-2010	E	4.03

5   HIGH-FREQUENCY FLOODING

High-frequency flooding, also known as nuisance flooding, recurrent flooding, or sunny-day flooding, are flood events caused by tides and/or minor storm surge that occur more than once per year. High-frequency flooding mostly affects low-lying and exposed assets or infrastructure, such as roads, public storm-, waste- and fresh-water systems (Sweet et. al 2018) and is likely more disruptive (a nuisance) than damaging. However, the cumulative effects of high-frequency flooding may be a serious problem to residents who live and work in these low-lying areas. The number of high-frequency flood days is accelerating in the study area in response to RSLC.

Flooding from rainfall and inadequate storm water systems are closely related to high-frequency flooding but are treated separated in this study. It is common for municipalities in the study area to have gravity-based storm water systems that are unable to drain water when tidal level exceeds the elevation of the storm drain. When this happens, water starts ponding around the drain and may flood many of the same low-lying areas as high-frequency flooding. The frequency and impact of rainfall flooding will increase as the probability of the tide level exceeding storm drains will increases in response to RSLC.

The primary focus of the NCBB study is managing risk to severe storm surge events (i.e. Hurricane Sandy), not flooding associated with inadequate storm sewer systems and/or high-frequency flooding. It is USACE policy (ER 1165-2-21) that storm water systems are a local non-federal responsibility. While flooding from high frequency flooding and inadequate storm water systems is not the focus of the NCBB study, it is acknowledged that nonstructural and storm surge barrier measures may not provide any relief from these problems. Therefore, complementary measures to address these problems will likely be investigated and may be recommended for implementation at the local non-federal level.

5.1   National Weather Service Flood Stages

The National Weather Service (NWS) with the help of NOAA and USGS provide real time flood status of stream gages and tidal stations (Figure 5-1). The NWS has established three coastal flood severity thresholds: minor, moderate, and major flood stages. The NWS minor and moderate flood stages are the most representative of high-frequency flooding events right now. However, all three flood stages will be evaluated here since NWS major flood stage could eventually occur at frequency consistent with high-frequency flooding in the future in response to RSLC.

The definition of minor, moderate, and major flooding is provided herein by NWS. The definitions are taken from the NWS website for Sandy Hook, NJ so that impacts are specific to Monmouth County, NJ. However, impacts experienced described at this station are generally representative of the entire study area.

- **Minor Flooding** - flooding begins along sections of NJ Route 36 in Middletown Township as water backs up into tidal streams in the community. Flooding begins along the access road to the Gateway National Recreation Area's Sandy Hook Unit;

- **Moderate Flooding** - widespread flooding of roadways begins due to high water and/or wave action with many roads becoming impassable in Middletown Township, Atlantic Highlands, Highlands, Rumson and Sea Bright. Lives may be at risk when people put themselves in harm's way. Some damage to vulnerable structures may begin to occur;

- **Major Flooding** - flooding starts to become severe enough to begin causing structural damage along with widespread flooding of roadways in Middletown Township, Atlantic Highlands, Highlands, Rumson and Sea Bright. Vulnerable homes and businesses may be severely damaged or destroyed as water levels rise further above this threshold. Numerous roads become impassable and some neighborhoods may be isolated.
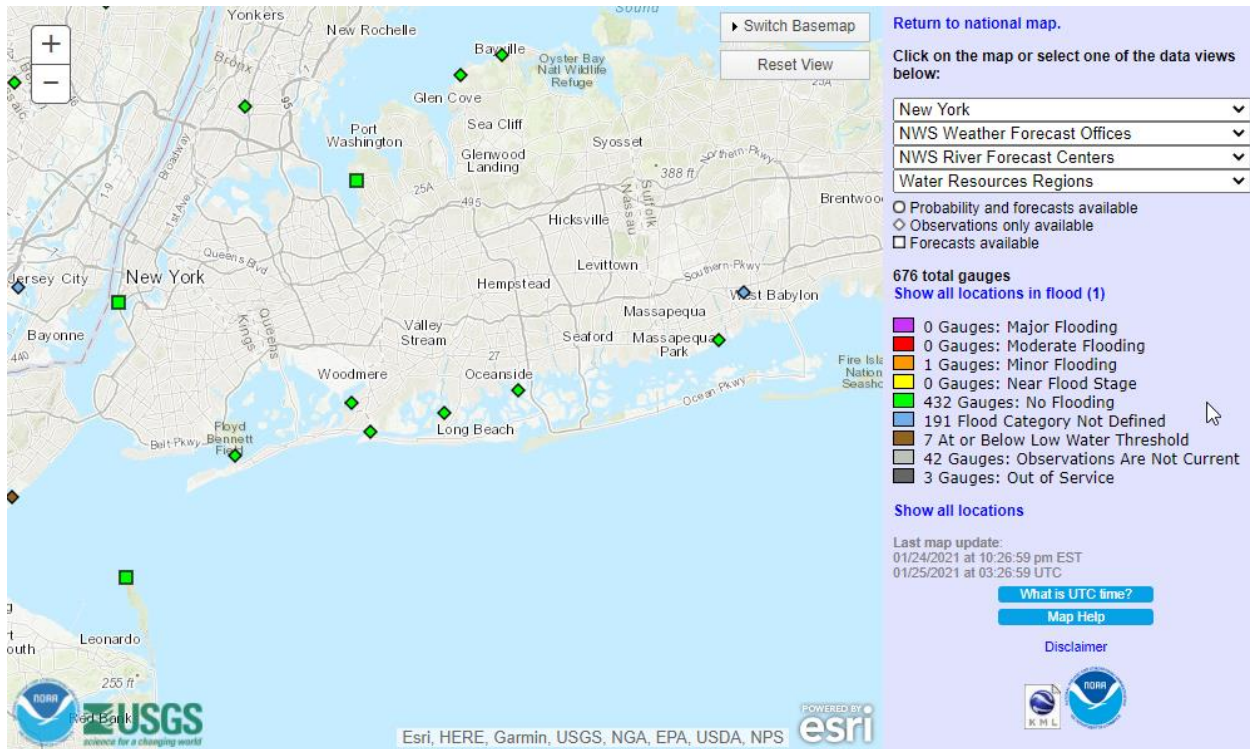
Figure 5-1:   NWS Real-Time Flood Monitoring Network

An example of the flood inundation area associated with the three NWS Flood stages is shown in Figure 5-2, and Figure 5-3 at Long Beach and Freeport. The impact of minor flooding can be seen to be very limited to a few particularly low-lying areas. The impact of moderate flooding is more widespread impacting some streets and properties and major flooding is widespread impacting several streets and blocks near the bay shoreline.

There are several NWS stations in the study area with documented flood stages. The flood stages are reported on the NWS website in feet MLWW:

https://water.weather.gov/ahps/region.php?state=ny

The NWS flood stages are converted to feet NAVD88 in Table 5-1 for floodplain mapping. NWS minor flood stages are typically 1 to 1.5 feet above MHHW. Moderate and major flood stages are typically an additional 1 and 2 feet, respectively, above the minor flood stage. The NWS minor flood stage elevations are pretty consistent across the study area, 3.2 to 3.4 feet NAVD88, with the exception of Great South Bay where the tidal range is smaller.

Table 5-1:   NWS Flood Stages

Location	Gage	Minor	Moderate	Major
		NAVD88		
Sandy Hook	SDHN4	4.0	5.0	6.0
The Battery	BATN6	4.4	5.7	7.2
East Rockaway Inlet	RKWN6	3.2	4.2	5.2
Hog Island	HOGN6	3.2	4.2	5.2
Freeport	FRPM6	3.4	3.9	4.6
Lindenhurst	LNDN6	2.3	2.8	3.3
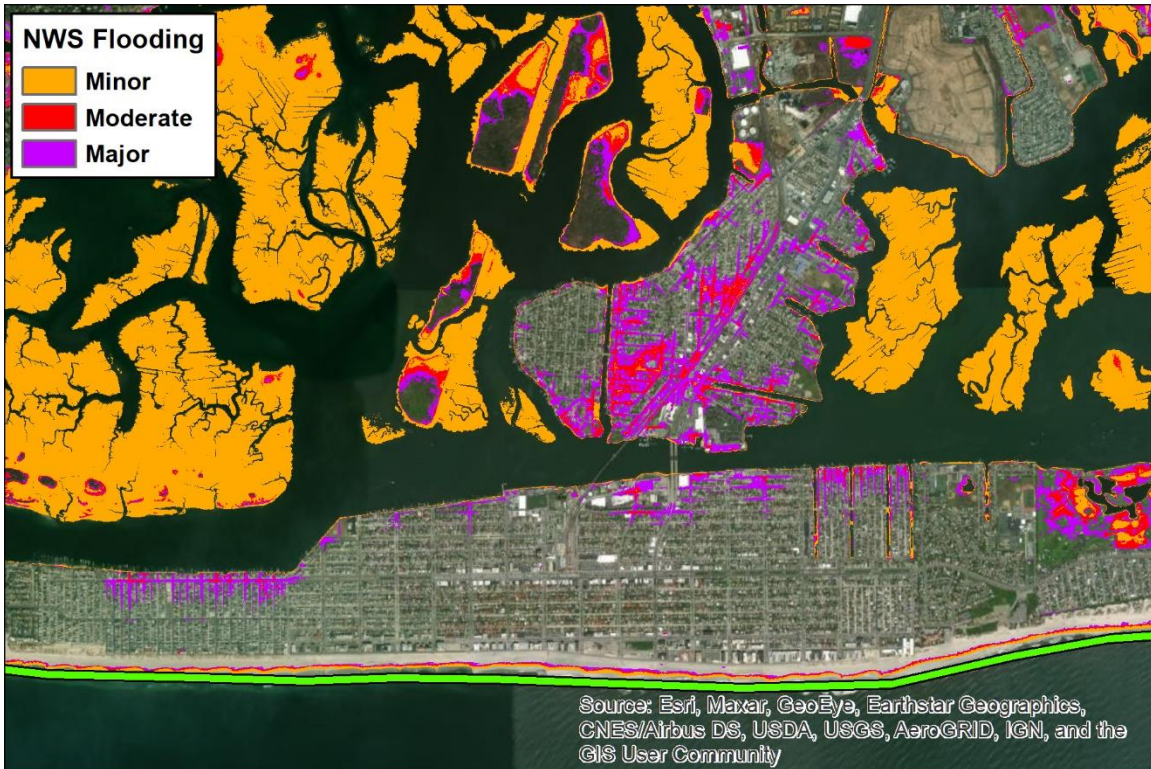
Figure 5-2:   Floodplain associated with NWS Stages at Long Beach and Island Park, NY
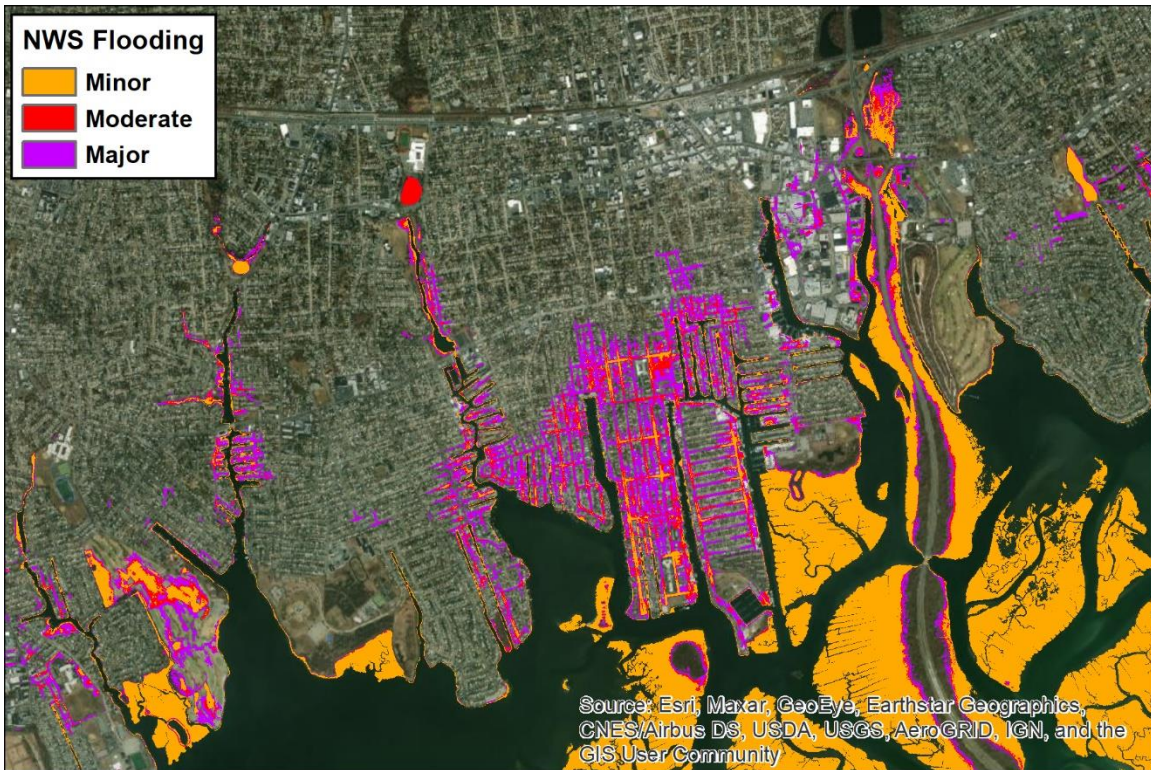
Figure 5-3:   Floodplain associated with NWS Stages at Freeport, NY

5.2   Historical High-Frequency Flooding

Sandy Hook, NJ has one of the longest tidal record (1932-Present) out of any of NOAA or USGS stations and is therefore well suited for investigating how often high-frequency flooding has occurred in the past and how rate of flooding has been affected by historic RSLC. Hourly verified data from NOAA CO-OPS station at Sandy Hook, NJ was downloaded from 1932-2020. The number of days in which the daily maximum water level equaled or exceeded the NWS flood stages was calculated. The top panel of Figure 5-4 shows historic record of water levels and a dot for any day in which the NWS flood stages were exceeded. The bottom panel of Figure 5-4 shows a histogram of the total number of days in a given year that the NWS flood stages were exceeded. It is readily observed from Figure 5-4 that annual rate of NWS minor flooding has increased over time, with a dramatic increase in the last 20 years. The annual rate of NWS moderate flooding has a seen a small but visible increase and with little or no increase in NWS major flooding.
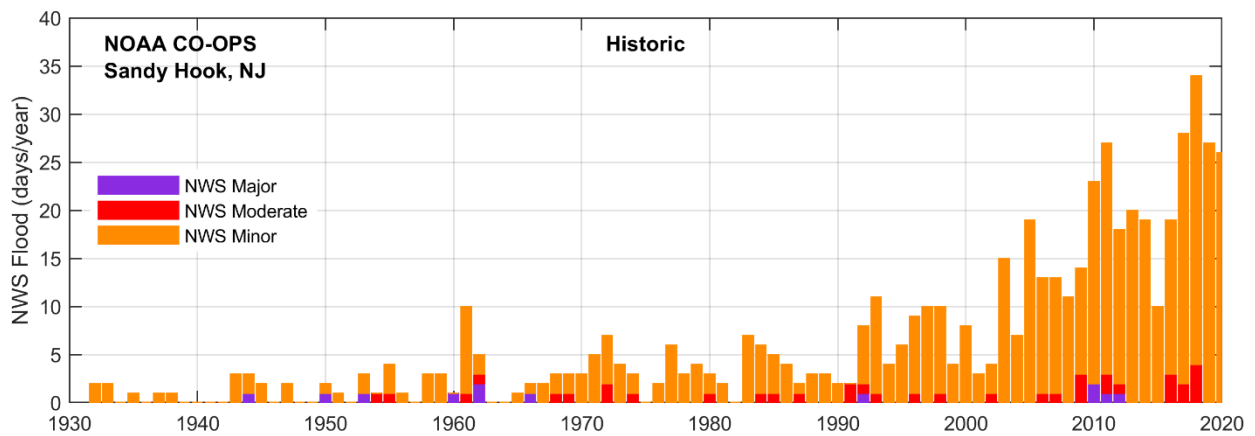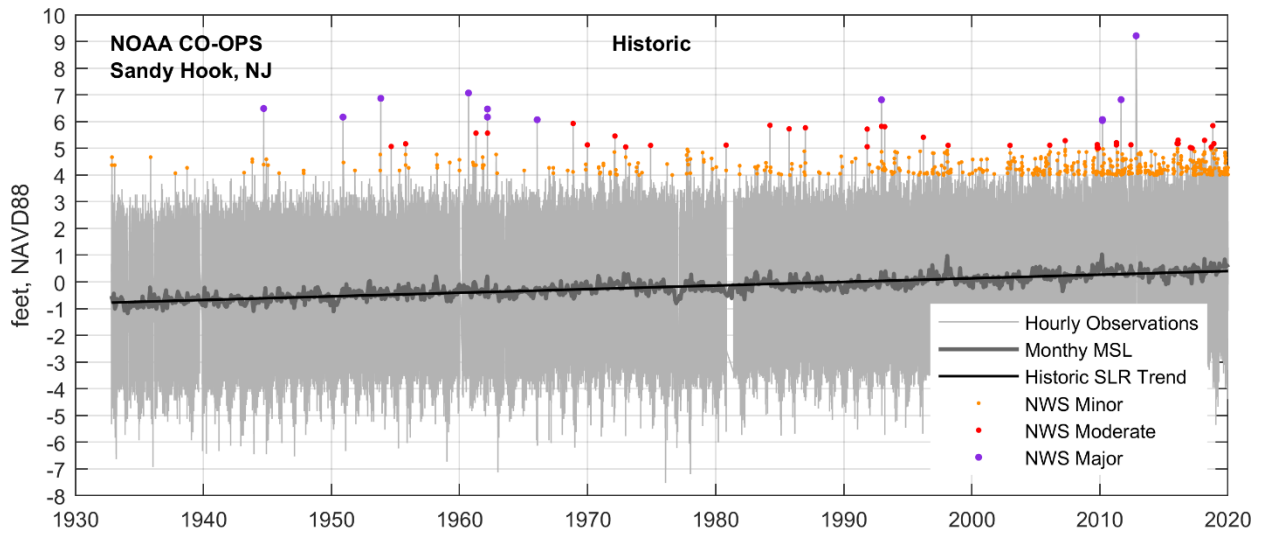
Figure 5-4:   Historic High-Frequency Flooding at Sandy Hook, NJ

To isolate the impact of historic RSLC on the frequency of flooding, the analysis was repeated with the historic SLR trend removed so that the mean sea level remained the same as in 1933 over the period of record. Figure 5-5 shows that if no RSLC had occurred since 1933, the frequency of NWS minor flooding would still only be a couple times per year, significantly lower than in actuality, and that primary driver of the increase in high-frequency flooding over the last 100 years has been RSLC, not changes in the tidal range or meteorological conditions.
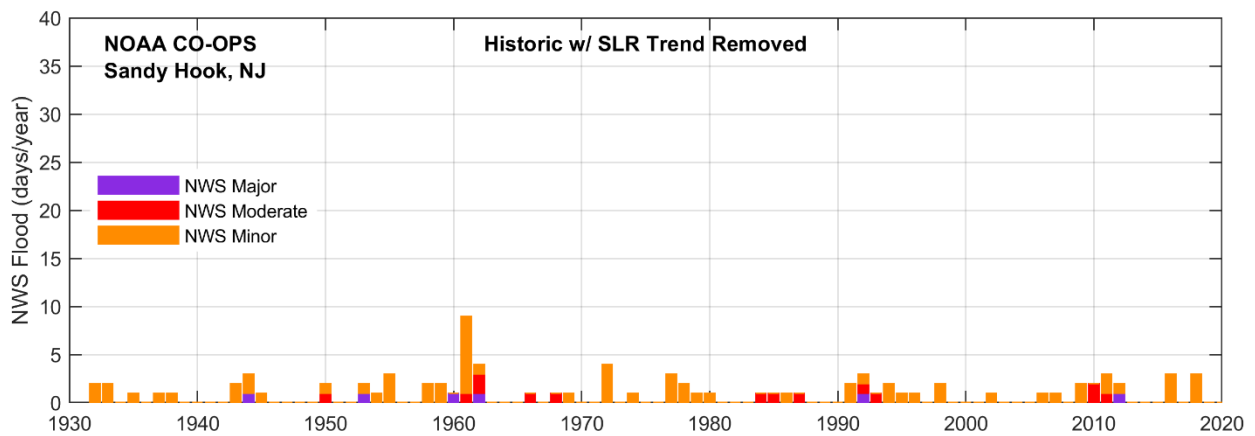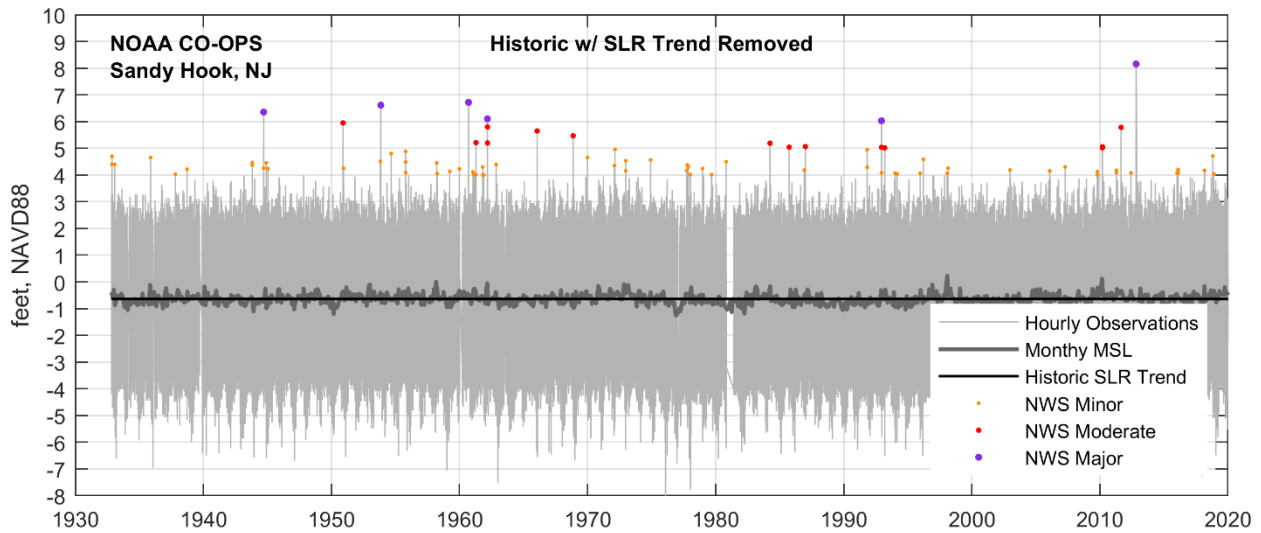
Figure 5-5:   Impact of SLC on Historic High-Frequency Flooding

5.3   Future High-Frequency Flooding

The previous section showed the dramatic impact RSLC has had on frequency of flooding over the last 100 years. This section shows how the rate of high-frequency flooding will be affected by future RSLC. To complete this analysis a recent 25-year period of the NOAA tidal record (1992-2016) was assumed to repeat over and over again until 2130. However, the three USACE SLC projections were added to the observed water levels. The top panel of Figure 5-6 shows the hourly water level observations and future projections with the USACE-Low SLC scenario applied and a dot for any day in which the NWS flood stages were exceeded. The middle and bottom panel of Figure 5-6 shows a histogram of the total number of days in a given year that the NWS flood stages were exceeded. The bottom panel shows the same information as the middle panel, but zooms in on NWS flood days (per year) between 0 and 40. The results in Figure 5-6 show that Sandy Hook is experiencing an acceleration in NWS minor flood days that will only get worse in the future. It also indicates that the increase already underway in NWS minor flooding will begin to occur in the future for the NWS moderate and major flooding. A significant increase in NWS moderate and major flooding appears to occur after 2030 and 2080 respectively.

The same analysis was repeated for the USACE-Intermediate and USACE-High RSLC scenarios in Figure 5-7 and Figure 5-8. Annual NWS flood days from the analyses are tabulated in Table 5-2. It is difficult to say or know what the tipping point (days per year) is for NWS minor, moderate, and major flooding before the impacts to roads and infrastructure are unacceptable. However, the analysis shows that major investments in bulkheads and storm water systems (i.e. pump stations) are likely to be required in the future for the portions of the study area to be inhabitable.

Table 5-2:   High-Frequency Flood Occurrences (Days Per Year)

Year	NWS Minor Flood			NWS Moderate Flood			NWS Major Flood		
	Low	Int	High	Low	Int	High	Low	Int	High
1935	0.8	0.8	0.8	0.0	0.0	0.0	0.0	0.0	0.0
1960	2.5	2.5	2.5	0.5	0.5	0.5	0.3	0.3	0.3
1985	3.4	3.4	3.4	0.4	0.4	0.4	0.0	0.0	0.0
2010	17.0	17.0	17.0	1.1	1.1	1.1	0.4	0.4	0.4
2020	26.2	30.7	49.6	2.1	2.3	3.1	0.3	0.3	0.4
2030	39.4	51.8	108.3	3.1	4.5	13.6	0.0	0.0	1.1
2055	70.5	127.5	315.0	6.5	17.7	151.2	0.2	1.3	25.8
2080	117.6	248.1	363.3	15.2	71.7	352.7	1.2	6.9	271.4
2105	172.0	339.6	363.6	33.2	201.5	363.6	2.6	47.1	363.4
2130	215.5	359.2	362.5	51.6	316.7	362.5	2.9	140.2	362.5

Note: 10-year running mean filter applied to determine annual flood occurrences
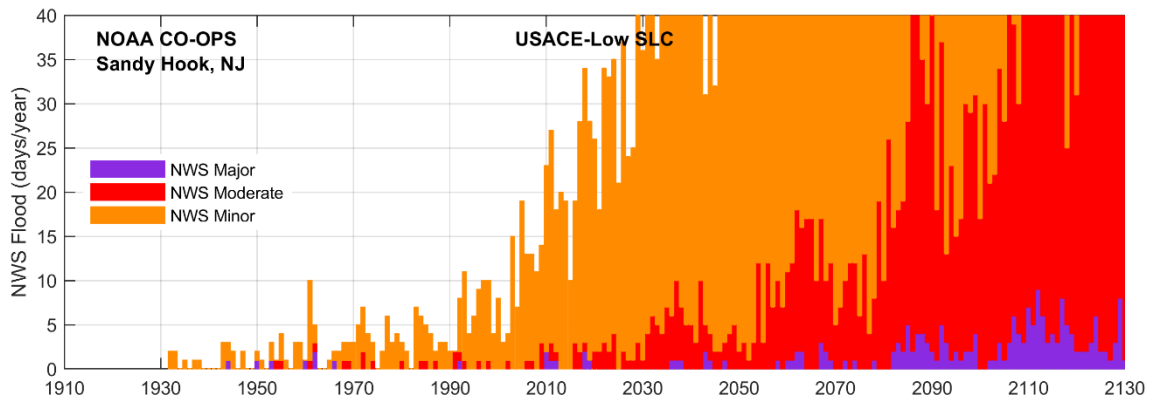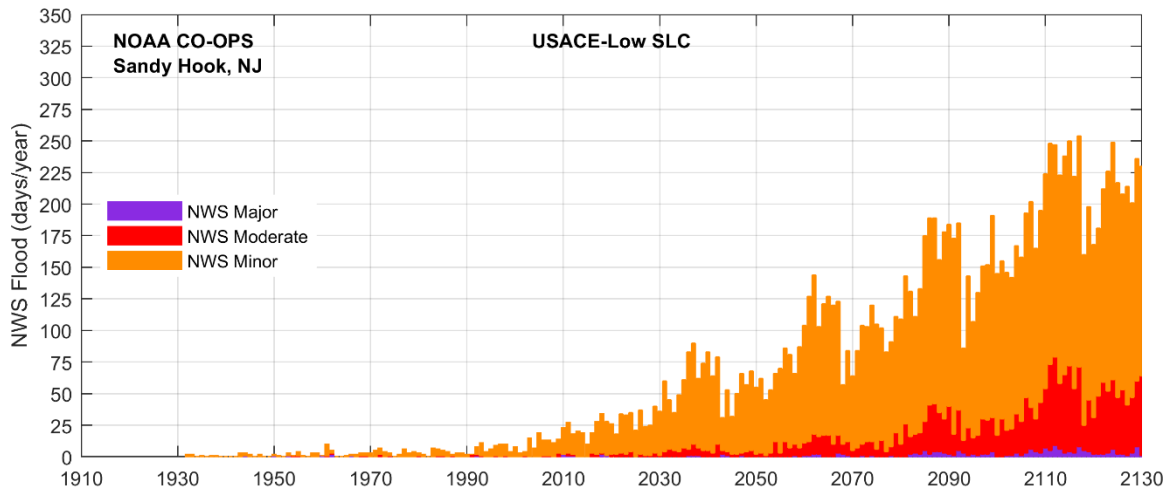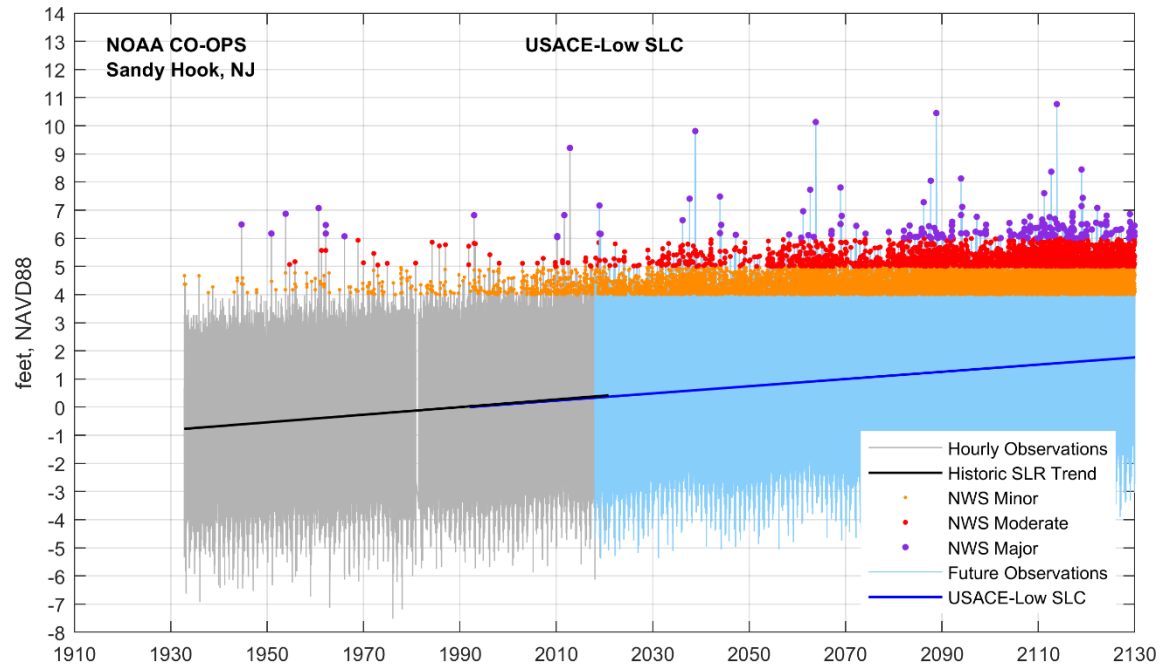
Figure 5-6:   *Future High-Frequency Flooding – USACE-Low SLC*
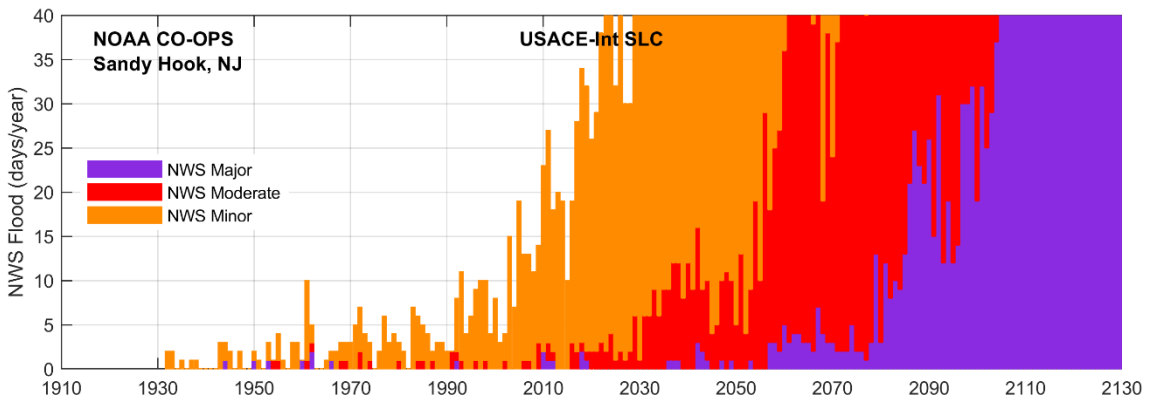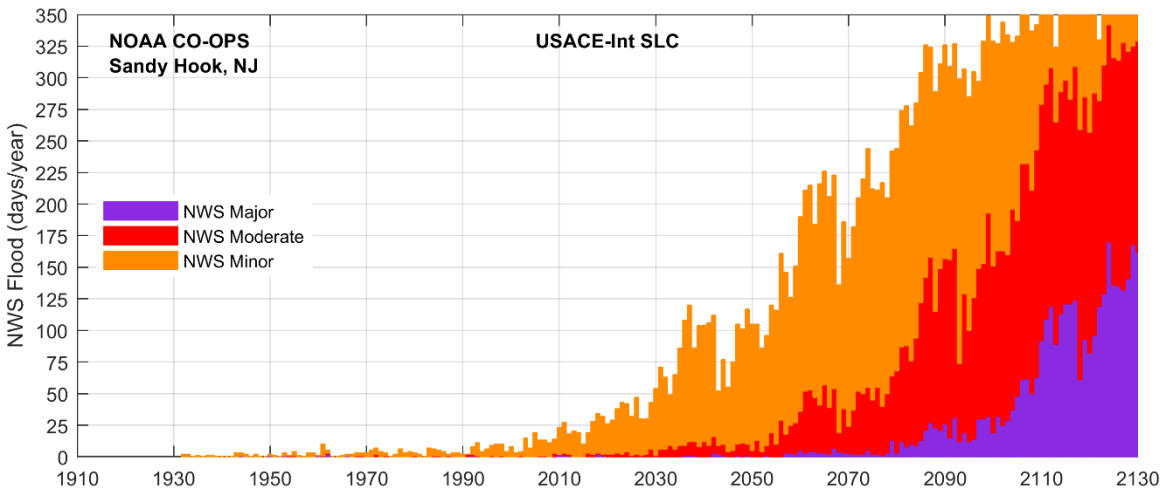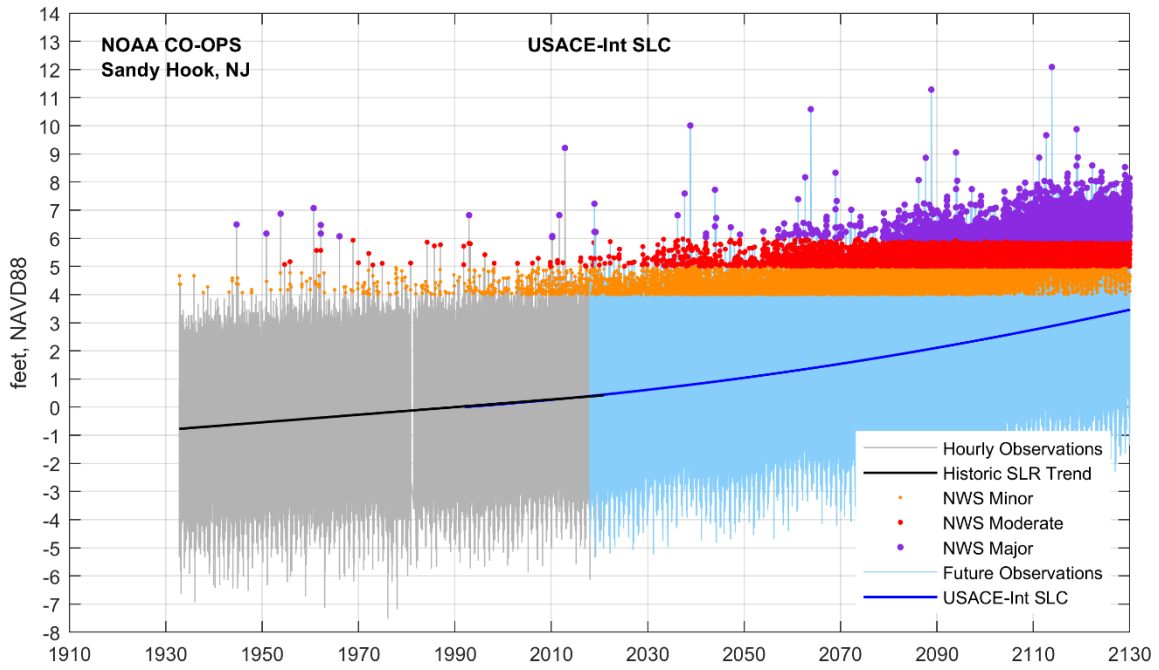
Figure 5-7:   *Future High-Frequency Flooding – USACE-Intermediate SLC*
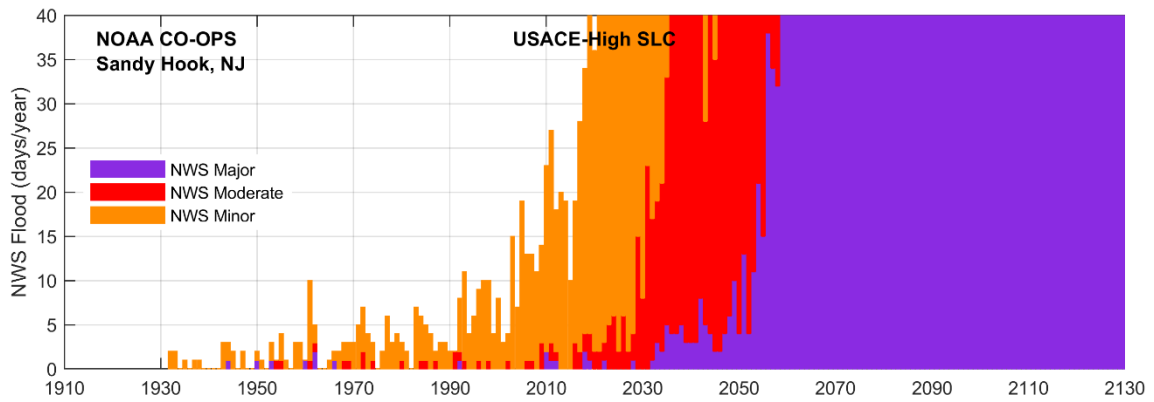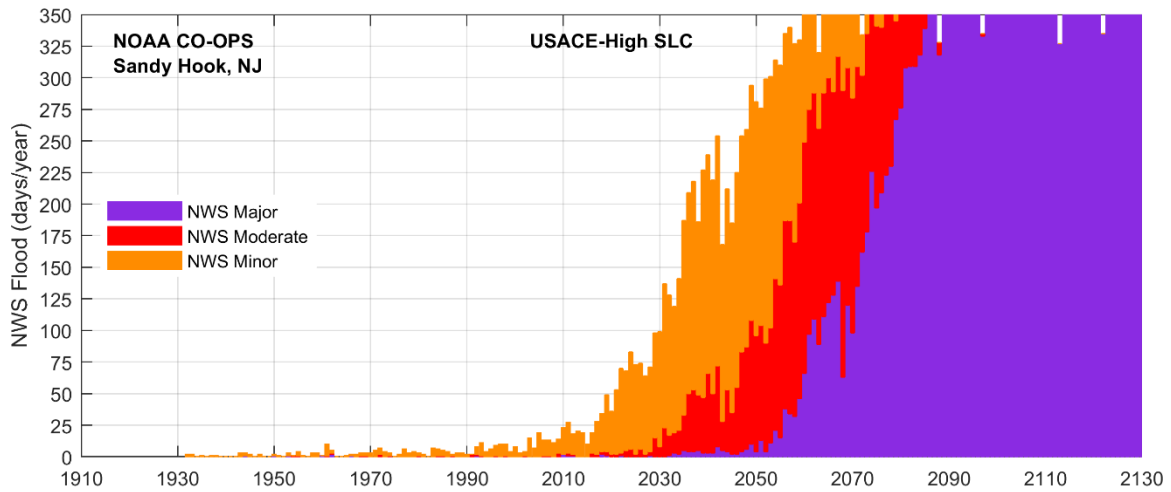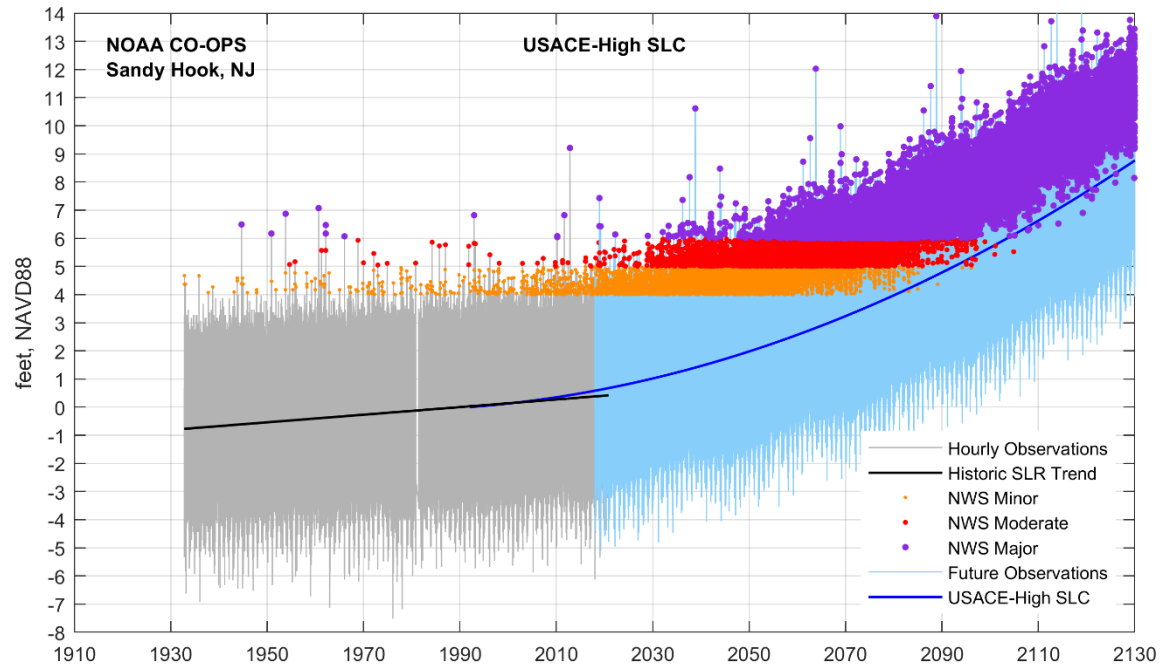
Figure 5-8:   *Future High-Frequency Flooding – USACE-High SLC*

6   STORM SURGE MODELING

6.1   NACCS

The North Atlantic Coast Comprehensive Study (NACCS) was authorized under the Disaster Relief Appropriations Act, PL 113-2, in response to Superstorm Sandy. The Act provided the USACE up to $20 Million to conduct a study with the goal to (1) reduce flood risk to vulnerable coastal populations, and (2) promote resilient coastal communities to ensure a sustainable and robust coastal landscape system, considering future sea level change and climate change scenarios.

As part of the NACCS, the US Army Engineer Research and Development Center (ERDC) completed a coastal storm wave and water level modeling effort for the U.S. North Atlantic Coast. This modeling study provides nearshore wind, wave, and water level estimates and the associated marginal and joint probabilities critical for effective coastal storm risk management. This modeling effort involved the application of a suite of high-fidelity numerical models within the Coastal Storm Modeling System (CSTORM-MS) to 1050 synthetic tropical storms and 100 historical extra-tropical storms. Documentation of the numerical modeling effort is provided in Cialone et al. 2015 and documentation of the statistical evaluation is proved in Nadal-Caraballo et al. 2015. Products of the study are available for viewing and download on the Coastal Hazards System (CHS) website: https://chs.erdc.dren.mil/.

6.2   Modifications for NCBB

The USACE Engineer Research and Development Center (ERDC), Coastal and Hydraulics Lab (CHL) conducted a numerical modeling study to evaluate the effectiveness of storm surge barriers in reducing water levels in the study area. As part of this numerical modeling study the existing condition water levels in the study area were updated to ensure that the existing and with-project water levels were consistent and derived from a common model, set of storms, and statistical evaluation. A detailed discussion of the ERDC numerical modeling report is provided in the Draft Report: Storm Surge Comparison for Proposed Nassau County Back Bays Inlet Closures (Norberto C. Nadal-Caraballo, Gregory Slusarczyk, Mary A. Cialone, and Robert W. Hampson, 2021).

The ADCIRC mesh developed for the North Atlantic Coast Comprehensive Study (NACCS) (Cialone et al. 2015) was modified to provide detailed representation of the Nassau County Back Bay (NCBB) study area. There were two major changes implemented in the NACCS grid, that is, refinement of the study area and de-refining of the remote area (Chesapeake Bay) while the original boundary of the domain was not altered. Refinement of the grid in the study area was necessary to fully capture and analyze the hydrodynamic processes of interest. Moreover, this procedure facilitated the implementation of the complex configurations of the storm surge barriers at the specific locations required by the study sponsor. The purpose of grid de-refining is to reduce the mesh resolution in areas remote from the area of interest to decrease model simulation times without significantly affecting the flow volume exchange between de-resolved and the study areas. Besides the grid refinement in the study area, the topographic and bathymetric data were updated in the study region with data from Year 2014 Lidar surveys. The elevation of the Long Beach dunes was set to +14 ft NAVD88 in accordance with the Federal CSRM project.

A total of 1050 synthetic tropical cyclones were designed and simulated in the NACCS. However, not all of these storms affect the NCBB region. Using Gaussian process metamodeling (GPM) and a design of experiments (DoE) approach, CHL selected subset of the NACCS synthetic tropical cyclones to maximize

coverage of the storm parameter and probability spaces and produce storm surges across the NCBB region while reducing the hydrodynamic modeling requirements. A set of approximately 25 tropical cyclones was selected for modeling in order to complete the frequency distributions of response for both the with- and without-project conditions. Although the subset of storms does not include extratropical storms (nor'easters), the combined frequency distributions for both tropical and extratropical storms is generated by ERDC using GPM.

Modeling results are applied throughout the NCBB study to define wave and water level Annual Exceedance Probabilities (AEP). The water level AEP are based on the "Base + Linear superposition of 96 random tides" simulations and the mean confidence interval. The wave height AEP are based on the "Base Conditions + 1 random tide" simulations and the mean confidence interval. The water levels represent the peak water level observed during a storm due to the combination of storm surge, astronomical tide, wave-setup, currents, and winds. The water levels are computed stillwater levels, which do not include individual wave crests that could increase the instantaneous water surface.

6.3   Model Validation

6.3.1   ADCIRC Model Validation

The NACCS model validation procedure, documented in Cialone et al. (2015), included a harmonic analysis to ensure that the model is responding correctly to astronomical forcing at 143 NOAA gage locations, 2 of which are in the near the study area: Sandy Hook, NJ and The Battery, NY. In addition, a comparison of the model to measurements for seven storm conditions was performed to ensure that the model is responding to meteorological forcing. The seven storms are Hurricanes Sandy, Irene, Isabel, Josephine, and Gloria and extratropical storms ET070 (North American Blizzard of 1996) and ET073. Cialone et al. (2015) concluded that "consistency in the model's ability to predict water levels for the seven validation storm events provided a level of confidence in what can be expected from the model", and "from the harmonic analysis conducted for the long-term simulation, it was determined that the model accurately predicts response to tidal forcing".

Since model validation conducted for the NACCS study focused on the available NOAA gage locations in the Atlantic Ocean, ERDC performed an additional analysis for USGS gages located in the NCBB study area. The additional model validation analyses compared observed water levels to modeled (ADCIRC) water levels for Hurricane Sandy at five USGS gauges that were active during the storm events. Figure 6-1 compares the observed and modeled peak water levels at one of the USGS stations (USGS 01311145, East Rockaway Inlet Atlantic Beach, NY). Model validation results at the five stations showed similar trends, the modeled (red line) and observed (green line) peak water level during Hurricane Sandy are in excellent agreement. However, the observed water levels 6 hours before and 6 hours after the peak of the storm are under predicted by the model.
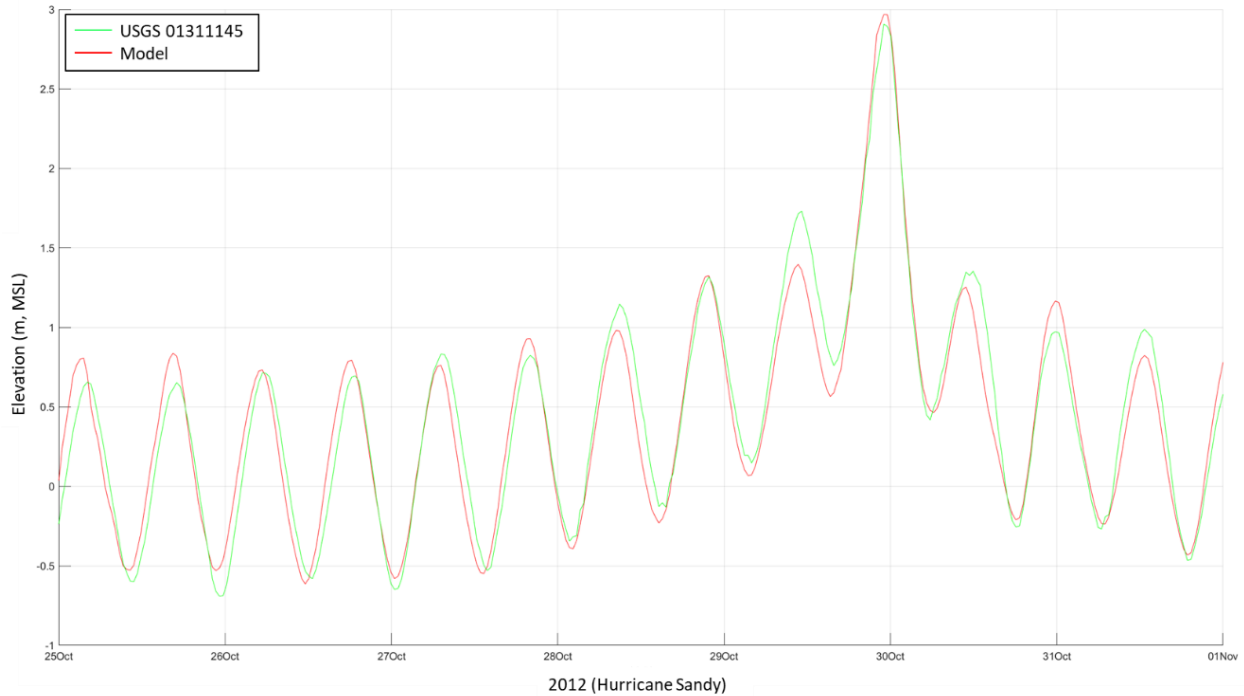
Figure 6-1: *NACCS Model Validation during Hurricane Sandy at Atlantic Beach, NY*

6.4 Hazard Curve Comparison to NOAA, USGS, FIMP, FEMA

NAP and ERDC analyzed the USGS tide gage records for the study area. The analysis compares the NACCS AEP values at several NOAA stations and back bay locations in the NCBB study area to values derived from NOAA observations, USGS observations, values developed for the Fire Island to Montauk Point (FIMP) General Reevaluation Report (GRR), and the 2014 FEMA Region II Coastal Storm Surge Study. NAP's evaluation of the AEP water levels in the NCBB study area shows that the NACCS water levels are consistently higher than water levels derived from NOAA and USGS measurements. Because the damages are so sensitive to changes in water level, the PDT decided to revise the NACCS water level statistics using the lower 16% confidence interval between the 99% and 10% AEPs. Modifications to the water elevations for the 2% AEP to 0.1% AEP are not recommended considering the higher uncertainty associated with less frequent extreme storm events so the mean (50%) confidence interval will be used from the 2% to 0.1% AEPs. The 5% AEP will be an average of the 16% and mean confidence interval to provide a smoother transition.

6.4.1 NOAA

The NOAA Center for Operational Oceanographic Products and Services (CO-OPS) operates several tidal gages in the region with a reliable history of water level observations dating as far back as 1893 at The Battery. A list of the three stations in the region that have periods of record long enough for NOAA to reliably estimate sea level trends and perform extreme water level analyses is shown in Table 6-1.

Water level statistics are presented here from two different sources, both derived from the NOAA water level measurements: (1) NOAA's published extreme water levels and (2) Nadal-Caraballo and Melby (2014,

TR-14-7). The statistical analysis methodology employed by NOAA is based on the use of monthly maximum data fitted by the generalized extreme value (GEV) distribution. GEV is a family of continuous probability distributions developed within extreme value theory to combine the Gumbel, Fréchet and Weibull families. Since the NOAA GEV water level statistics are based on monthly maximums, smaller storm events that occur in the same month as a larger storm event are omitted from the analysis and could cause an underestimation of the 99% annual exceedance probability (AEP).

Nadal-Caraballo and Melby (2014, TR-14-7) calculated water level statistics at 23 NOAA tidal gages based on verified water level measurements using a peak over threshold (POT) and Generalized Pareto Distribution (GPD) and Monte Carlo Life-Cycle. The Monte Carlo Life-Cycle allows tidal variations (i.e. spring/neap and high/low tides) to be incorporated. The water level statistics from Nadal-Caraballo and Melby (2014) were shown to agree well with those computed by NOAA GEV at the 10% AEP to 1% AEP. At the 99% AEP the TR-14-7 water levels are greater than the NOAA GEV as expected since the NOAA GEV misses some of the storm events that occur within the same month.

Table 6-1: NOAA Long-term Tidal Stations

Station Name	Station Number	Records Since
Montauk, NY	8510560	1947
The Battery, NY	8518750	1893
Sandy Hook, NJ	8531680	1932
Atlantic City, NJ	8534720	1911
Cape May, NJ	8536110	1965
Lewes, DE	8557380	1919

6.4.2   USGS

The US Geological Survey (USGS) operates five tidal gages in the NCBB study area, Table 6-2 and Figure 6-2, with water level observations dating as far back as 1997. The period of record for USGS tidal gages is not as long as the NOAA stations, but still provides meaningful information about the high-frequency water level statistics. ERDC-CHL obtained water level statistics at these 5 USGS tidal gages using a similar methodology as presented in Nadal-Caraballo and Melby in TR-14-7. The water level statistics at Atlantic Beach are not presented because the station did not record the peak water level during Hurricane Irene, the second largest storm at all the other USGS gages in the study area. The results of the water level statistics are shown for the other four USGS stations in Figure 6-3.

Table 6-2: USGS Tidal Stations

Station Name	Station Number	Records Since
East Rockaway Inlet at Atlantic Beach	01311145	Aug 2002*
Hog Island Channel at Island Park	01311143	Oct 2010
Reynolds Channel at Point Lookout	01310740	Dec 1997
Hudson Bay at Freeport	01310521	Oct 1999
Great South Bay at Lindenhurst	01309225	July 2002

* Peak water level during Hurricane Irene not recorded

Figure 6-2:   USGS Tidal Stations
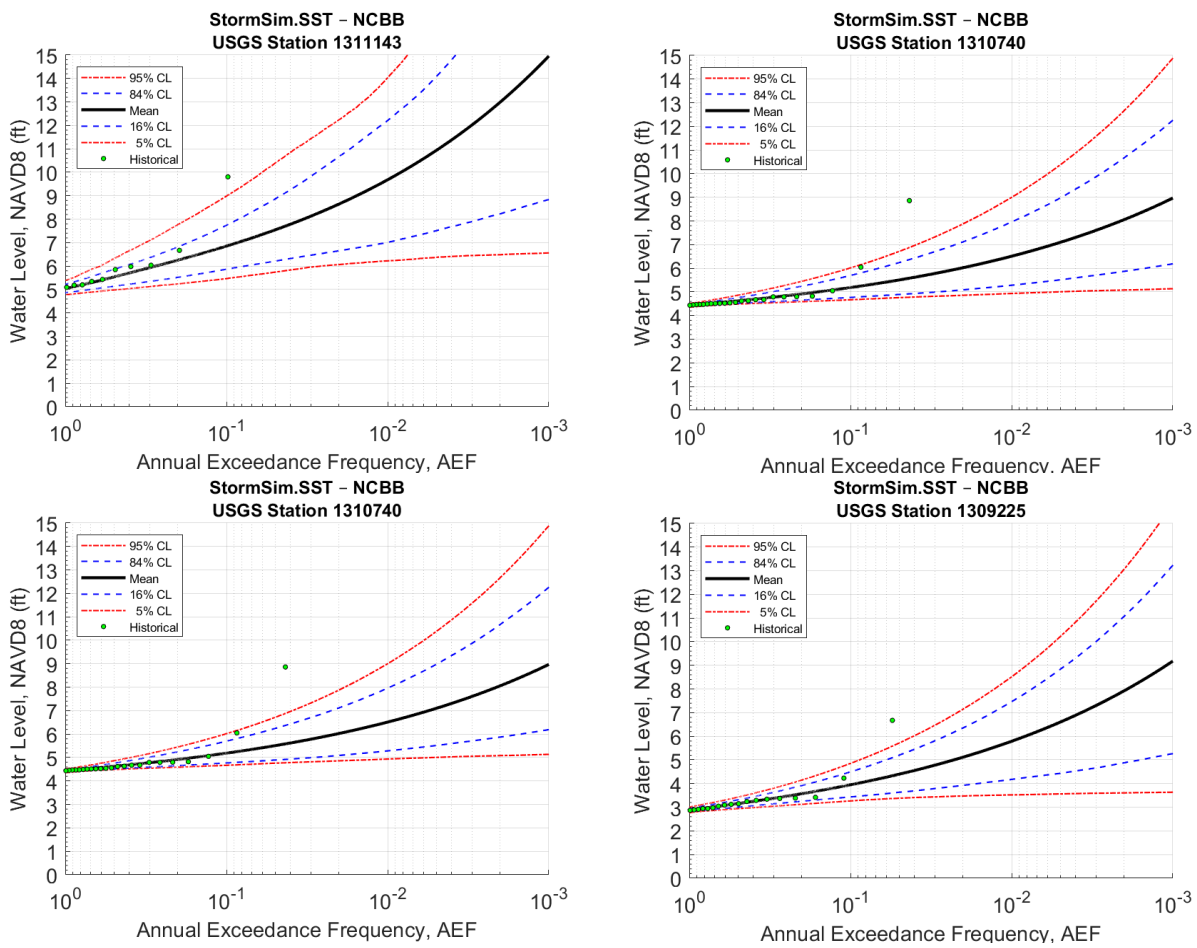
Figure 6-3:   USGS Derived Hazard Curves at 4 Tidal Stations

6.4.3   FIMP GRR

In support of the Fire Island to Montauk Point (FIMP) General Reevaluation Report (GRR), NAN completed a numerical modeling investigation that addressed a comprehensive list of physical processes (wind

conditions, barometric pressure, astronomic tide, wave conditions, barrier island overwash and breaching, and localized wind and wave setup) by merging hydrodynamic, wave, and sediment transport models. Water level statistics for FIMP are based on an improved 1-D Empirical Simulation Technique (EST) that accounted for other, equally probably, astronomical tide timings relative to each individual storm's timing.

The FIMP modeling effort relied on a total of 36 historical storm events, 14 tropical storms and 22 extratropical storms. Historical tropical storms from 1930 through 2001 and extratropical storms from 1950 through 1998 were considered for the storm set. To develop stage-frequency relationships, several supplemental storms were selected for numerical modeling. These included variation in the timing of major historical events such that different astronomical tide scenarios could be considered. An overview of the FIMP save points available in the NCBB study area is shown in Figure 6-4.
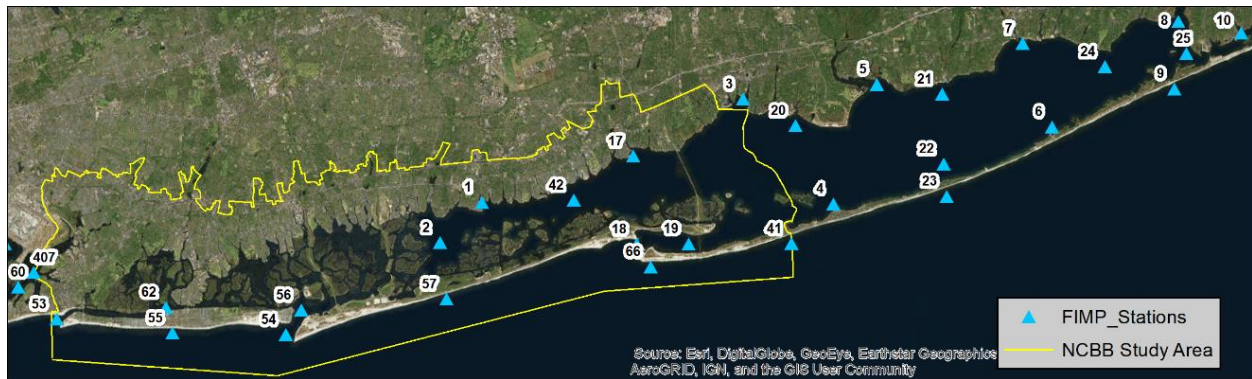
Figure 6-4:   FIMP Save Points

In 2012 Hurricane Sandy caused extensive coastal erosion, extensive overwash, and three breaches of the barrier islands. One of the breaches, the Wilderness Breach, is within the Fire Island National Seashore and was not closed following the storm (Figure 6-5). After the initial formation of the breach during Hurricane Sandy, it grew rapidly for several months and remains open at present. Observations and modeling results have shown that, at its current size, the Wilderness Breach has not significantly altered tidal elevations in Great South Bay or Moriches Bay (Aretxabaleta et al. 2014, van Ormondt et al. 2015, USACE, 2016). However, the FIMP GRR model simulations show that the breach will significantly increase storm tide elevations within Great South Bay during larger storm events.

In 2014 the numerical modeling results and baseline water level statistics for the FIMP GRR were updated to reflect the Wilderness Beach. The remainder of the barrier island topography was not updated and is based on a relatively healthy dune and berm condition captured in a 2000 LIDAR survey. However, FIMP numerical modeling results were also performed for a future vulnerable condition (FVC) that represents a barrier island topography that has a lower dune height and narrower berm width than the 2014 baseline conditions (BLC). Figure 6-6 compares the 2014 baseline conditions and FVC illustrating the impact the pre-storm barrier island topography has on bay water levels. It is noted that the NACCS model includes the Wilderness Breach and the barrier island topography based on post-Sandy LIDAR data that may be more comparable to the FIMP FVC.
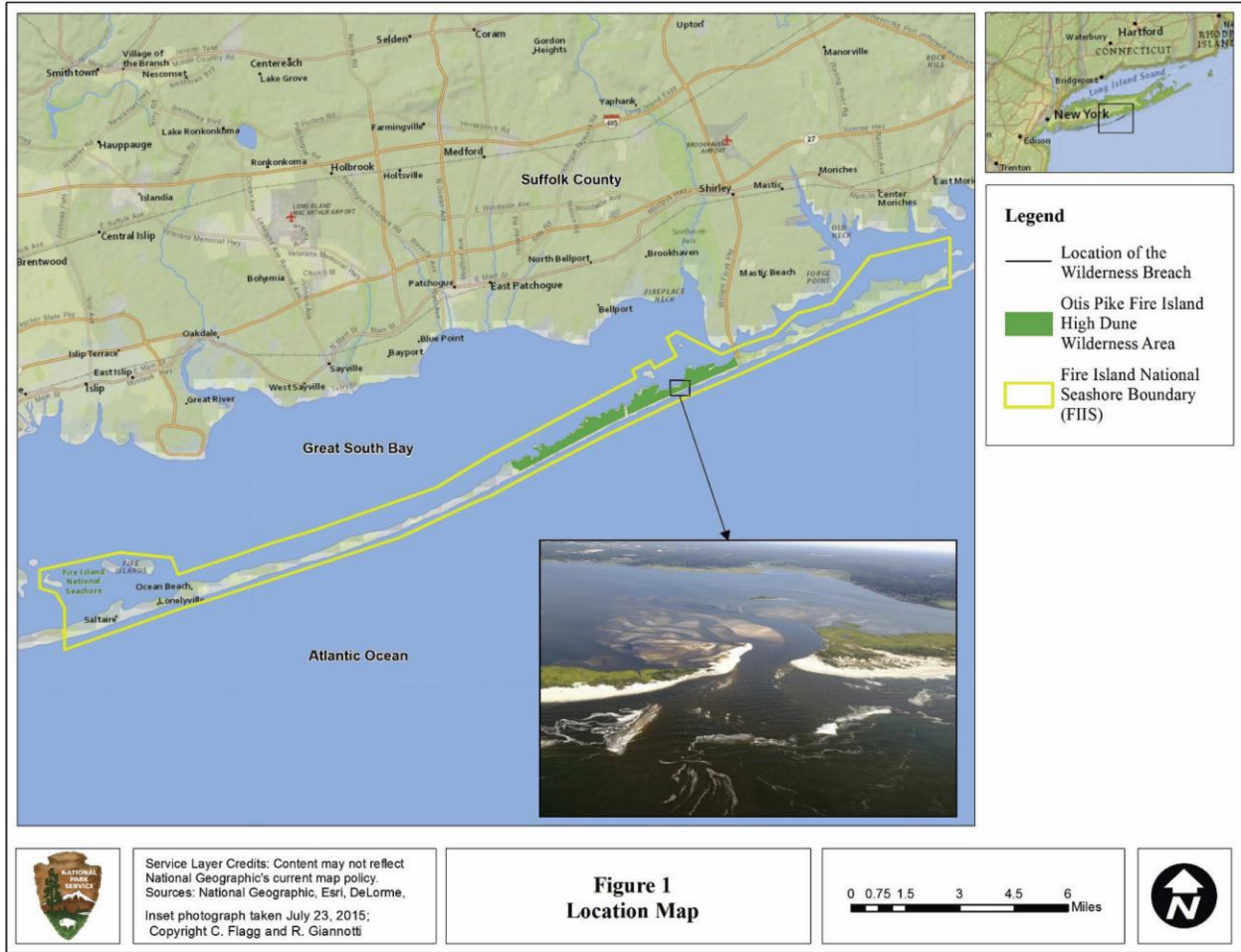
Figure 6-5:   Location of Wilderness Breach
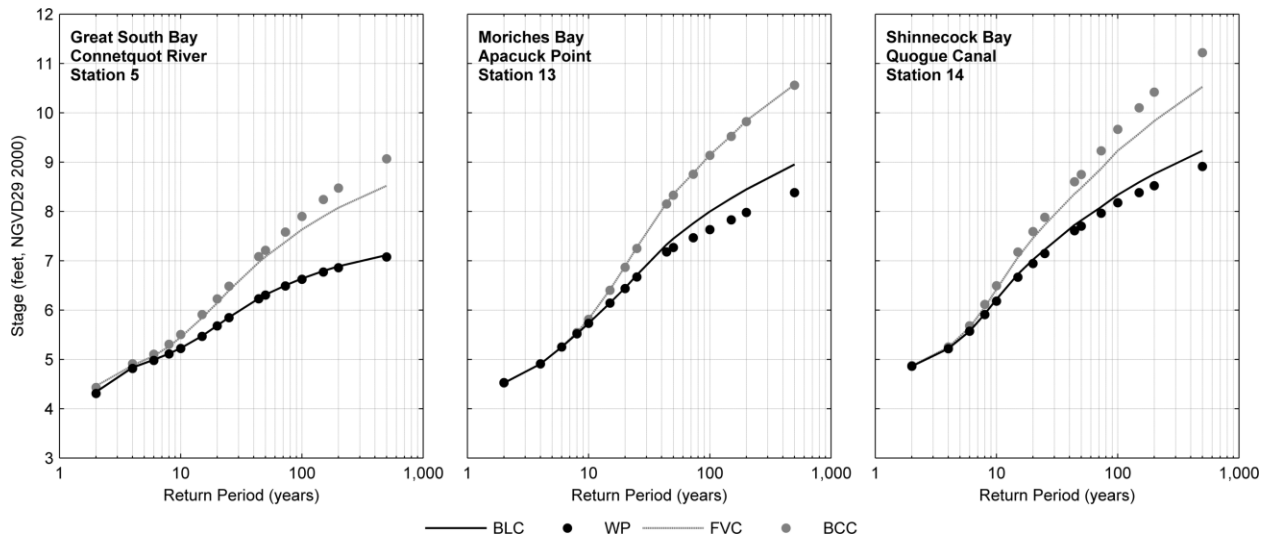
Figure 6-6:   FIMP Baseline and Future Vulnerable Water Levels

6.4.4 FEMA Region II

In 2014 FEMA completed the Region II Coastal Storm Surge Study that included new numerical modeling and updated water level statistics. The FEMA Region II approach is similar to NACCS with a suite of 159 tropical events and 60 extratropical storms (30 unique storms simulated at two randomly selected tidal phases). The statistical method used for analysis of tropical storms is called the Joint Probability Method (JPM) and for the extratropical storms, a modified version of the Empirical Simulation Technique (EST) was used to develop storm statistics. The FEMA water level statistics represent the upper 84-percent confidence limit, not the mean.

The FEMA Region II model results will be used to update flood maps in New York City and New Jersey (from Hudson River to Cape May). However, the FEMA Region II model results for NYC were successfully appealed by NYC and are in the process of being revised. The FEMA water levels presented here do not include any revisions associated with the NYC appeal. The FEMA Region II model is not being used to update the flood maps in Nassau County or Delaware Bay. The FIMP GRR modeling is the basis for the FEMA flood maps in Nassau County.

Figure 6-7:   FEMA Region II Save Points

6.4.5 Vertical Datum, Sea Level Rise, and Uncertainty

Adjustments to the water level statistics are necessary to ensure that comparisons between the data sources are made to a common vertical datum (feet, NAVD88) and sea level rise trends are removed. The local NAVD88-MSL relationship is based on published values at NOAA and USGS gages and at locations between gages estimated using NOAA VDatum. In addition, all water level statistics represent the mean or 50% probability curve unless otherwise noted.

Sea level trends are removed to ensure that all water level statistics are consistent with the current National Tidal Datum Epoch (NTDE) of 1983-2001 with a midpoint of 1992.5. Time series of water level observations at NOAA stations are detrended using the historic (linear) rate of RSLC with a zero crossing in 1992.5 (TR-14-7). The reported values in TR-14-7 included an additional adjustment from 1992.5 to 2014, present-day MSL at the time of the report. The 1992.5 to 2014 adjustment (Table 6 in TR-14-7) has been subtracted from the values published in TR-14-7 so that the water levels are relative to 1992.5.

At USGS stations, water level observations are detrended using the historic (linear) rate of RSLC at Sandy Hook, NJ with a zero crossing in 2019. The USGS water level statistics are then adjusted to the current NTDE by subtracting the historic rate of RSLC from 1992.5 to 2019 (0.35 feet).

FIMP water level statistics are published in feet, NGVD29 relative to MSL in 2000. Originally FIMP numerical model results were converted from MSL to NGVD29 by adding 0.5 feet over the entire modeling domain. FIMP water elevations are converted back to MSL by subtracting 0.5 feet and then adjusted to NAVD88 based on VDATUM. The water levels are adjusted to the current NTDE by subtracting 0.10 feet.

NACCS and FEMA water levels are published in meters, MSL relative to the current NTDE. Therefore the only adjustment needed is to convert to feet, NAVD88 which is performed here using NOAA VDATUM. FEMA water level statistics for Region II are reported at the upper 84-percent confidence limit.

6.4.6   Comparison

A comparison of the water level statistics at three NOAA stations in the region is shown in Table 6-3. A comparison of the water level statistics at nine back bay stations (Figure 6-8) in the study area are shown in Table 6-4 and Table 6-5.

Table 6-3:   Water Level Comparison at NOAA Stations

Station / Source	Annual Exceedance Probability						
	99%	50.0%	20.0%	10.0%	5.0%	2.0%	1.0%
	Return Period (years)						
	1	2	5	10	20	50	100
Water Level Elevations in Feet, NAVD88 (Current NTDE, 1983-2001)							
Montauk, NY							
NACCS	3.4	4.3	5.3	5.9	6.5	7.1	7.8
NOAA TR-14-7	3.0			4.4		5.7	6.3
NOAA GEV	2.4	3.4		4.7			6.7
The Battery, NY							
NACCS	4.6	5.4	6.6	7.4	8.4	9.8	11.1
NOAA TR-14-7	4.5			5.8		7.1	7.7
NOAA GEV	3.8	4.7		5.8			7.8
FIMP		4.8		6.6	7.6	8.9	9.9
FEMA Region II			6.8	6.9	8.1	10.0	11.6
Sandy Hook, NJ							
NACCS	4.7	5.5	6.6	7.5	8.3	9.6	10.9
NOAA TR-14-7	4.8			6.3		7.8	8.5
NOAA GEV	4.0	5.0		6.4			9.2
FIMP		4.9		6.7	7.7	8.9	9.9
FEMA Region II			6.2	7.5	8.6	10.2	11.4

Figure 6-8:   *Eastern and Western Back Bay Stations for Comparison*

Table 6-4:   *Water Level Comparison at Western Back Bay Stations*

Location and Source	Annual Exceedance Probability						
	99%	50.0%	20.0%	10.0%	5.0%	2.0%	1.0%
	Return Period (years)						
	1	2	5	10	20	50	100
Grass Hock Channel (Jamaica Bay)							
NACCS*	4.9	5.6	6.5	7.2	7.9	9.0	10.1
FIMP 2006		4.8	5.7	6.6	7.6	9.2	10.8
FIMP 2014		4.8	5.7	6.6	7.6	9.2	10.8
FEMA RII			5.2	6.3	7.3	8.5	9.4
Island Park							
NACCS	4.9	5.5	6.2	6.9	7.7	9.0	10.1
USGS	4.8	5.2	5.9	6.5	7.2	8.3	9.3
Reynolds Channel							
NACCS	4.8	5.4	6.1	6.8	7.7	9.0	10.0
FIMP 2006		4.6	5.4	6.0	6.6	7.4	7.8
FIMP 2014		4.8	5.5	6.2	7.0	7.7	8.0
FEMA RII			4.2	5.3	6.3	7.7	9.1
Pt. Lookout							
NACCS	4.5	5.1	5.8	6.4	7.0	8.1	9.1
USGS	4.1	4.3	4.6	4.8	5.2	5.7	6.2
FIMP 2006		4.1	5.0	5.6	6.1	6.7	7.1
FIMP 2014		4.4	5.3	5.9	6.4	7.0	7.3
FEMA RII			5.0	6.2	7.2	8.6	10.0
Freeport							
NACCS	4.6	5.2	5.9	6.4	7.1	8.5	9.6
USGS	4.0	4.2	4.5	4.7	5.0	5.5	6.0
FEMA RII			5.3	6.5	7.5	8.8	9.9

Notes: *NACCS model results from Coastal Hazards System website shown

Table 6-5:   Water Level Comparison at Eastern Back Bay Stations

Location and Source	Annual Exceedance Probability						
	99%	50.0%	20.0%	10.0%	5.0%	2.0%	1.0%
	Return Period (years)						
	1	2	5	10	20	50	100
South Oyster Bay							
NACCS	3.6	4.2	4.9	5.6	6.3	7.4	8.4
FIMP 2006		3.4	4.1	4.6	5.0	5.6	5.9
FIMP 2014		3.8	4.7	5.1	5.5	6.1	6.4
FEMA RII			5.6	6.7	7.6	8.7	9.5
Unqua Point							
NACCS	3.5	4.2	5.0	5.7	6.4	7.6	8.7
FIMP 2006		3.2	3.9	4.4	4.8	5.3	5.7
FIMP 2014		3.7	4.5	4.9	5.4	5.9	6.2
FEMA RII			5.7	6.9	7.8	9.0	9.7
Lindenhurst							
NACCS	3.1	3.8	4.4	5.3	6.2	7.4	8.2
USGS	2.5	2.8	3.2	3.6	4.1	4.8	5.4
FIMP 2006		2.6	3.3	3.7	3.9	4.3	4.6
FIMP 2014		3.4	4.1	4.5	4.8	5.2	5.4
Fire Island Bridge							
NACCS	2.7	3.3	3.9	4.4	5.0	6.1	7.1
FIMP 2006		2.6	3.1	3.5	3.7	4.2	4.7
FIMP 2014		3.0	3.5	3.9	4.3	4.8	5.0
Brown Point							
NACCS*	2.8	3.5	4.5	5.2	6.0	6.9	7.7
FIMP 2006		2.2	3.1	3.4	3.6	3.9	4.1
FIMP 2014		3.6	4.3	4.6	4.8	5.0	5.2
Watch Hill							
NACCS*	2.9	3.6	4.6	5.4	6.2	7.3	8.1
FIMP 2006		2.3	3.0	3.4	3.6	3.9	4.1
FIMP 2014		3.5	4.1	4.6	4.9	5.2	5.4

Notes: *NACCS model results from Coastal Hazards System website shown

Water levels in the NCBB study area are complex and affected by tidal and storm surge propagation through the inlets, local wind-driven surge along the bay-axis, and overwash across the barrier islands. Numerical modeling performed for the FIMP GRR showed that the dynamic nature of the barrier island topography and inlets/breaches connecting the back bay to the ocean could significantly influence water levels in the NCBB study area. Therefore, the evaluation of the NACCS AEP water levels starts by comparing results at the NOAA stations with long-term records that are generally located along the open ocean. Confidence in the NACCS ADCIRC model is greater at these stations since the model calibration and validation was performed here.

Comparison of the NACCS AEP water levels the NOAA stations to water levels derived from the long-term measurements (TR-14-7), as shown in Table 6-3, indicates that NACCS water levels are 1.1 to 1.6 feet

higher than NOAA TR-14-7 at the 10% AEP (10-year) and 1.5 to 3.2 feet higher at the 1% AEP (100-year). At the 99% AEP (1-year) the NACCS and NOAA TR-14-7 water levels are in good agreement. Nadal-Caraballo et al. (2015) note that AEP water levels derived from NOAA measurements may be lower than from NACCS JPM-OS methodology because of the short record length and relatively sparse extreme storm occurrences. However, records at several of the NOAA stations exceeds 100 years and the NOAA derived AEP values should be considered more and more reliable at estimating water levels moving from the low-frequency to high-frequency water levels.

In the NCBB study area, the AEP water level evaluation is split into two areas, western back bay stations and eastern back bay stations. The western back bay stations are located in Nassau County west of the Jones Beach Causeway. The eastern back bay stations are located in east of the Jones Beach causeway in South Oyster and Great South Bay. The FIMP GRR numerical modeling indicates that the eastern stations are more likely to be affected by the dynamic nature of the barrier island topography and inlets/breaches.

Comparison of the NACCS AEP water levels to the USGS and FIMP water levels at the western back bay stations, Table 6-4, indicates that NACCS water levels are 0.1 to 0.6 feet higher than USGS at the 99% AEP and 0.4 to 1.7 feet higher than USGS at the 10% AEP. The FIMP GRR AEP water levels are generally somewhere in the middle between the NACCS and USGS water levels. Figure 6-9 shows the NACCS, USGS, and FIMP water levels at Island Park, NY, Pt. Lookout, NY, and Freeport, NY.

Comparison of the NACCS AEP water levels to the USGS and FIMP water levels at Lindenhurst, the only USGS station in eastern back bay, Table 6-5, indicates that NACCS water levels are 0.6 feet higher than USGS at the 99% AEP and 1.7 feet higher than USGS at the 10% AEP. The FIMP 2006 AEP water levels are in good agreement with the USGS water levels. However, the updated FIMP 2014 water levels, that include the Wilderness Breach, are only 0.4 feet lower than the NACCS at the 50% AEP and 0.8 feet lower than NACCS at the 10% AEP. Figure 6-9 shows the NACCS, USGS, and FIMP water levels at Lindenhurst, NY.

The differences between the FIMP 2006 and FIMP 2014 water levels indicate that the Wilderness Breach, which is also present in the NACCS model bathymetry, could be partially responsible for the large differences observed between the NACCS and USGS water levels in South Oyster and Great South Bay. The two storms of record in the USGS dataset, Hurricane Sandy and Hurricane Irene, and 7 of the top 8 events at Lindenhurst occurred before the Wilderness Breach opened in October 2012 during Hurricane Sandy. The observed differences between NACCS and USGS high-frequency AEP water levels at the western back bay stations are more consistent with the differences observed between NACCS and NOAA TR-14-7 at the open ocean stations.
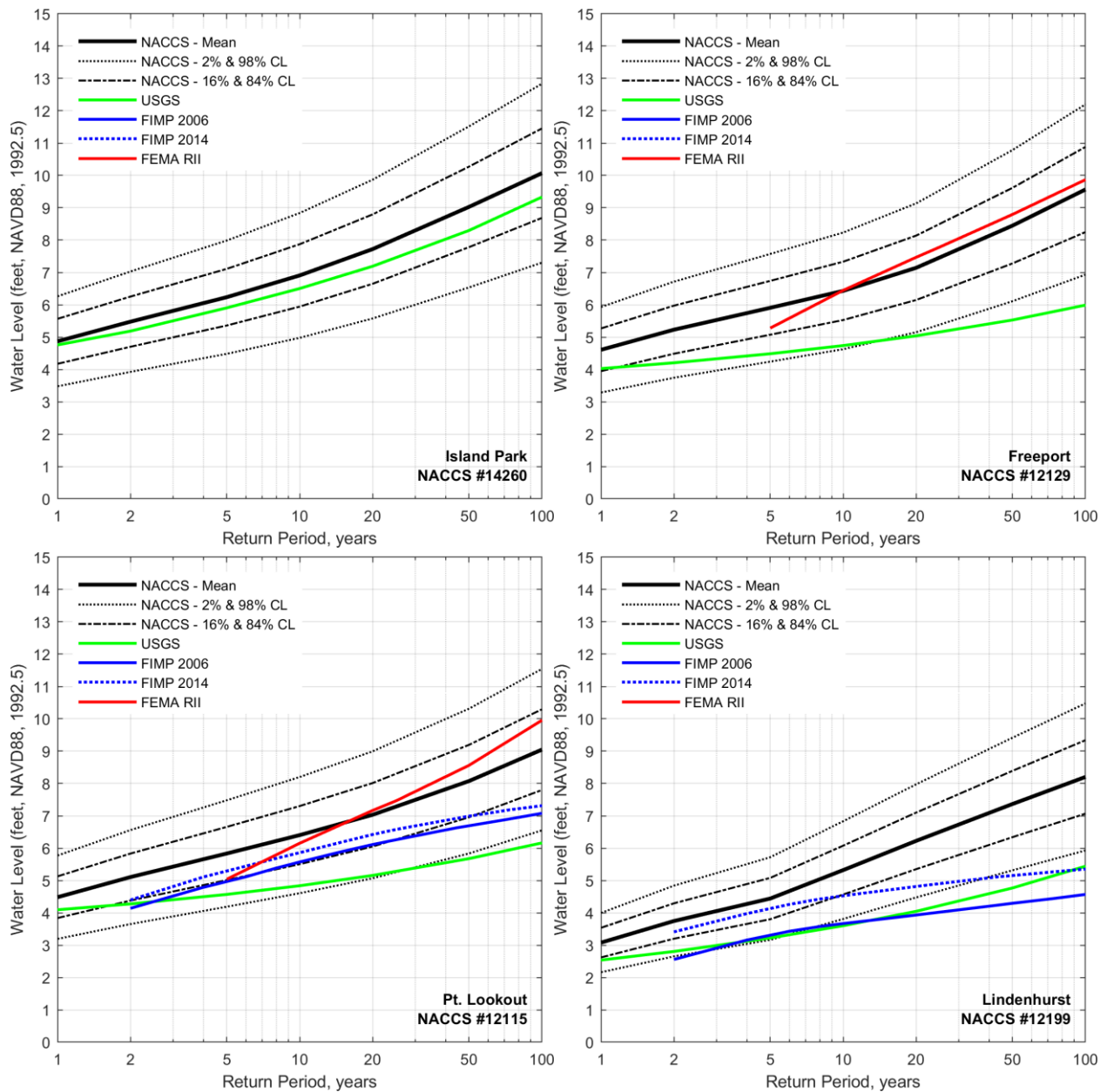
Figure 6-9:   *Water Level Hazard Curves in NCBB Study Area*

6.4.7   Recommendation

Evaluation of the AEP water levels in the NCBB study area shows that NACCS water levels are consistently higher than water levels derived from NOAA and USGS measurements and the AEP water levels developed for the FIMP GRR. NACCS water levels at the 10% AEP are 1.2 to 1.6 feet higher than other values at NOAA stations and 0.4 to 1.7 feet higher than other values at USGS stations. Differences in South Oyster Bay and Great South Bay may be partially attributed to the Wilderness Breach and lower barrier island topography in the NACCS model bathymetry. However, the observed differences between NACCS and NOAA water levels at the open ocean NOAA stations indicate that the high-frequency water levels (10% AEP) are likely overestimated in the NCBB study area.

After review of the NACCS AEP water level evaluation and sensitivity of the FWOP damages to a 1 foot reduction in the water levels, it is recommended to lower the NACCS water level between the 99% AEP and 10% AEP applied in the FWOP damage calculations. Modifications to the water elevations for the 2% AEP to 0.1% AEP are not recommended considering the higher uncertainty associated with less frequent extreme storm events. Validation of the NACCS model to Hurricane Sandy observations in the NCBB study area provides confidence in NACCS model and its ability to simulate storm surge in the NCBB study area in the existing conditions and storm surge barrier alternatives.

The recommended approach to revising the NACCS water level statistics is to use the lower 16% confidence interval between the 99% and 10% AEPs and mean confidence interval from the 2% to 0.1% AEP. The 5% AEP will be an average of the 16% and mean confidence interval to provide a smoother transition. Figure 6-10 provides an example of the revised NACCS water levels. The 16% confidence interval from NACCS is found to be in better agreement with FIMP 2014 hazard curves and USGS derived curves. Using the 16% confidence interval instead of the mean will result in a reduction of the 1-year water elevations by approximately 0.5 feet and the 10-year water levels by approximately 1.0 feet. The advantage of using the lower NACCS confidence interval to define the high-frequency end of the hazard curve, as opposed to a linear or percent reduction, is that this approach may be replicated in the With-Project modeling (i.e. storm surge barriers) allowing for a fair estimation of the reduction in water levels and damages.
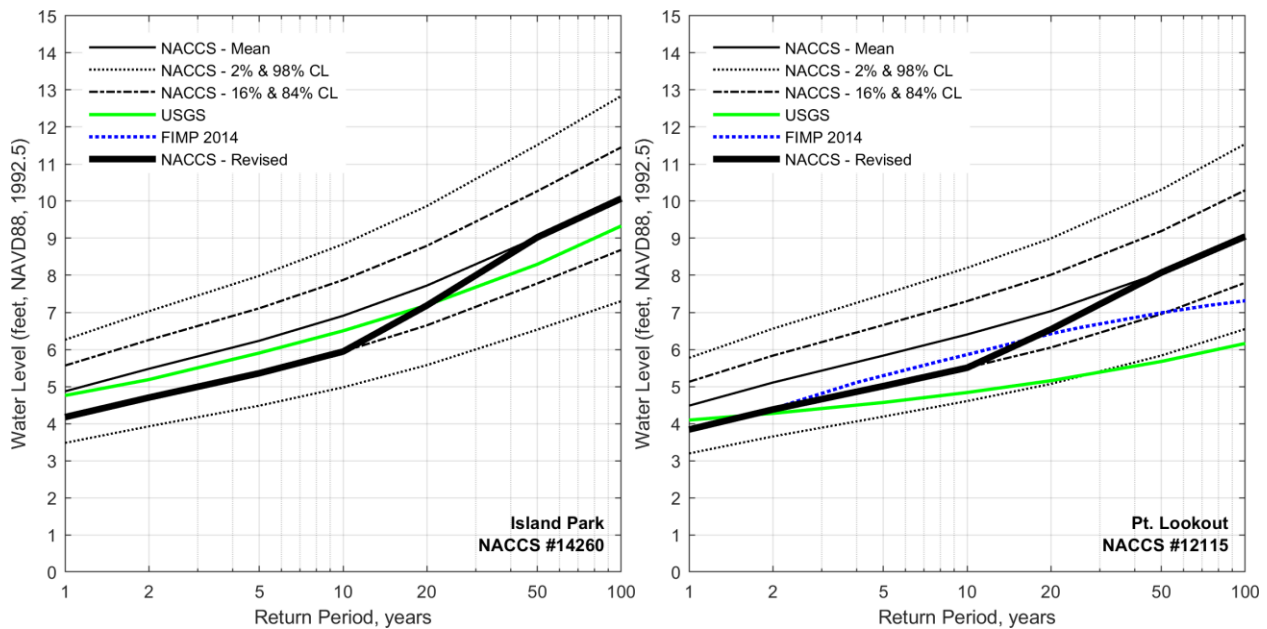
Figure 6-10:   *Example of Revised Water Level Hazard Curves in NCBB Study Area*

6.5   Representative NACCS Model Results

Table 6-6 presents the NACCS AEP water levels for 9 representative stations in the study area. The high-frequency water levels in Table 6-6 are revised using the 16% confidence limit as described in Section 6.4.The variability in water levels within the study area is captured by Figure 6-11, which shows a map of the 1% AEP water levels. It is apparent from these tables and figures that the back bay AEP water levels increase from east to west, with the highest water levels in the vicinity of Bay Park and Long Beach.

Table 6-6:   *NCBB Baseline Water Level AEP at Representative Stations*

Location	Save Point	Return Period (years)							
		1	2	5	10	20	50	100	500
		Annual Exceedance Probability							
		99%	50%	20%	10%	5%	2%	1%	0.2%
Long Beach	14230	4.1	4.6	5.3	5.9	7.2	9.1	10.1	12.2
Bay Park	12084	4.4	4.9	5.6	6.1	7.4	9.3	10.4	12.5
Lido Beach	12080	4.1	4.7	5.3	5.9	7.2	9.0	10.0	12.1
Freeport	12129	4.0	4.5	5.1	5.6	6.7	8.5	9.6	11.7
Seaford	14401	3.5	4.1	4.7	5.2	6.3	7.9	9.0	11.4
Lindenhurst	12199	3.0	3.5	4.1	4.9	6.1	7.7	8.5	11.0
Great Cove	3652	3.3	3.8	4.3	4.8	5.8	7.3	8.5	11.3
Ocean Beach	3656	2.1	2.7	3.3	3.9	4.9	6.3	7.3	9.9
Patchogue	3671	2.4	3.0	3.7	4.4	5.5	7.2	8.3	11.8

Note: All elevations are in feet NAVD88, relative to NTDE (1983-2001), Revised high-frequency values
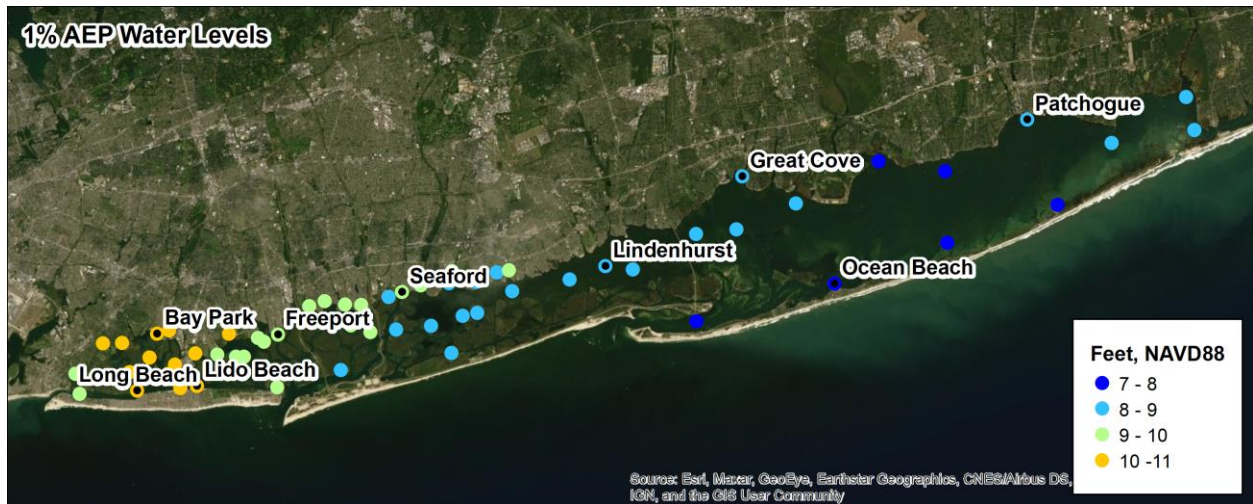
Figure 6-11:   *NCBB Baseline 1% AEP Water Levels*

6.6 Storm Surge Barrier Modeling

6.6.1 Approach to Modeling Storm Surge with Storm Surge Barriers

Due to the complex network of inlets and bays that control the flow of water between the ocean and back bays, NAP requested assistance from ERDC-CHL in evaluating the effectiveness of inlet closures in reducing water levels in the NCBB study area. To answer these questions ERDC-CHL leveraged the existing NACCS CSTORM-MS. The Project Delivery Team (PDT) identified five closure alternatives with different combinations of inlet and bay closures and floodwalls to evaluate. CSTORM-MS model simulations are performed for the five alternatives and baseline conditions using a subset of 25 tropical cyclones and three historical storms. Model results are used to develop frequency distributions of peak water levels that may be applied in economic analyses of flood damages and benefits. A Draft Technical Report by Slusarczyk et al. (2021) provides a detailed description of the storm surge modeling effort and discussion of the modeling results.

The effectiveness of the storm surge barriers (SSB) at reducing water levels in the study area captured in the water level hazard curves at nine locations throughout the study area (Figure 6-12). The nine locations selected capture effectiveness and impacts of the closure structures throughout the study area and outside the study area in Great South Bay.
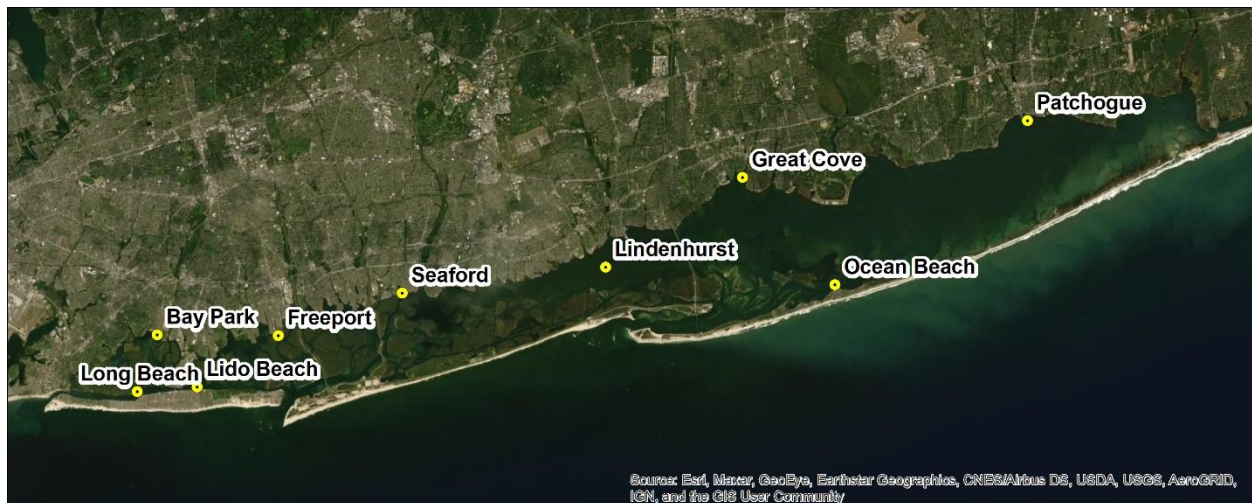
Figure 6-12: NACCS Save Points Evaluated for Storm Surge Barriers

6.6.2 Summary of Storm Surge Barrier Model Results

Two principal processes are responsible for back bay flooding in the NCBB study area: (1) storm surge propagation through tidal inlets and (2) local wind-driven storm surge along the east-west bay axis. Effective SSB alternatives must address both processes.

Four SSB alternatives were identified by the PDT irrespective of CBRA constraints. Figure 6-13 shows the four SSB alternatives as well as one additional perimeter plan (floodwall) alternative. Alternative 1A consists of three storm surge barriers at each of the three inlets (East Rockaway Inlet, Jones Inlet, and Fire Island Inlet) in the study area. Three additional SSB alternatives (Alternatives 1B, 1C, 1D) were developed

by the PDT with storm surge barriers across the bay, "bay closures," to reduce flooding from the local wind-driven surge along the bay. Alternative 2 consist of floodwalls along the entire developed bay shoreline in Nassau County. The hazard curves for the five alternatives is presented in Figure 6-14.

Model results for Alternative 1A indicate that inlet closures alone are only able to reduce the 1% Annual Exceedance Probability (AEP) water elevation by approximately one foot, from 10 feet NAVD88 to 9 feet NAVD88. Even with the three inlets closed, winds push water in Great South Bay westward into the study area limiting the effectiveness of Alternative 1A. An example of the ineffectiveness of Alternative 1 is captured in the model results for Hurricane Sandy as provided in Figure 6-15. If the three inlets closures had been in place during Hurricane Sandy, the model predicts up to a one foot reduction in water elevations.

The PDT developed Alternatives 1B, 1C, and 1D to reduce impacts from local wind-driven surge in Nassau County. ERDC storm surge model results for Alternatives 1B, 1C, and 1D indicate that the combination of inlet closures and bay closures is successful at reducing water elevations inside the SSB system. However, outside the SSB system, specifically east of the bay closures in Great South Bay, the 1% AEP water elevations increase by 2 to 4 feet over extensive areas (10 to 20 miles). An increase in water elevations is the result of local wind-driven storm surge "piling up" at the bay closures. An example of the induced flooding caused by the bay closures is captured in the model results for Hurricane Sandy as provided in Attachment 2. SSB alternatives with bay closures (Alternatives 1B, 1C, 1D) are likely to have been dropped from further consideration due to the substantial increase in flooding to communities outside the storm surge barrier.

Storm surge modeling results for Alternative 2, perimeter plan around the entire Nassau County back bay shoreline (~30 miles), show the potential for a 0.5 to 1 ft increase in the 1% AEP water level. However, these model results are not representative of the impacts of a significantly smaller and more localized floodwall (4 miles) at the City of Long Beach. Detailed modeling will be performed prior to the Final Report to confirm that the impact of the floodwall at the City of Long Beach is not significant. The floodwall along the City of Long Beach is not expected to significantly increase water levels in the adjacent areas.

All four of the SSB alternatives have at least one SSB located entirely within the footprint of a system unit. Figure 6-16 includes a figure of the four SSB alternatives and CBRA system units. Eliminating storm surge barrier (SSB) features located in CBRA system units will render the SSB alternatives even less effective at reducing storm surge by severely handicapping their ability to block storm surge from both of the principal processes responsible for back bay flooding

Figure 6-13:   Storm Surge Barrier Alternatives
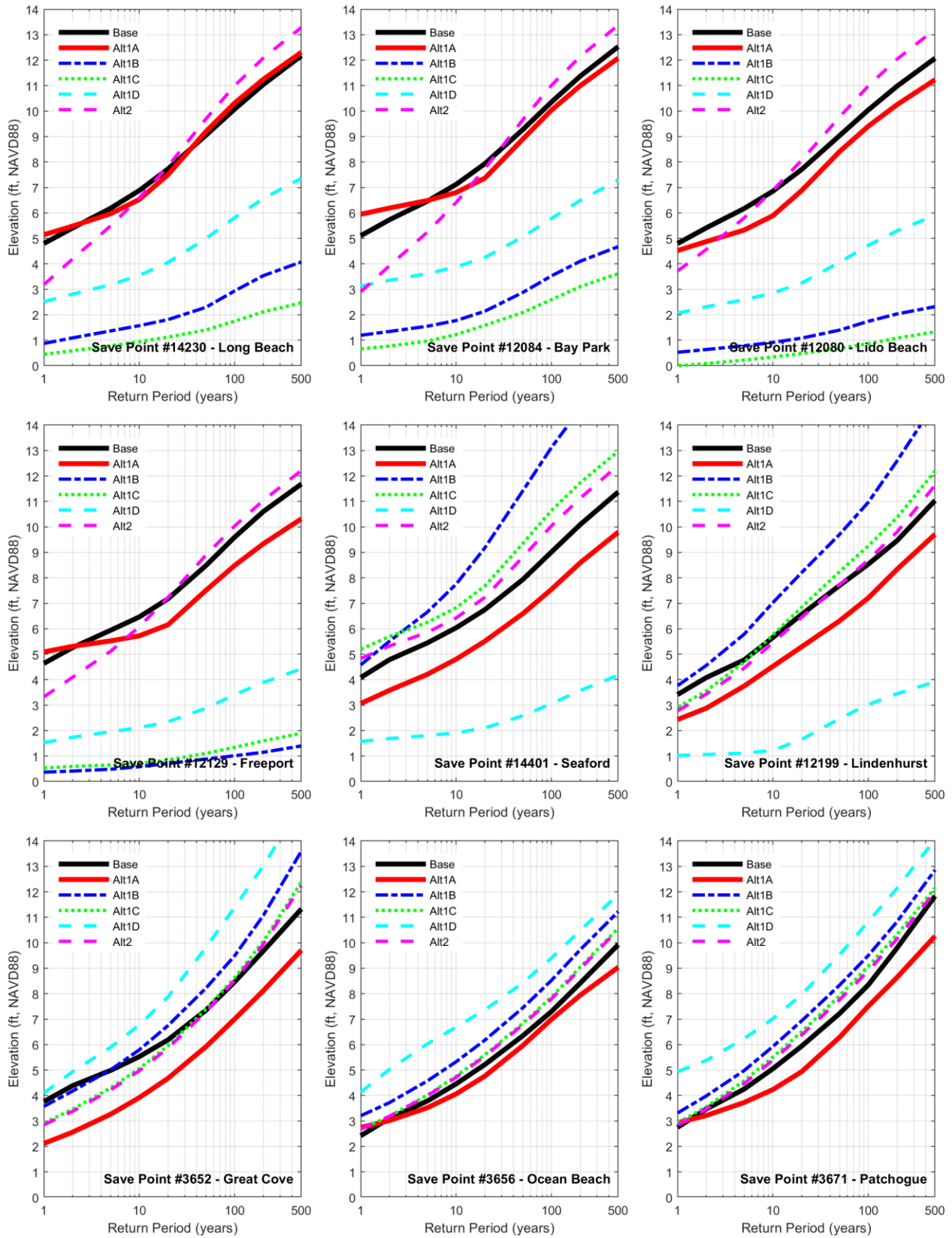
Figure 6-14:   Storm Surge Barrier Water Level Hazard Curves
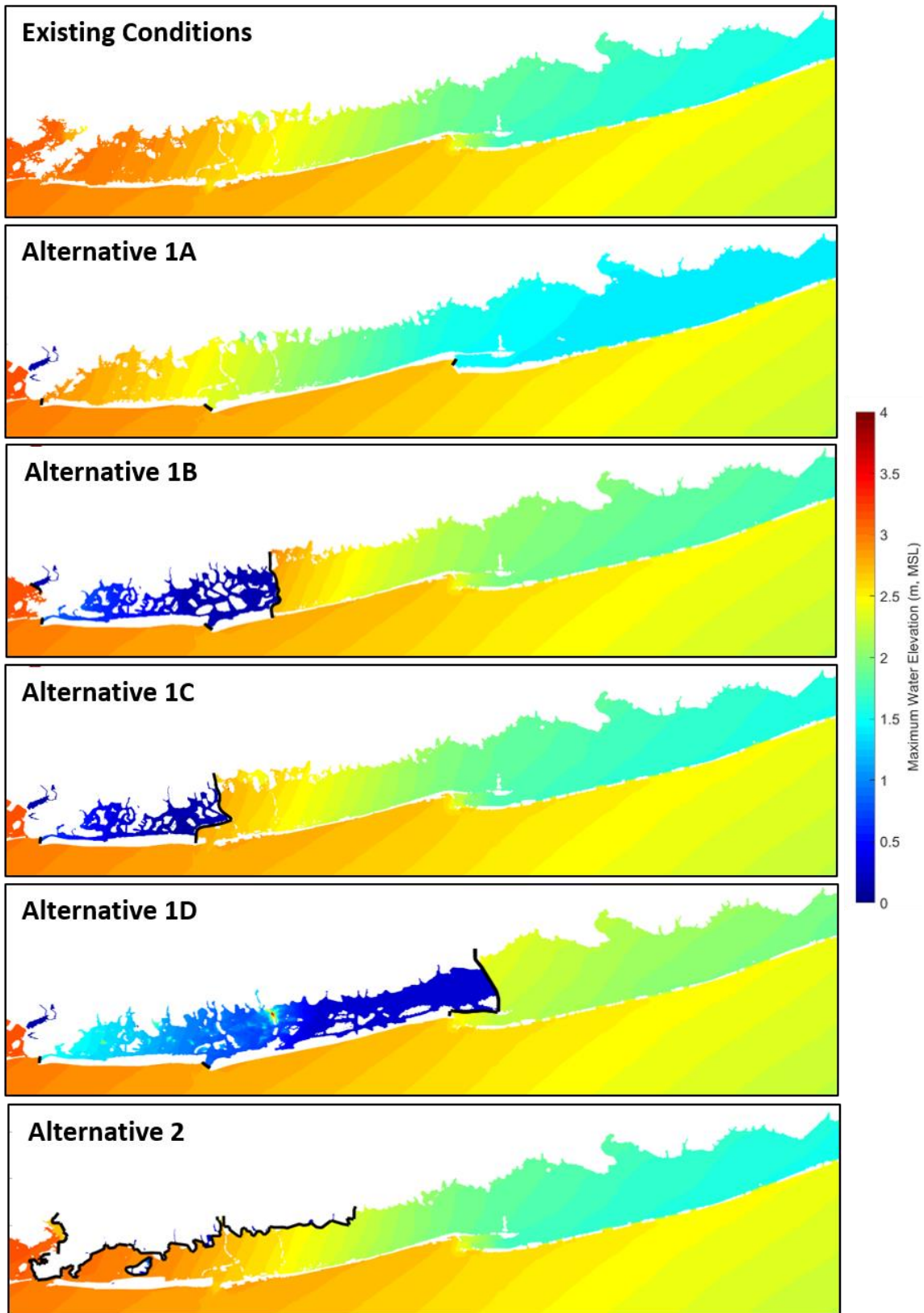
Figure 6-15: Storm Surge Model Results for Hurricane Sandy
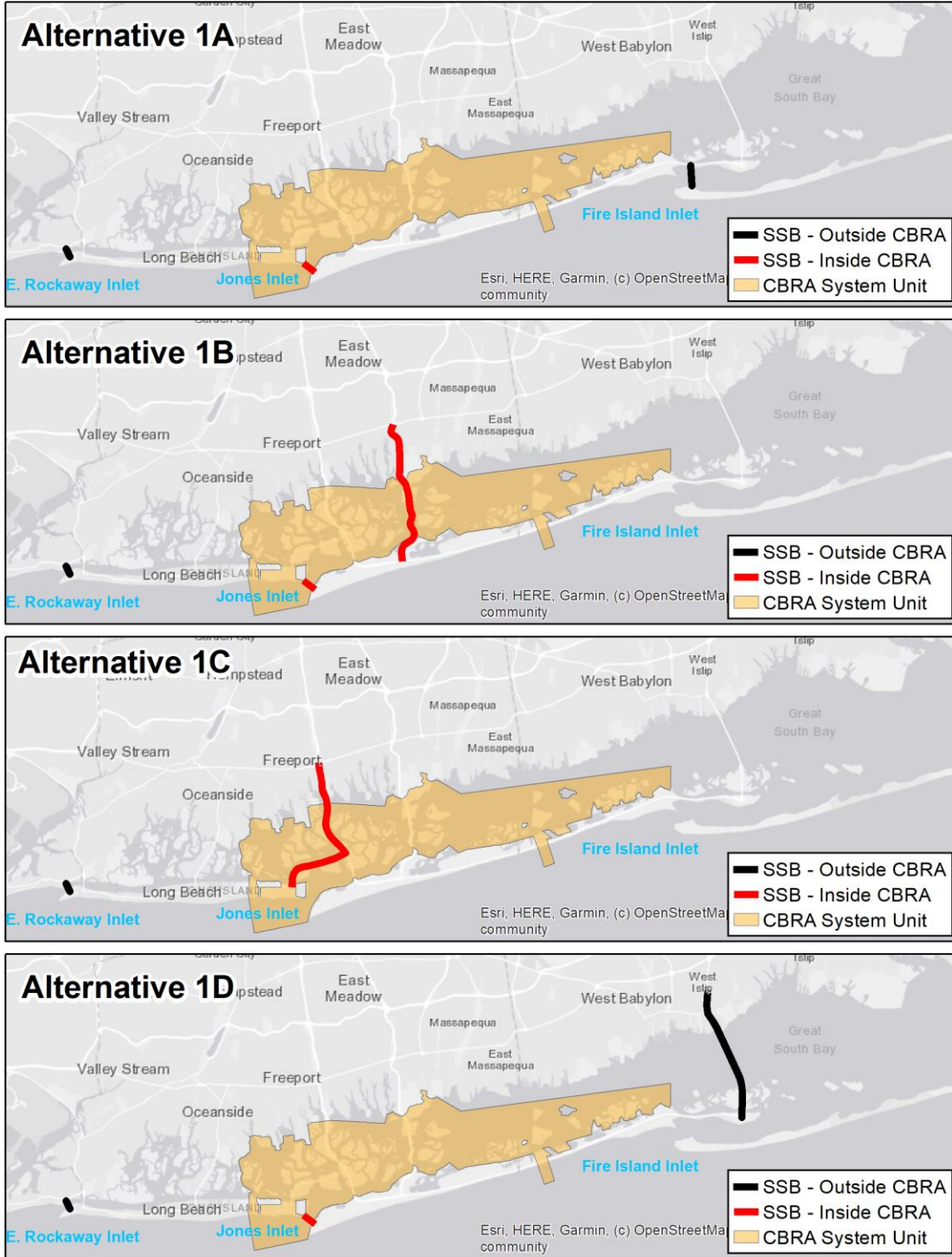
Figure 6-16:   Storm Surge Barrier Alternatives (1A to 1D) and CBRA System Unit

7   WAVE OVERTOPPING

7.1   Overview

Wave overtopping is of principal concern for structures constructed for flood risk management. The design crest elevation of flood risk management structure is often determined by the design still water level and required freeboard, height above still water level, to prevent wave overtopping from damaging the structure during the design storm event.

EurOtop (2016) describes wave overtopping as:

> *Overtopping discharge occurs because of waves running up the face of a seawall or dike. If wave run-up levels are high enough water will reach and pass over the crest of the structure. This defines the 'green water' overtopping case where a continuous sheet of water passes over the crest. In cases where the structure is vertical, the wave may impact against the wall and send a vertical plume of water of the crest. A second form of overtopping occurs when waves break on the seaward face of the structure and produce significant volumes of splash 'whitewater'. These droplets may then be carried over the wall either under their own momentum or as a consequence of an onshore wind.*
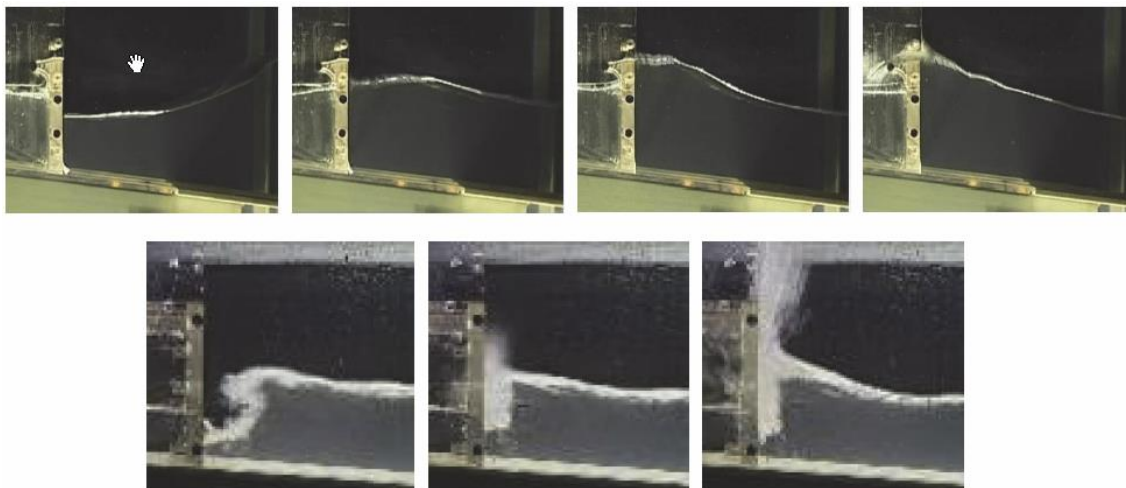
Figure 7-1:   Wave Overtopping at Vertical Wall (EurOtop, 2016)

The top panel and bottom panel of Figure 7-1show an example 'green water' and 'white water' overtopping at a vertical structure respectively.

The wave overtopping rate, q, reported in this study is the mean overtopping discharge (liters/s/m). Wave overtopping occurs in sporadic short pulses and is not constant over time. It is coastal engineering practice to use mean wave overtopping rates in engineering applications since available design formulas are based on the mean overtopping rate due to its ability to be easily measured in laboratory studies.

7.2   Wave Conditions

Wave conditions in the NCBB study area are fetch-limited waves generated by local wind conditions. In fetch-limited conditions, wave heights are limited by the distance of open water in which the waves can grow. Wave conditions throughout the bay are also affected by the shallow water depths, marshes, and

orientation relative to the wind directions. A sampling of the 100-year wave conditions at 6 representative locations throughout the study area is provided in Table 7-1.

In the design or assessment of coastal structures with respect to wave overtopping, the two primary hydraulic parameters (water level and wave height and wave period) may be derived from a joint probability analysis (EurOtop, 2016). If both water level and wave height are determined for a certain return period, then the wave overtopping discharge for the combination of these extreme conditions will be larger than the actual wave overtopping occurring with the return period (EurOtop, 2016). This is caused by the fact that the combination of these two extreme values will have a lower probability of occurrence if the two are not fully correlated (EurOtop, 2016).

The "H_{m0} – Joint" and "T_p – Joint" columns in Table 7-1, Table 7-2, and Table 7-3 represent the joint probability or most likely wave height and wave period associated with the 1% AEP water level event. The joint probability of the wave height and water levels was determined from time series of NACCS model results at each of the representative stations. The maximum wave height within 1 hour of the maximum water level was identified from the time series. Scatter plots showing the relationship between the peak water level and wave height is presented in Figure 7-3 and Figure 7-4. These figures also show the relationship between the wave height and wave period associated with the peak water levels. A linear curve was fit to the scatter data to obtain the joint probability relationship.

Table 7-1: Representative Wave Conditions, Joint Probability for 1% AEP

Station	ID	SWEL (ft, NAVD88)	H_{m0} (ft)	H_{m0}-Joint (ft)	T_p-Joint (s)
Bay Park	12084	10.4	4.0	3.6	3.7
Island Park	14260	10.2	4.3	3.9	4.5
Long Beach	14230	10.1	4.5	3.5	5.2
Lido Beach	12080	10.0	5.2	4.0	3.9
Oceanside	14276	10.0	4.8	5.0	3.9
Freeport	12129	9.6	4.7	4.1	4.6

Notes: Still Water Elevation (SWEL), Joint probabilities values shown based on curve fit.

Table 7-2: Representative Wave Conditions, Joint Probability for 5% AEP

Station	ID	SWEL (ft, NAVD88)	H_{m0} (ft)	H_{m0}-Joint (ft)	T_p-Joint (s)
Bay Park	12084	7.4	3.4	2.6	3.4
Island Park	14260	7.3	3.6	2.8	3.8
Long Beach	14230	7.2	3.9	2.5	4.3
Lido Beach	12080	7.2	4.5	3.0	3.5
Oceanside	14276	7.1	4.1	3.7	3.7
Freeport	12129	6.7	4.3	2.9	3.9

Notes: Still Water Elevation (SWEL), Joint probabilities values shown based on curve fit.

Table 7-3:   Representative Wave Conditions, Joint Probability for 20% AEP

Station	ID	SWEL (ft, NAVD88)	H_{m0} (ft)	H_{m0}-Joint (ft)	Tp-Joint (s)
Bay Park	12084	5.6	3.0	2.0	3.1
Island Park	14260	5.5	3.1	2.1	3.5
Long Beach	14230	5.3	3.4	1.9	3.8
Lido Beach	12080	5.3	3.8	2.3	3.3
Oceanside	14276	5.3	3.6	2.8	3.6
Freeport	12129	5.1	3.8	2.3	3.6

Notes: Still Water Elevation (SWEL), Joint probabilities values shown based on curve fit.
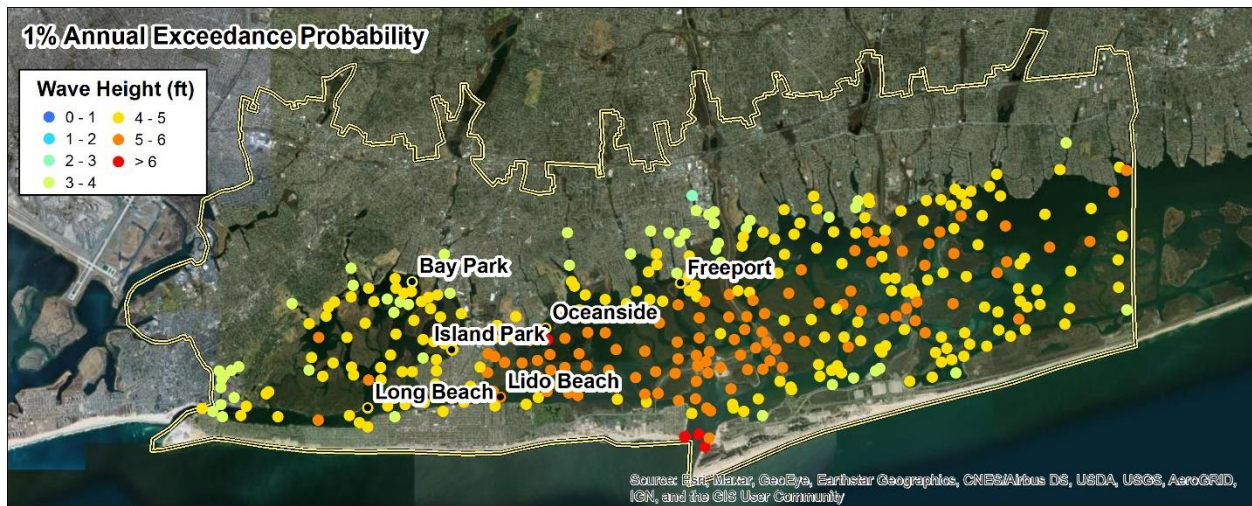

Figure 7-2:   NACCS 1% AEP Peak Wave Height and Representative Stations
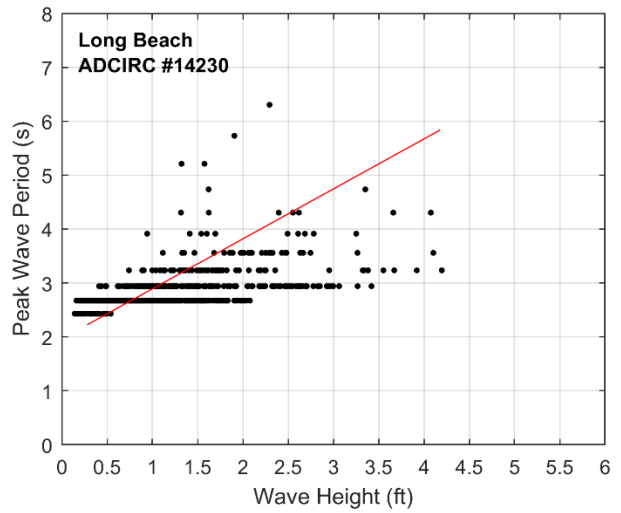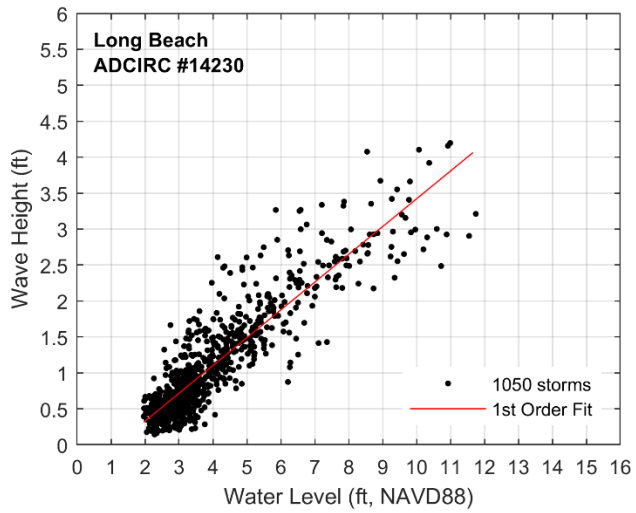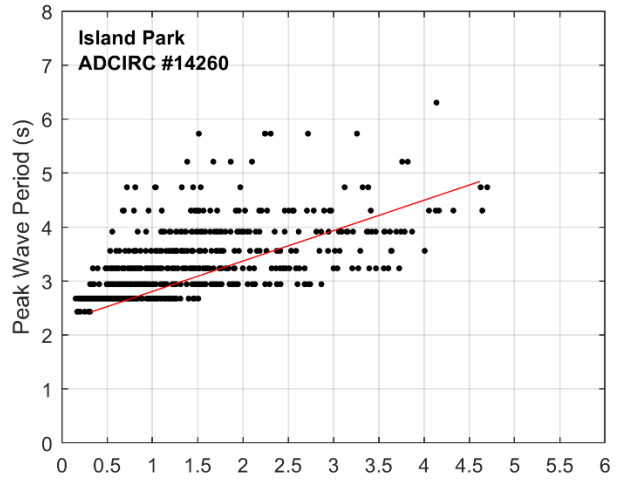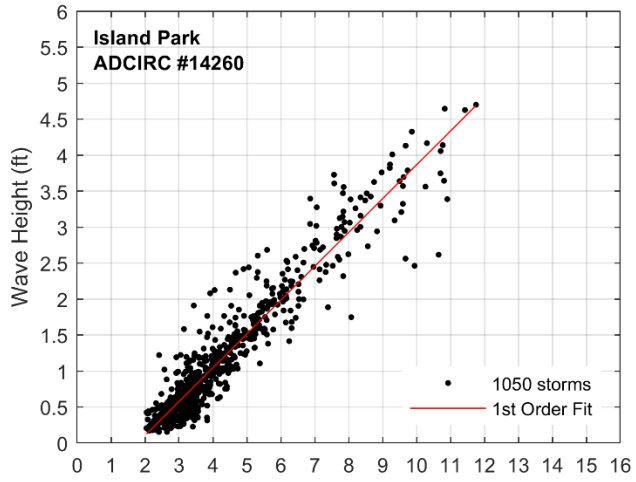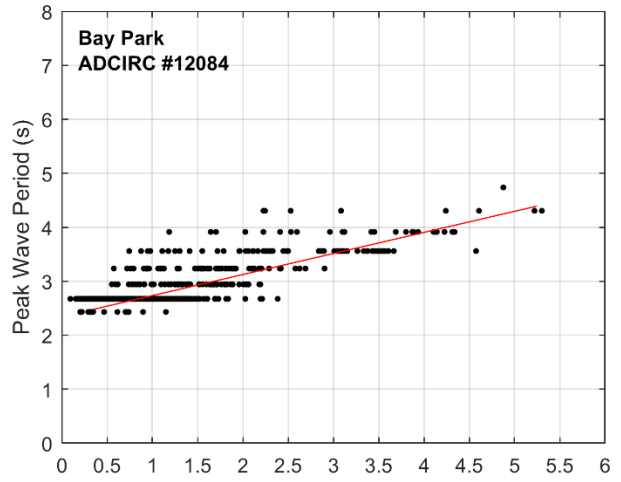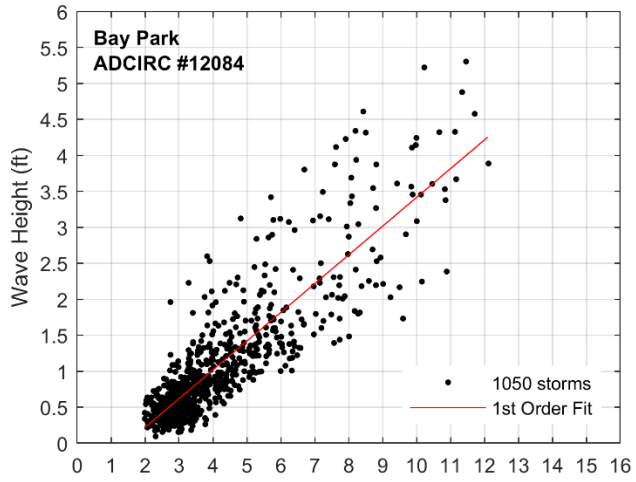
Figure 7-3:   *Joint Wave Probability, Bay Park, Island Park, and Long Beach*
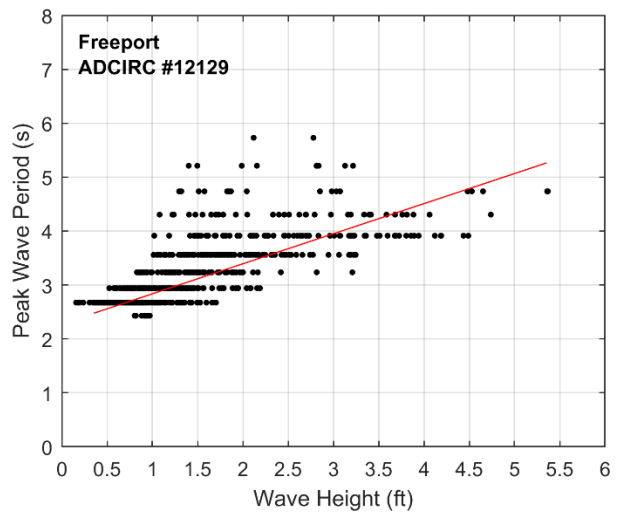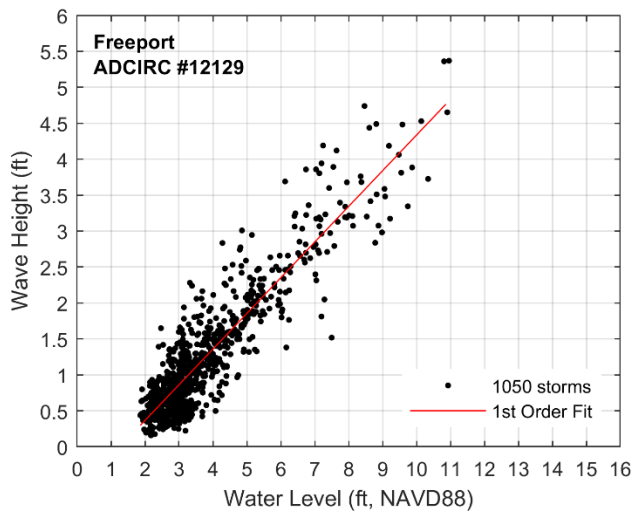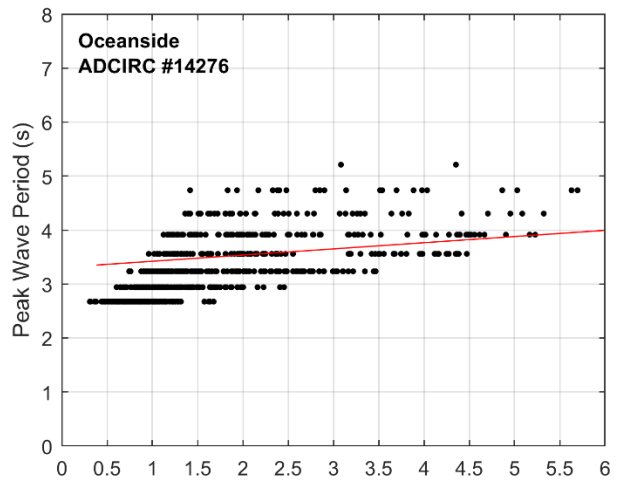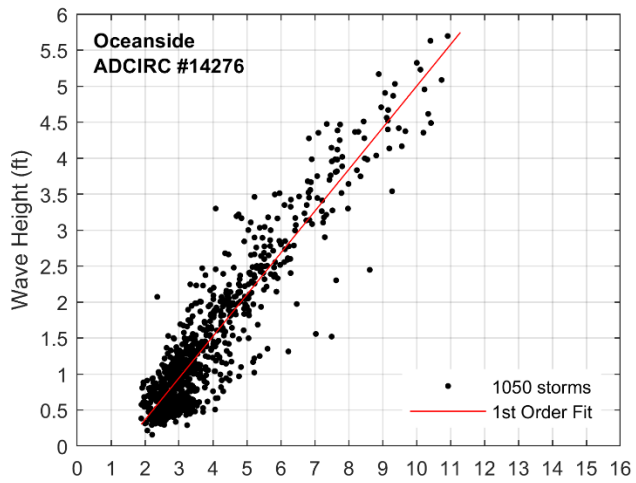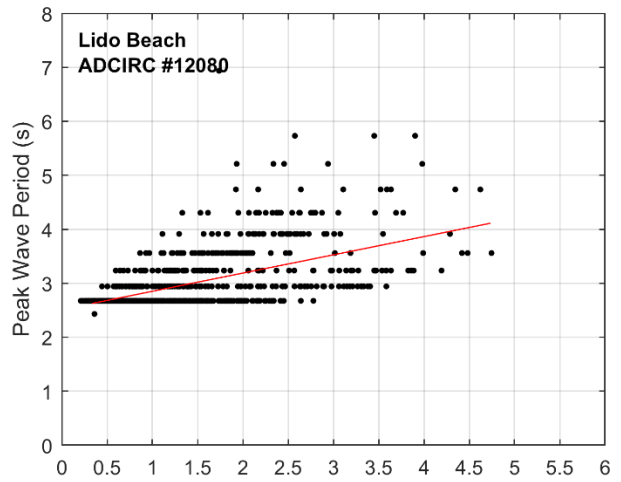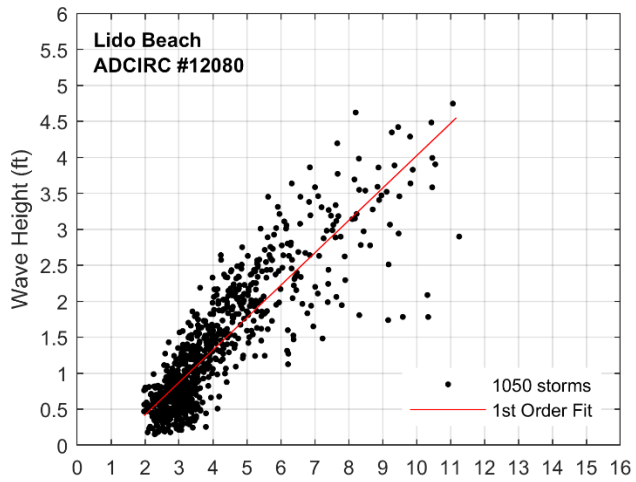
Figure 7-4:   Joint Wave Probability, Lido Beach, Oceanside, and Freeport

7.3 Tolerable Wave Overtopping Rates

Floodwalls that are exposed to heavy wave overtopping for many hours are susceptible to structural failure (Goda, 2000). Therefore, floodwalls are often designed to limit wave overtopping below a tolerable overtopping rate based on the structure type, property and operation, and people and vehicles. EM 1110-2-1100 provides guidelines for critical mean wave overtopping rates of several structure types before the structure begins to exhibit damage which may eventually lead to structural failure. Based on available literature including European and United States reference documents including Table 7-4, a tolerable mean wave overtopping rate of 10 liters/s/m is selected for floodwalls, rubble slopes (armored levees), and bay closures in the NCBB study. Floodwalls with an adequate splash apron could handle higher rates of wave overtopping before suffering structural damage and failure. However, houses and infrastructure are located in close proximity to the floodwalls and higher rates of overtopping could cause damage to houses and infrastructure, localized flooding/ponding, and threat to life safety.

Table 7-4:   *Tolerable Values of Mean Wave Overtopping (EM 1110-2-1100)*

q m^3/s per m q litres/s per m

	SAFETY OF TRAFFIC		STRUCTURAL SAFETY			
	VEHICLES	PEDESTRIANS	BUILDINGS	EMBANKMENT SEAWALLS	GRASS SEA-DIKES	REVETMENTS
10^0 (1000)						Damage even for paved promenade
(200)				Damage even if fully protected	Damage	Damage if promenade not paved
10^{-1} (100)	Unsafe at any speed	Very dangerous				(50)
			Structural damage	Damage if back slope not protected		(20)
10^{-2} (10)				Damage if crest not protected	Start of damage	
						(2)
10^{-3} (1)			Dangerous on grass sea dikes, and horizontal composite breakwaters			
	Unsafe parking on horizontal composit breakwaters	Dangerous on vertical wall breakwaters			No damage	
10^{-4} (0.1)	Unsafe parking on vertical wall breakwaters					
				No damage		(0.03) (0.02)
10^{-5} (0.01)		Uncomfortable but not dangerous	Minor damage to fittings, sign posts, etc.		No damage	
	Unsafe driving at high speed					(0.004)
10^{-6} (0.001)		Wet, but not uncomfortable				
	Safe driving at all speeds		No damage			
10^{-7} (0.0001)						

EurOtop (2016) and EM 1110-2-1100 highlight the importance of peak wave overtopping from a single wave on tolerable wave overtopping values. Overtopping discharge from a single wave can be more than 100 times the mean overtopping discharge during the storm peak (EM 1110-2-1100) and is often responsible for structural damages. Peak wave overtopping volumes have been shown to be strongly dependent on the wave height (EurOtop, 2016). For a given mean overtopping discharge, small waves only give small overtopping volumes, whereas large waves may give a much larger overtopping volumes for a single wave (EurOtop, 2016). In that sense mean tolerable overtopping rates should also be coupled to the wave height (EurOtop, 2016). Since the design wave conditions in the NCBB study area are relatively small, the tolerable mean wave overtopping rate selected for this study should be considered conservative relative to higher wave energy environments.

7.4   Overtopping Formulas

7.4.1   Vertical Wall

Mean wave overtopping rates are calculated for vertical walls using empirical formulas provided by EurOtop (2016). Results from EurOtop are compared to Franco and Franco (1999) as described in EM 1110-2-1100 and Ward and Ahrens (1992). The primary parameters in all of these wave overtopping formulas are the crest freeboard (R_c) and wave height (H_{m0}) as shown in Figure 7-5. The water depth (h), slope of foreshore (1:m), and wave period are important parameters in shallow water.
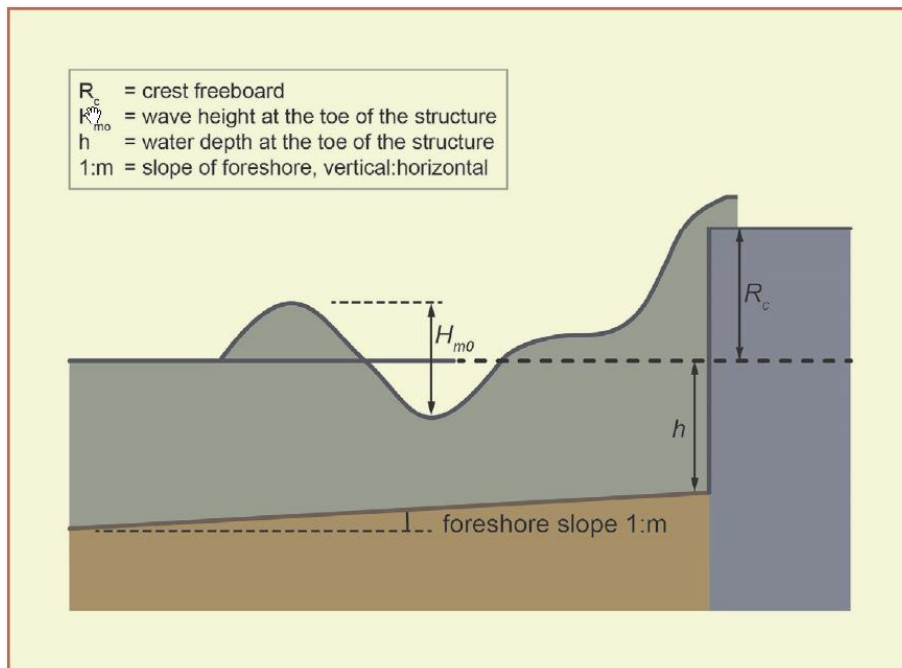

Figure 7-5:   Wave Overtopping Parameters (EurOtop, 2016)

The five wave overtopping formulas for vertical walls evaluated here are:

- EurOtop equations 7.1 and 7.2 for non-impulsive wave conditions;
- EurOtop equations 7.5 and 7.6 for non-impulsive wave conditions with an influencing foreshore;
- EurOtop equations 7.6, 7.8, 7.9, and 7.10 for impulsive wave conditions;
- Franco & Franco (1999), Table VI-5-13 in EM 1110-2-1100;
- Ward & Ahrens (1992), Group 1 Seawalls.

The general equation for the empirical formulas are

$$Q = a \, exp[-(bR)^c]$$

where Q and R are the non-dimensional representation of the mean wave overtopping rate, q, and freeboard, R_c ,

$$Q = \frac{q}{\sqrt{gH_{m0}^3}} \, , \qquad R = \frac{R_c}{H_{m0}}$$

and a, b, and c are constants. This general equation is used by Franco & Franco (1999) and the EurOtop formulas for non-impulsive (i.e. non-breaking) wave conditions. The empirical formulas for Ward and Ahrens (1992) and EurOtop formula for impulsive wave conditions follow this general form but also include parameters based on the water depth, slope of foreshore, and wave period. A comparison of three EurOtop formulas are shown in Figure 7-6, where the strong dependence of wave overtopping on the relative freeboard is shown. It is apparent from Figure 7-6 that under small relative freeboard conditions, $R_c/H_{m0} < 1$, the three wave overtopping formulas produce similar results. As the relative freeboard increases the impulsive wave (breaking wave) conditions produce higher rates of wave overtopping and the impact of the foreshore becomes more significant.

The EurOtop Manual provides two sets of formulas, the "Mean value approach" and "Design or assessment approach". The mean value approach should be used to predict or compare with test data and the design or assessment approach includes a partial safety factor with one standard deviation above the mean value approach. The difference between the approaches is shown in Figure 7-7 for non-impulsive wave conditions.
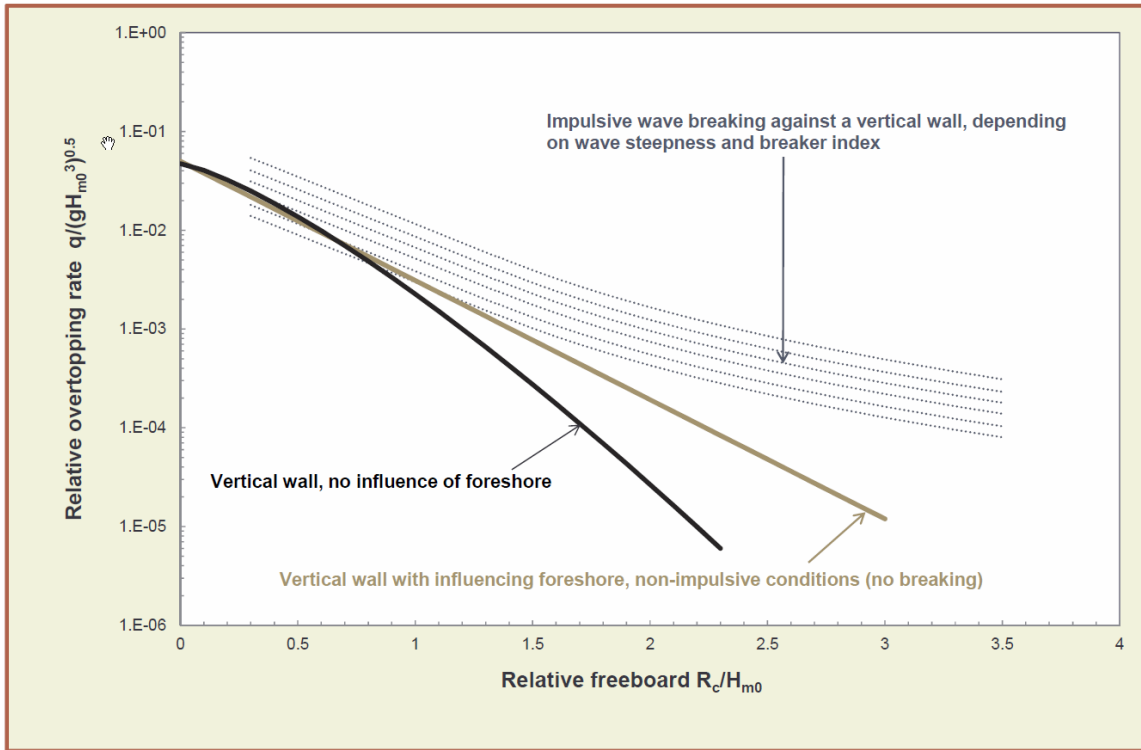
*Figure 7-6:   Non-dimensional Overtopping and Freeboard (EurOtop, 2016)*
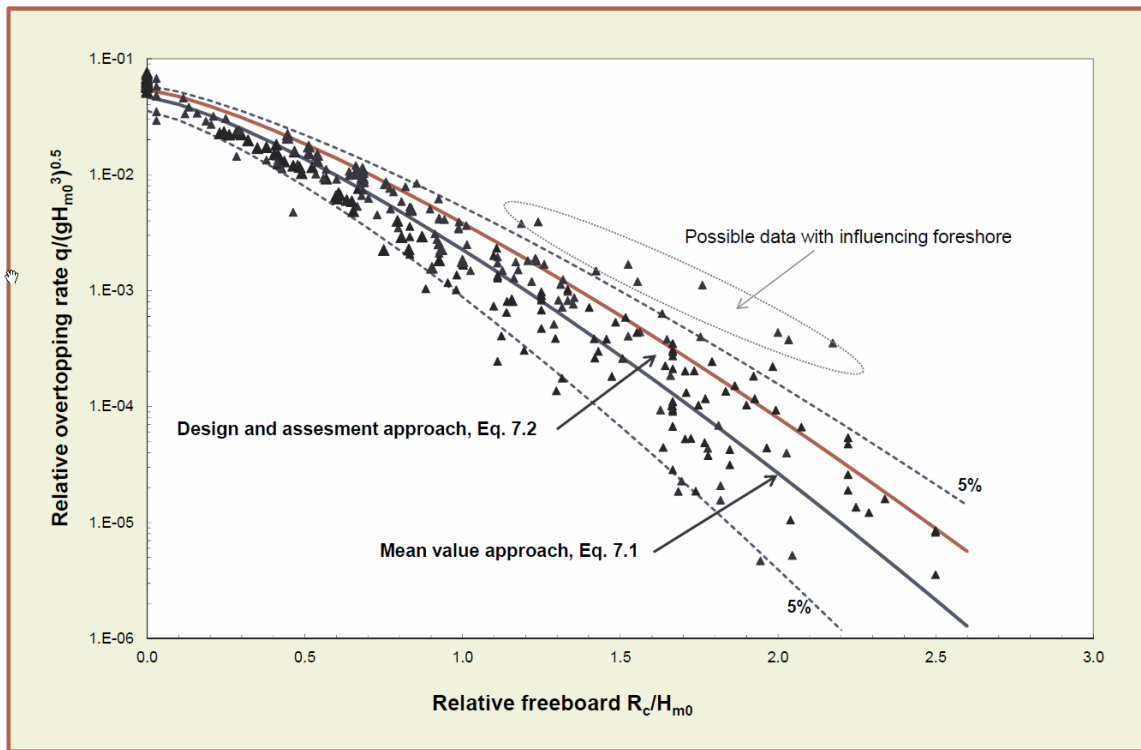
Figure 7-7:   Mean Value and Design Approaches (EurOtop, 2016)

7.4.2 Rubble Slope

The primary focus of the wave overtopping analysis is on vertical walls (i.e. floodwalls) since they are the primary measure under consideration in the Perimeter Plan. However, there are some locations where a rubble slope (i.e. armored levee) is more appropriate and economical. Mean wave overtopping rates are calculated for rubble slopes using empirical formulas provided by EurOtop (2016). The general formula for the rubble slope is the same as the vertical wall with other influence factors that account for roughness associated with the armor stone, oblique wave attack, crest berm, composite slopes, and wave wall at crest. EurOtop (2016) provides a formula for the "Mean value approach" and "Design or assessment approach".

7.4.3 Comparison of Formulas

Due to the size of the study area, there will be considerable variability in the local site conditions, such as the wave conditions, water depth, and foreshore slope. Rather than perform a detailed analysis at every site, several representative sites are selected throughout the study area and the sensitivity to the wave overtopping formulas is evaluated. This approach provides confidence in the results and a deeper understanding of the most important parameters governing wave overtopping in the study area.

Two sets of wave conditions are evaluated:

- Wave Height = 1 m, Wave Period = 4 s, Water Depth = 3m;

- Wave Height = 2 m, Wave Period = 8 s, Water Depth = 3m;

The first set of wave conditions are fairly representative of the design wave conditions found in the NCBB study area. The second set of wave conditions are included to illustrate how the results are affected by the wave height and wave period. Figure 7-8 presents the wave overtopping results on a vertical wall for the first two wave conditions over a range of freeboard heights in terms of the relative wave overtopping and relative freeboard.

In order to provide context to the non-dimensional figures, the tolerable wave overtopping rate of 50, 10, and 2 liters/s/m, is plotted in Figure 7-8. The intersection of the wave overtopping formulas and tolerable rate of wave overtopping represents the relative freeboard, R_c/H_{m0}, required to limit wave overtopping below this tolerable rate. For the 1 meter wave height conditions, a relative freeboard of about 0.8 is required to limit wave overtopping below 10 liters/s/m for all the formulas except Ward & Ahrens, which requires a higher freeboard. Said differently, the freeboard must be equal to or greater than 80 percent of the wave height. For the 2 meter wave height conditions, a relative freeboard of 1.2 is required to limit wave overtopping below the tolerable rate.

It is apparent from this analysis that the required relative freeboard for a vertical wall is not very sensitive to the wave overtopping formula, especially in the 1 meter waves, with the exception of Ward & Ahrens. Ward & Ahrens based their formula on physical lab experiments with impulsive wave conditions with wave heights generally greater than 2m and wave periods between 8 and 12 seconds. Therefore, the Ward & Ahrens formula is better suited for larger wave conditions not found within the NCBB study area. It can be seen from Figure 7-8 that Ward & Ahrens produce similar results to the impulsive EurOtop formulas for the 2 meter wave conditions within the 50/liter/s/m to 2/liters/s/m overtopping range.

Wave overtopping for the rubble slope (solid blue line) is very similar to vertical walls and it is expected that the required relative freeboard will be similar between the vertical wall and rubble slope.
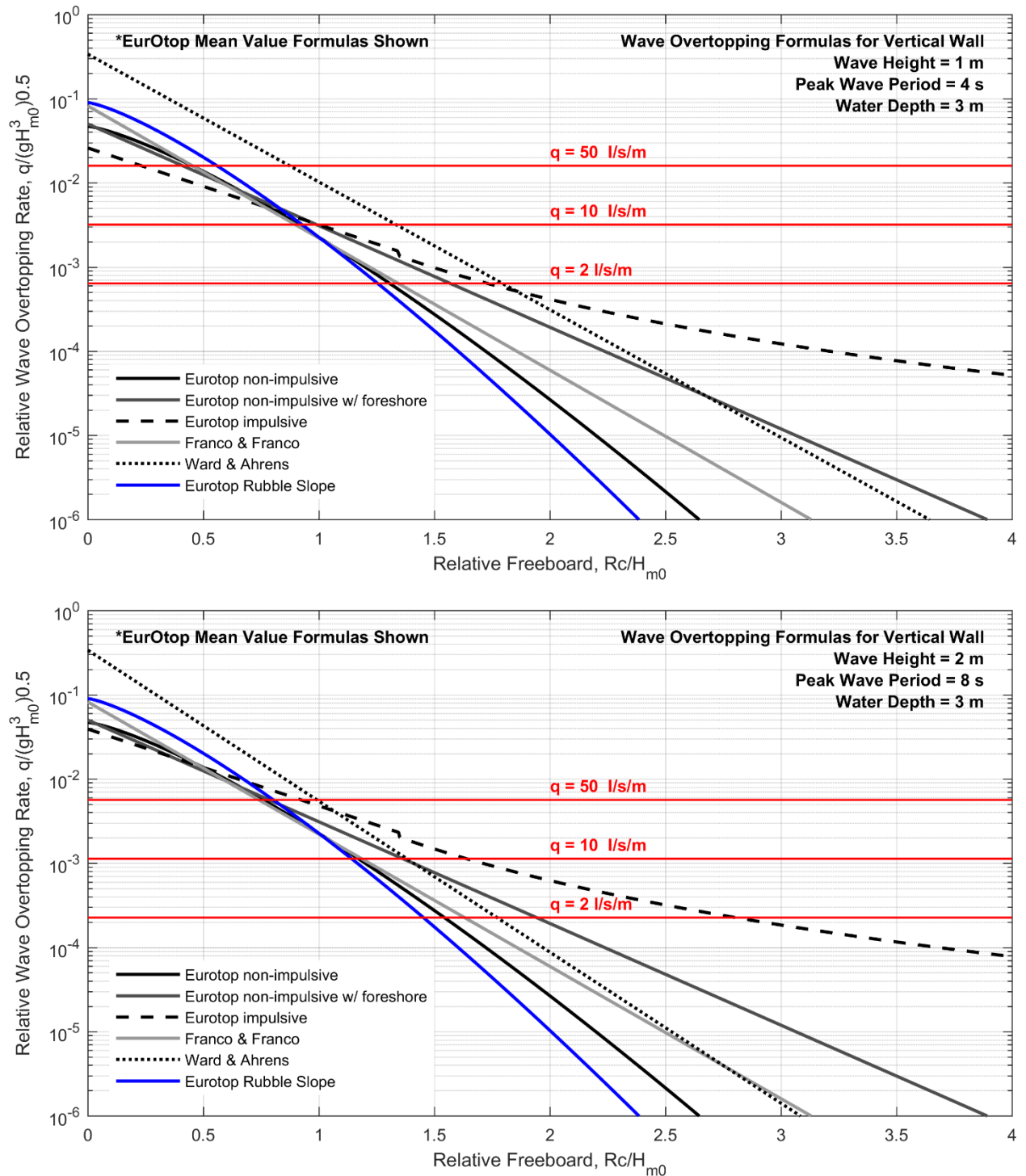

Figure 7-8:   Wave Overtopping Formulas for Vertical Wall

7.5 Overtopping Results

7.5.1 Vertical Wall

The results from the wave overtopping analysis at the 6 representative locations are presented in Table 7-5. The required relative freeboard, R_c/H_{m0}, and freeboard height, R_c, to keep wave overtopping below the tolerable threshold, 10 liters/s/m, are given. The results in Table 7-5 are based on the EurOtop equation for non-impulsive conditions with an influencing foreshore. The more conservative "design approach" formula was applied. The required freeboard height varies between 4.0 and 6.9 feet.

Table 7-5:   Wave Overtopping Results at Vertical Wall, Relative Freeboard (1% AEP)

Station	ID	SWEL (ft, NAVD88)	H_{m0}-Joint (ft)	Tp-Joint (s)	R_c/H_{m0} (-)	Rc (ft)
Bay Park	12084	10.4	3.6	3.7	1.2	4.2
Island Park	14260	10.2	3.9	4.5	1.2	4.9
Long Beach	14230	10.1	3.5	5.2	1.2	4.0
Lido Beach	12080	10.0	4.0	3.9	1.3	5.1
Oceanside	14276	10.0	5.0	3.9	1.4	6.9
Freeport	12129	9.6	4.1	4.6	1.3	5.3

Table 7-6:   Wave Overtopping Results at Vertical Wall, Relative Freeboard (5% AEP)

Station	ID	SWEL (ft, NAVD88)	H_{m0}-Joint (ft)	Tp-Joint (s)	R_c/H_{m0} (-)	Rc (ft)
Bay Park	12084	7.9	2.6	3.4	1.0	2.6
Island Park	14260	7.8	2.8	3.8	1.1	3.0
Long Beach	14230	7.7	2.5	4.3	1.0	2.5
Lido Beach	12080	7.7	3.0	3.5	1.1	3.2
Oceanside	14276	7.7	3.7	3.7	1.2	4.4
Freeport	12129	7.2	2.9	3.9	1.1	3.1

Table 7-7:   Wave Overtopping Results at Vertical Wall, Relative Freeboard (20% AEP)

Station	ID	SWEL (ft, NAVD88)	H_{m0}-Joint (ft)	Tp-Joint (s)	R_c/H_{m0} (-)	Rc (ft)
Bay Park	12084	5.6	2.0	3.1	0.9	1.7
Island Park	14260	5.5	2.1	3.5	0.9	1.9
Long Beach	14230	5.3	1.9	3.8	0.8	1.6
Lido Beach	12080	5.3	2.3	3.3	0.9	2.2
Oceanside	14276	5.3	2.8	3.6	1.0	2.9
Freeport	12129	5.1	2.3	3.6	0.9	2.2

The sensitivity of the relative freeboard height to EurOtop "mean value" and "design approach", as well as the Franco & Franco equation, are presented in Table 7-8. Differences between the three equations are relatively small and the EurOtop "design approach" generally requires the greatest relative freeboard. Results for Ward & Ahrens are not presented here because the wave conditions in the NCBB are smaller than the range of values used in their laboratory experiment. The EurOtop impulsive wave conditions

actually produces smaller required freeboard elevations for these wave conditions and is not presented here. It is more likely that the wave conditions will be non-impulsive during the design conditions considering the small wave periods, small wave heights, and water depths during the 1% AEP.

Table 7-8:   Relative Freeboard Sensitivity, Vertical Wall (1% AEP)

Station	ID	EurOtop w/ Foreshore Mean Value Approach	EurOtop w/ Foreshore Design Approach	Franco & Franco
Bay Park	12084	1.04	1.19	0.94
Island Park	14260	1.09	1.25	0.97
Long Beach	14230	1.02	1.17	0.92
Lido Beach	12080	1.10	1.26	0.99
Oceanside	14276	1.22	1.38	1.08
Freeport	12129	1.12	1.28	1.00

7.5.2   Rubble Slope

The results from the wave overtopping analysis at the 6 representative locations are presented in Table 7-9. The required relative freeboard, R_c/H_{m0}, and freeboard height, R_c, to keep wave overtopping below the tolerable threshold, 10 liters/s/m, are given. The results in Table 7-9 are based on the EurOtop equation for rubble slopes using the more conservative "design approach" formula. The required freeboard height varies between 3.7 and 6.0 feet.

Table 7-9:   Wave Overtopping Results at Rubble Slope, Relative Freeboard (1% AEP)

Station	ID	SWEL (ft, NAVD88)	H_{m0}-Joint (ft)	Tp-Joint (s)	R_c/H_{m0} (-)	Rc (ft)
Bay Park	12084	10.4	3.6	3.7	1.1	3.9
Island Park	14260	10.2	3.9	4.5	1.1	4.5
Long Beach	14230	10.1	3.5	5.2	1.1	3.7
Lido Beach	12080	10.0	4.0	3.9	1.1	4.6
Oceanside	14276	10.0	5.0	3.9	1.2	6.0
Freeport	12129	9.6	4.1	4.6	1.1	4.8

Table 7-10:   Wave Overtopping Results at Rubble Slope, Relative Freeboard (5% AEP)

Station	ID	SWEL (ft, NAVD88)	H_{m0}-Joint (ft)	Tp-Joint (s)	R_c/H_{m0} (-)	Rc (ft)
Bay Park	12084	7.9	2.6	3.4	1.0	2.6
Island Park	14260	7.8	2.8	3.8	1.0	2.9
Long Beach	14230	7.7	2.5	4.3	1.0	2.5
Lido Beach	12080	7.7	3.0	3.5	1.0	3.1
Oceanside	14276	7.7	3.7	3.7	1.1	4.0
Freeport	12129	7.2	2.9	3.9	1.0	3.0

Table 7-11:   Wave Overtopping Results at Rubble Slope, Relative Freeboard (20% AEP)

Station	ID	SWEL (ft, NAVD88)	H_{m0}-Joint (ft)	Tp-Joint (s)	R_C/H_{m0} (-)	Rc (ft)
Bay Park	12084	5.6	2.0	3.1	0.9	1.8
Island Park	14260	5.5	2.1	3.5	0.9	2.0
Long Beach	14230	5.3	1.9	3.8	0.9	1.7
Lido Beach	12080	5.3	2.3	3.3	0.9	2.2
Oceanside	14276	5.3	2.8	3.6	1.0	2.8
Freeport	12129	5.1	2.3	3.6	0.9	2.2

8 TOTAL WATER LEVEL AND CREST ELEVATIONS

8.1 Total Water Level Components

The total water level component analysis identifies all the contributions to the water surface elevation applied in the design structural crest elevations. The significant water level components for the NCBB study area are shown below:

- **Mean Sea Level**

  – Mean Sea Level (MSL) is a tidal datum, is mean or average sea level computed over a 19-year period, known as the National Tidal Datum Epoch (NTDE). The present 19-year reference period used by NOAA is the 1983-2001 NTDE.

  – Relative Sea Level Change (RSLC) is a combination of both global and local SLC including local vertical land motion (subsidence or uplift).

- **Astronomical Tide** is the semi-diurnal (twice daily) periodic rise and fall of a body of water resulting from gravitational interactions between Sun, Moon, and Earth.

- **Non-Tidal Residuals**

  – Seasonal variations in sea level from <u>regular</u> fluctuations in coastal temperatures, salinities, winds, atmospheric pressures, and ocean currents.

  – Interannual variations in sea level from <u>irregular</u> fluctuations in coastal temperatures, salinities, winds, atmospheric pressures, and ocean currents (El Niño).

  – Storm Surge is the increased water level due to storm winds over the ocean and the resultant wind stress on the ocean surface.

- **Wave-induced Components**

  – Wave Setup is the increase in water level from wave breaking in the nearshore.

  – Freeboard is additional height of a structure (i.e. levee, floodwall) above the still water level required to limit wave overtopping below a tolerable discharge. On sloped structures such as levees the freeboard height is related to wave runup.

8.2 Design Crest Elevations

Preliminary crest elevations for structural measures (Floodwalls, Levees, Storm Surge Barriers) are based on the 1% AEP with 50% assurance provided in the NCBB Baseline and NACCS hazard curves. Additional, alternatives were developed based on the 5% AEP and 20% AEP, both with a 50% assurance. It is emphasized that there is no policy requirement that USACE projects be designed to the 1% AEP water level or any minimum performance standard. In subsequent phases of the NCBB Feasibility Study the performance of the measures will be optimized to maximize NED benefits, which could result in higher or lower performance.

The relative contribution of each respective total water level component towards the perimeter plan design crest elevation at three representative locations is provided in Table 8-1, Table 8-2, and Table 8-3 for the 1% AEP, 5% AEP, and 20% AEP respectively. The NCBB CSTORM-MS and NACCS water level hazard

curves include several of the total water level components: MSL, astronomical tide, storm surge, and wave setup. The water level hazard curves represent the joint probability of all the components combined and the exact relative contribution of each component is not well defined. However, the relative contribution of each component is estimated here based on the well-known tidal amplitudes (MHW) and approximate estimates of wave setup based on the wave heights.

RSLC is included by adding 1.8 feet, based on the USACE Intermediate SLC scenario. The required freeboard for each structure was determined based on wave overtopping calculations and tolerable overtopping rate. Seasonal variations in sea level are included based on average seasonal fluctuation during peak hurricane season (August, September, October) observed NOAA tidal gage at Sandy Hook. Inter-annual variations in sea level are not included in the TWL estimate or design crest elevations at this time and rarely exceed 0.5 feet.

Design and cost estimates of the perimeter plan floodwalls and levees are based on a crest elevation of 16 feet NAVD88, 13 feet NAVD88, and 9 feet NAVD88 for the 1% AEP, 5% AEP, and 20% AEP. Due to the spatial variability in water levels, wave conditions, and wave overtopping the required crest elevation of the perimeter plan features could be higher or lower than the preliminary crest elevations.

Table 8-1:   Perimeter Plan Crest Elevations and Total Water Level Components (1% AEP)

Component	Long Beach (feet)		Lido Beach (feet)		Freeport (feet)	
MSL (feet, NAVD88)	-0.3		-0.4		-.3	
Astronomical Tide	1.8[1]	10.1[2]	1.8[1]	10.0[2]	1.6[1]	9.6[2]
Storm Surge	8.4		8.4		8.1	
Wave Setup	0.2		0.2		0.2	
RSLC	1.8		1.8		1.8	
Seasonal Variations	0.2		0.2		0.2	
Freeboard	4.0[3]		5.1[3]		5.3[3]	
Total Water Level (feet, NAVD88)	**16.1**		**17.1**		**16.9**	

Notes: [1]MHW shown; [2]Value from NACCS hazard curve in feet, NAVD88; [3]Freeboard based on wave overtopping of vertical wall.

Table 8-2:   Perimeter Plan Crest Elevations and Total Water Level Components (5% AEP)

Component	Long Beach (feet)		Lido Beach (feet)		Freeport (feet)	
MSL (feet, NAVD88)	-0.3		-0.4		-.3	
Astronomical Tide	1.8[1]	7.7[2]	1.8[1]	7.7[2]	1.6[1]	7.2[2]
Storm Surge	6.0		5.9		5.7	
Wave Setup	0.2		0.2		0.2	
RSLC	1.8		1.8		1.8	
Seasonal Variations	0.2		0.2		0.2	
Freeboard	2.5[3]		3.2[3]		3.1[3]	
Total Water Level (feet, NAVD88)	**12.3**		**12.9**		**12.3**	

Notes: [1]MHW shown; [2]Value from NACCS hazard curve in feet, NAVD88; [3]Freeboard based on wave overtopping of vertical wall.

Table 8-3: Perimeter Plan Crest Elevations and Total Water Level Components (20% AEP)

Component	Long Beach (feet)		Lido Beach (feet)		Freeport (feet)	
MSL (feet, NAVD88)	-0.3		-0.4		-.3	
Astronomical Tide	1.8[1]	5.3[2]	1.8[1]	5.3[2]	1.6[1]	5.1[2]
Storm Surge	3.6		3.7		3.6	
Wave Setup	0.2		0.2		0.2	
RSLC	1.8		1.8		1.8	
Seasonal Variations	0.2		0.2		0.2	
Freeboard	1.6[3]		2.2[3]		2.2[3]	
Total Water Level (feet, NAVD88)	**9.0**		**9.5**		**9.3**	

Notes: [1]MHW shown; [2]Value from NACCS hazard curve in feet, NAVD88; [3]Freeboard based on wave overtopping of vertical wall.

9   PERFORMANCE

ER 1105-2-101 requires risk assessment for CSRM studies. At this stage of the NCBB CSRM Study the risk assessment provides additional information about the relative project performance, structural performance and reliability, and life safety that is not provided by the NED economic results. In addition, the impact of sea level change on the system performance is helpful to consider the strengths, weaknesses, and adaptability of different alternatives. The focus here is on nonstructural (elevating structures) and perimeter plans (floodwalls), storm surge barriers are not included. Definitions for a few commonly used terms in this section are provided below:

Annual Exceedance Probability (AEP) - The probability that a certain threshold may be exceeded at a location in any given year, considering the full range of possible values, and if appropriate, incorporation of project performance. The AEP is expressed as a percentage. An event having a one in 100 chance of occurring in any single year would be described as the one percent AEP event.

Assurance - The probability that a target stage will not be exceeded during the occurrence of a flood of specified exceedance probability considering the full range of uncertainties. Term selected to replace "conditional non-exceedance probability" (CNP).

Long-Term Exceedance Probability (LTEP) - The probability of capacity exceedance during a specified period. For example, 30-year exceedance probability refers to the probability of one or more exceedances of the capacity of a measure during a 30-year period; formerly long-term risk. This accounts for the repeated annual exposure to flood risk over time.

9.1   Structural Performance and Reliability

There are significant differences in the reliability and consequences of failure between nonstructural and perimeter plans. Perimeter plans in the NCBB study area are far from trivial in extent and complexity. Every road closure, rail closure, miter gate, and structure transition are failure points that require active intervention in advance of storm events. In addition, perimeter plans are exposed to waves, wave overtopping, and possible failure over several miles along the system. Storage capacity of perimeter plans is limited, and flood damages occur rapidly after wave overtopping begins. Failure of a floodwall, transition, or closure/gate will quickly overwhelm any storage capacity resulting in high velocities, rapid increases in flood elevations, conditions that may increase the risk of life loss.

Nonstructural plans generally provide exceptional reliability, require little active intervention, and independent failure points. Failure of a single structure will not lead to failure of the entire system. In addition, people located inside elevated structures will be able to evacuate vertically inside the structure or to the roof to greater elevations, potentially reducing life loss.

9.2   Project "System" Performance

Project performance is evaluated for four plans:

- Nonstructural plans with structures elevated to the 1% AEP

- 1% AEP Perimeter Plan

- 5% AEP Perimeter Plan

- 20% AEP Perimeter Plan

At this stage of the study both the nonstructural and perimeter plans have been designed for 1.8 feet of RSLC based on the USACE-Intermediate SLC scenario. Project Performance is evaluated by determining the AEP, LTEP, and assurance associated with the water level exceeding the design first floor elevation (Nonstructural) or floodwall crest elevation. It is assumed that when these water elevations are reached the elevated structures will begin to experience significant damages and in the case of the perimeter plan wave overtopping or wall failure will lead to significant damages.

Project performance (AEP, LTEP, and assurance) in the year 2080 assuming RSLC has followed the USACE-Intermediate SLC scenario (1.8 feet) is presented in Table 9-1. Since both the nonstructural plan and 1% AEP perimeter plan are designed to the 1% AEP in 2080, the AEP is equal to 1%, and the LTEP and assurances are the same.

The project performance of the four plans over a 100 year planning period is provided in Table 9-2. The table captures the impact RSLC has on project performance. The left side of Table 9-2 shows the AEP in 2030, 2055, 2080, 2105, and 2130. The right side of the table shows the LTEP over four 25-year periods. In the USACE-Intermediate SLC scenario the AEP for the 1% AEP Perimeter Plan increases from 0.41% at the start of the project (2030) to 1% in 2080 and then 3% in 2130. Another way to look at the project performance, is that the LTEP (probability of a single event exceeding the design water level) increases from 12% to 18% in the first 25-years of the project (2030-2055) to the second 25-years of the project (2055-2080). In the last 50-years of the project the LTEP increases from 28% (2080-2105) and 43% (2105-2030).

Table 9-1:   Project Performance: AEP, LTEP, Assurance at Year 2080 (USACE Int. SLC)

Plan	AEP		LTEP			Assurance by Event				
	Expected	90% Assurance	10-yr Period	30-yr Period	50-yr Period	10%	2%	1%	0.4%	0.2%
Nonstructural	1.00%	2.79%	9.6%	26.0%	39.5%	99.9%	79.6%	50.0%	21.1%	10.3%
Perimeter Plan, 1% AEP	1.00%	2.79%	9.6%	26.0%	39.5%	99.9%	79.6%	50.0%	21.1%	10.3%
Perimeter Plan, 5% AEP	5.00%	13.79%	40.1%	78.5%	92.3%	81.2%	14.3%	4.4%	1.0%	0.4%
Perimeter Plan, 20% AEP	20.00%	60.88%	89.3%	99.9%	100.0%	23.2%	1.0%	0.2%	0.0%	0.0%

Table 9-2:   Project Performance: AEP, LTEP sensitivity to SLC

Plan	Annual Exceedance Probability, Expected					Long-Term Exceedance Probability			
	2030	2055	2080	2105	2130	2030-2055	2055-2080	2080-2105	2105-2130
USACE Low SLC Scenario									
Nonstructural	0.37%	0.48%	0.61%	0.77%	0.96%	10.0%	12.7%	15.7%	19.3%
Perimeter Plan, 1% AEP	0.37%	0.48%	0.61%	0.77%	0.96%	10.0%	12.7%	15.7%	19.3%
Perimeter Plan, 5% AEP	1.99%	2.49%	3.10%	3.87%	4.83%	42.9%	50.4%	58.4%	66.7%
Perimeter Plan, 20% AEP	5.97%	7.75%	10.09%	13.86%	19.03%	82.7%	90.0%	95.6%	98.8%
USACE Int SLC Scenario									
Nonstructural	0.41%	0.62%	1.00%	1.67%	3.05%	11.9%	17.8%	27.6%	43.4%
Perimeter Plan, 1% AEP	0.41%	0.62%	1.00%	1.67%	3.05%	11.9%	17.8%	27.6%	43.4%
Perimeter Plan, 5% AEP	2.18%	3.17%	5.00%	9.32%	22.36%	48.3%	63.5%	82.8%	97.9%
Perimeter Plan, 20% AEP	6.64%	10.40%	20.00%	49.20%	100.00%	88.2%	97.9%	100.0%	100.0%
USACE High SLC Scenario									
Nonstructural	0.56%	1.36%	4.44%	34.57%	100.00%	19.7%	46.5%	96.7%	100.0%
Perimeter Plan, 1% AEP	0.56%	1.36%	4.44%	34.57%	100.00%	19.7%	46.5%	96.7%	100.0%
Perimeter Plan, 5% AEP	2.87%	7.29%	42.39%	100.00%	100.00%	67.9%	99.3%	100.0%	100.0%
Perimeter Plan, 20% AEP	9.21%	34.49%	100.00%	100.00%	100.00%	99.2%	100.0%	100.0%	100.0%

10 INTERIOR DRAINAGE

Any perimeter plan with-project (WP) conditions implemented in the study area would require upgrades to existing stormwater infrastructure. Any upgrades to the existing stormwater infrastructure would ensure that the proposed perimeter plan doesn't increase flooding during heavy rainfall events where the perimeter plan might block overland runoff, forcing all the stormwater to be funneled into the stormwater infrastructure. Given the large study area, and initial phase of screening, detailed assessment for each reach (e.g. determination of runoff, storage, pipe sizing, minimum facilities, pump sizing, etc.) was infeasible. As such, a conservative assumption was made that all necessary stormwater management upgrades would be in the form of pump stations. Following Cycle 1 screening of the perimeter plan, a desktop assessment was performed to estimate the number of pump stations required in each reach of the proposed perimeter plans.

The first step was to determine contributory drainage area to each segment of the WP perimeter plan alternatives. ArcGIS was utilized for this delineation of contributory drainage areas, by which each major tributary was identified via the National Hydrography Dataset (NHD) coverage, and sub-delineated as necessary to isolate all streamlines crossing each WP segment. Sub-delineations were backchecked using National Elevation Dataset (NED) elevation data, and Google Earth. Table 10-1 lists estimated drainage area to each segment/streamline crossing location, and Figure 10-1 depicts drainage area delineations in plan view. Perimeter plan segments fell into two categories, with the majority having less than 5 sq mi drainage areas, and two having greater than 30 sq. mi. drainage areas.

Table 10-1:   NCBB Drainage Areas

Plan	DA Name	DA (Acres)	DA (SQ MI)
East Rockaway	Parsonage Creek	3,196	4.99
East Rockaway	Mill River	22,180	34.66
East Rockaway	Un. Western Drainage	451	0.70
East Rockaway	Un. Middle Drainage	564	0.88
East Rockaway	Bedell Creek	1,410	2.20
Freeport	Freeport Creek	20,547	32.10
Freeport	Un. Eastern Drainage	318	0.50
Freeport	Un. Western Drainage	1,141	1.78
Freeport	Milburn Creek	3,127	4.89
Island Park	Island Park (All)	744	1.16
Long Beach	Long Beach (All)	1,632	2.55

A two-tiered approach was taken based on contributory drainage areas. Those segments of the perimeter plan with smaller drainage areas (9 of 11), consistent with previous NAN projects that analyzed interior drainage were assessed using an analogue approach, using similar assumptions. Segments with much larger drainage areas (2 of 11) were analyzed with an alternate method, to more realistically account for peak flows and required pumping on a larger scale. It is anticipated that both methods will be refined in subsequent phases of screening, as the study incorporates additional information.
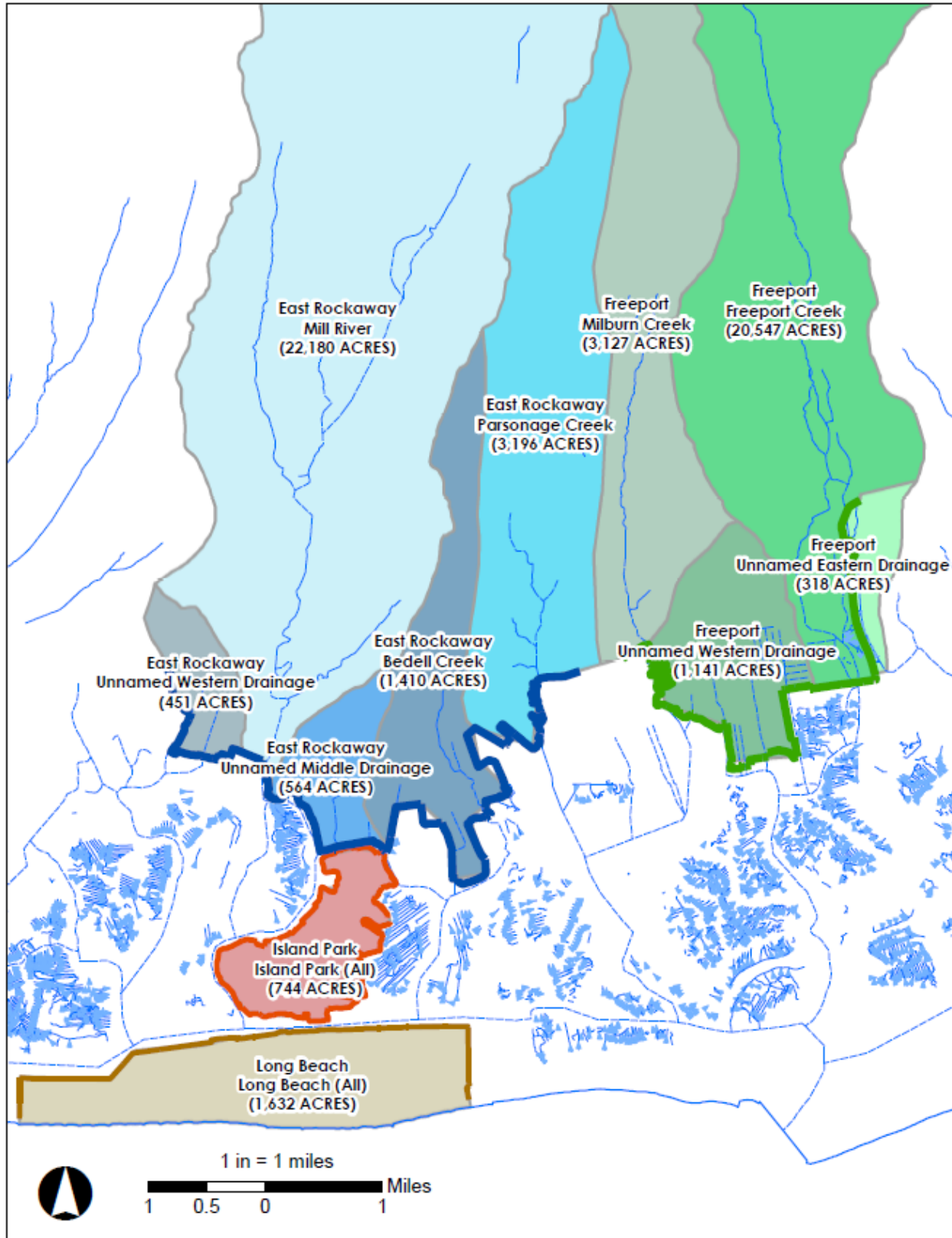
Figure 10-1: NCBB Drainage Areas

Smaller Drainage Areas

Smaller drainage areas (less than 5 sq mi contributory area) within the study limits were assessed using an analogue approach using data from a previous NAN interior drainage study (USACE, 2018). The previous NAN study provided estimates of both 1% Annual Exceedance Probability (AEP) peak flows, and estimates for pumping requirements recommended as part of the TSP. For this study, NAN pump sizes were compiled and normalized to the fraction of the 1% AEP peak flow required for capacity, to allow direct application to NCBB interior drainage areas. Specific peak flows for the previous NAN study were reported between 516 to 920 cfs/sq mi, with required pump sizes ranging from 56 to 200 cfs, with an average of 108 cfs. Normalized, this produces an average pumping requirement of 0.27 of the 1% AEP peak flow (Table 10-2). Both specific discharge estimates (cfs/sq mi), and the average pumping requirement fraction (0.27) were then applied to all smaller drainage areas, i.e. 177 cfs/sq mi.

Table 10-2: Summary of Previous NAN Study Interior Drainage Calculations

Drainage Subbasin	DA (AC)	DA (SQ MI)	1% AEP Peak Flow	Pump Required Alt 1 (CFS)	Pump Required Alt 2 (CFS)	Average CFS/SQMI	Average Pump Size Fraction of 1% AEP
Hammels H1	104.5	0.16328125	400	100		612	0.25
Hammels H2	139	0.2171875	642	160	180	829	0.28
Arverne A1	72.5	0.11328125	248	70		618	0.28
Arverne A2	139.5	0.21796875	474	120	180	826	0.38
Arverne A3	208.6	0.3259375	789	200	300	920	0.38
Edgemere E1	191.7	0.29953125	582	140	210	701	0.36
Edgemere E2	273.9	0.42796875	782	180	120	280	0.15
Canarsie C1	119.7	0.18703125	455	70	150	802	0.15
Canarsie C2	69.3	0.10828125	245	56		517	0.23
Canarsie C3	84.1	0.13140625	323	84		639	0.26
Cedarhurst-Lawrence L1	93.3	0.14578125	343	90		617	0.26
Motts Basin North M1	28.1	0.04390625	122	26		592	0.21
			AVERAGE	108	AVERAGE	663	0.27
						AVERAGE	177.04

Larger Drainage Areas

As there are no USGS stream gages within the study area, effort was given to determine flood-frequency relationships for proximate USGS gages. Gages utilized for this assessment were determined to be generally hydrologically similar to the study area. Annual maximum peak flow data for each gage were analyzed in HEC-SSP to determine approximate flood-frequency relationships for each USGS gage. Table 10-3 lists USGS gages utilized in this analysis, and Table 10-4 summarizes flood frequency results at each gage.

For this initial analysis, the 1% AEP peak flows were utilized for comparison and further calculations. To apply these flood-frequency estimates to the largest two ungaged drainage areas, peak flows were normalized by drainage area to estimate an average peak cfs/sq. mi, as shown in Table 10-5. Given the perceived lack of storage available in these densely populated areas, it was conservatively assumed that pump stations in the largest drainage areas would require capacity to pump the full 1% AEP peak.

Table 10-3:   Proximate USGS Gages utilized for Flood Frequency Analysis

USGS Site Number	USGS Site Name	DA (SQ MI)
1309500	MASSAPEQUA CREEK AT MASSAPEQUA NY	38.6
1310000	BELLMORE CREEK AT BELLMORE NY	14.2
1310500	EAST MEADOW BROOK AT FREEPORT NY	28.7
1311000	PINES BROOK AT MALVERNE NY	10.1
1311500	VALLEY STREAM AT VALLEY STREAM NY	3.77

Table 10-4:   Flood Frequency Estimates for Proximate USGS Gages

HEC-SSP Bulletin 17C Flood Frequency Estimates					
Annual Exceedance Probability (AEP) (%)	MASSAPEQUA CREEK AT MASSAPEQUA NY	BELLMORE CREEK AT BELLMORE NY	EAST MEADOW BROOK AT FREEPORT NY	PINES BROOK AT MALVERNE NY	VALLEY STREAM AT VALLEY STREAM NY
0.2	745.5	368	1526.4	1356.4	424.8
0.5	640.2	305.9	1344.3	1132.9	384.1
1	562.1	262.3	1203.5	970.1	352.8
2	485.4	221.4	1060.1	813.3	320.8
5	386.1	171.1	865.6	615.8	277.1
10	312.1	135.7	713.9	474.1	242.3
20	238.4	102.1	556.2	339.3	204.8
50	137.2	58.5	327.5	168.9	146.2
80	75.1	33	179.5	77.7	102.1
90	53.7	24.3	127.3	50.2	83.9
95	40.2	18.8	94.4	34.4	71
99	22.8	11.6	51.8	16.2	51.4

Table 10-5:   Flood Frequency Estimates – Normalized by Drainage Area

USGS Site Number	USGS Site Name	DA (SQ MI)	1% AEP (CFS)	1% AEP (CFS/SQMI)
1309500	MASSAPEQUA CREEK AT MASSAPEQUA NY	38.6	562.1	14.56
1310000	BELLMORE CREEK AT BELLMORE NY	14.2	262.3	18.47
1310500	EAST MEADOW BROOK AT FREEPORT NY	28.7	1203.5	41.93
1311000	PINES BROOK AT MALVERNE NY	10.1	970.1	96.05
1311500	VALLEY STREAM AT VALLEY STREAM NY	3.77	352.8	93.58
			AVERAGE	53

Results

This two-tiered approach to estimating potential interior drainage requirements was deemed appropriately detailed for the current screening level of design, however it is anticipated that both methods will be refined in subsequent phases of screening, as the study incorporates additional information. Average normalized 1% AEP peak flow of 177 cfs/sq mi from the previous NAN study data was used for smaller drainage areas, where for the larger two drainage areas, average normalized 1% AEP peak flow of 53 cfs/sq mi determined from the flood frequency analysis was used. For these initial pumping estimates, pump stations were assumed to have 100 cfs capacity, consistent with previous NAN and NAP studies of similar nature and scope. For consistency, larger drainage areas also use this 100 cfs capacity assumption. It is possible that larger pump sizing could be more efficient than several smaller pumps, however this was deemed appropriately conservative at this level of design. Pumping requirements estimated in number of 100 cfs pump stations required is supplied in Table 10-6.

Table 10-6:   Interior Drainage Analysis – Pump Stations Required

LOP Name	DA Name	DA (Acres)	DA (SQ MI)	Pumping Required (CFS)	Pumping Required (CFS) FFA	Number of 100 CFS pump stations
East Rockaway	Parsonage Creek	3,196	4.99	884		9
East Rockaway	Mill River	22,180	34.66		1834	19
East Rockaway	Unnamed Western Drainage	451	0.70	125		2
East Rockaway	Unnamed Middle Drainage	564	0.88	156		2
East Rockaway	Bedell Creek	1,410	2.20	390		4
Freeport	Freeport Creek	20,547	32.10		1699	17
Freeport	Unnamed Eastern Drainage	318	0.50	88		1
Freeport	Unnamed Western Drainage	1,141	1.78	316		4
Freeport	Milburn Creek	3,127	4.89	865		9
Island Park	Island Park (All)	744	1.16	206		3
Long Beach	Long Beach (All)	1,632	2.55	451		5
Constants						
NAN CFS/SQMI	177	(using 0.27 fraction of 1% AEP peak flow)				
FFA CFS/SQMI	53	(using full 1% AEP peak flow)				

11 LONG BEACH CSRR PROJECT

The U.S. Army Corps of Engineers, New York District, completed construction of the Long Beach Coastal Storm Risk Reduction (CSRR) Project in April of 2019. The $130 million project was performed in two phases over a three year period that included construction of 4 new groins and the rehabilitation of 18 existing groins, installing 284,000 tons of rock. The Corps also used 3.2 million cubic yards of sand to widen the beach and reinforce sand dunes, which play a crucial role in flood risk reduction. The Long Beach CSRR Project was constructed in response to extensive storm damages resulting from Hurricane Sandy and an increased vulnerability to future events, and made possible by the Disaster Relief Appropriations Act of 2013 (Public Law [P.L.] 113-2) passed by Congress.

The constructed plan, Figure 11-1, consists of constructing a berm from Point Lookout west to the western boundary of the City of Long Beach where the plan tapers into the existing shoreline in East Atlantic Beach (approximately 35,000 lf). Fronting the dune, a berm width of 110 ft at elevation +9 ft NAVD88 with a shore slope of 1V: 30H over the City of Long Beach The dune has a crest elevation of +14 ft NAVD88 for a crest width of 25 ft with a 1V:5H side slopes on the landward and seaward sides of the dune (1V:3H side slope on the landward side in front of the boardwalk in the City of Long Beach). The dune extends approximately 35,000 lf from Point Lookout to the western boundary of the City of Long Beach. Fifteen existing groins in the City of Long Beach and 2 existing groins in the Town of Hempstead (Point Lookout) will be rehabilitated. The terminal groin in the Town of Hempstead (Point Lookout) will also be rehabilitated and extended (100 ft). In addition, the project includes four new groins fronting the Town Park in the Town of Hempstead (construction of 2 additional groins deferred based on monitoring and determination of future needs) existing dune profile.

Figure 11-1:   Long Beach CSRR Design Profile

In regards to the NCBB CSRM study, the question is whether the proposed perimeter plan alternatives at the City of Long Beach would require modification of the existing Long Beach CSRR dune and beach, specifically whether the 14 ft NAVD88 dune crest elevation meets the performance criteria for a flood system around the City. For the NCBB 1% AEP perimeter plan at the City of Long Beach the dune and beach must also be able to withstand and limit wave overtopping during the 1% AEP storm. If the dune were to be overtopped and/or eroded, floodwaters would flow into the City of Long Beach and flood the community. The topography of the City of Long Beach is highest near the ocean and slopes gentle towards the bay shoreline. The proposed NCBB floodwalls would prevent ocean floodwaters from flowing into the bay. Instead the water would be trapped behind the floodwalls, accumulate, and flood the City. After the storm recedes, the stormwater infrastructure and pump stations would be able to collect and pump water

back into the bay, however it is not feasible to design these pump to be able to keep up with the rapid volume of water that could flood the City in the event of significant dune failure.

The Long Beach HSLRR did not include a detailed evaluation of the project performance and older analyses may not accurately reflect the storm climate since Hurricane Sandy would not have been included and is the storm of record for the study area. However, a detailed evaluation of the performance of several dune alternatives at Rockaway, NY which is located 5 miles west of Long Beach along the Atlantic Ocean with very similar storm climate, wave and water level conditions provides a reasonable initial estimate of the dune and seawall conditions required to meet a 1% AEP design. Appendix A1 of the East Rockaway to Rockaway Inlet and Jamaica Bay, NY HSGRR evaluated the performance of a three design beach profiles (Figure 11-2) with dune heights of +16 ft, +18 ft, and +20 ft NAVD88, as well as composite seawall (Figure 11-3). The three design beach profiles had an AEP of 2.3%, 1.4%, and 1% respectively (44 year, 70 year, and 100 year return periods). The composite seawall with a rubble mound structure backed by an impermeable vertical wall with a crest elevation of +17 ft NAVD88 had an AEP of 0.67% (150 year return period).
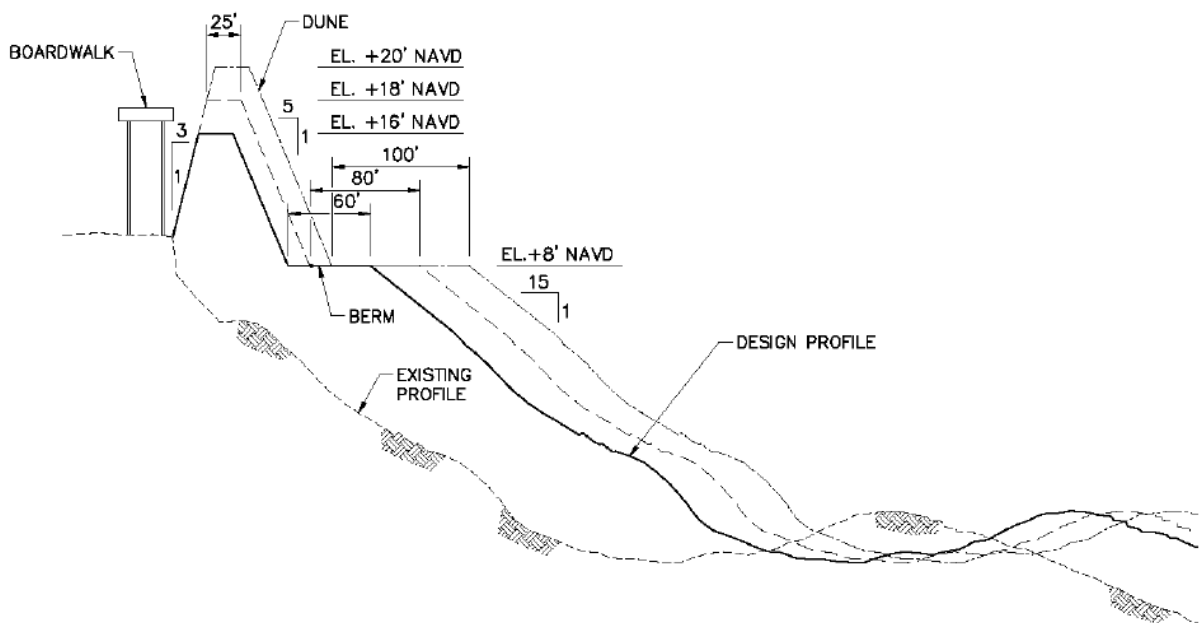
Figure 11-2:   Rockaway Design Beach and Dune Profiles
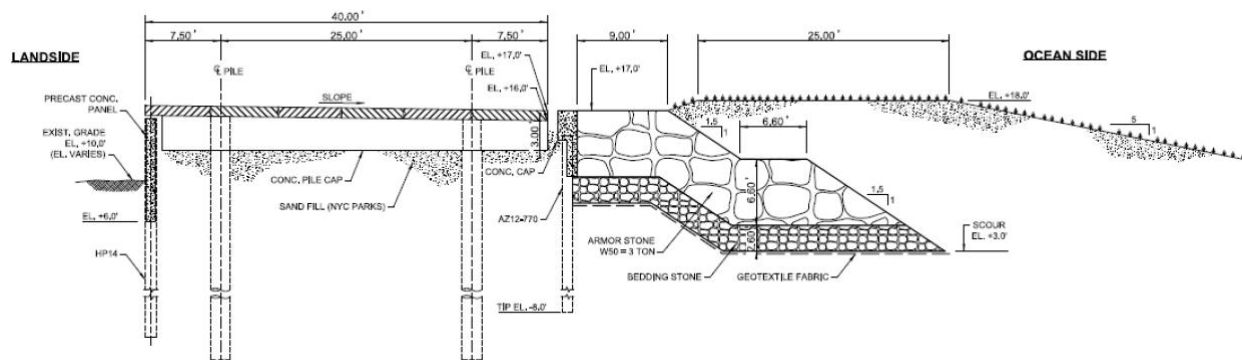
Figure 11-3:   *Rockaway Composite Seawall*

Based on the dune and seawall performance evaluation at Rockaway, NY it is expected that the existing Long Beach CSRR Project would not meet the requirements for the 1% AEP. A dune crest elevation of +20 ft NAVD88 or a smaller composite seawall structure with a crest elevation of approximately 16 ft NAVD88 would be required. While the existing dune height of +14 ft NAVD88 may meet the 5% and 20% AEP requirements, a more detailed risk assessment may show it is desirable from a life-safety and economic perspective to increase the height of the dunes to avoid a situation where the dune fails and floodwaters flow into and become trapped in the City of Long Beach.

Costs associated with modifications to the existing CSRR project in the City of Long Beach, such as higher dunes, would extend well beyond the additional sand required to construct the dune. Increasing the dune height would increase the footprint of the dune and push the design profile further seaward, increasing fill quantities and periodic nourishment quantities/frequency. In some erosion hot spots it may be difficult to maintain the expanded design profile between periodic nourishment operations. Modifying the dune height may also require obtaining new easements, since the existing easements are based on a specific dune crest elevation.

REFERENCES

Aretxabaleta, A. L., B. Butman, and N. K.Ganju. 2014 "Water level response in back-barrier bays unchanged following Hurricane Sandy", Geophys. Res. Lett., 41, 3163–3171, doi: 10.1002/2014GL059957.

Cialone, M. A., T. C. Massey, M. E. Anderson, A. S. Grzegorzewski, R. E. Jensen, A. Cialone, D. J. Mark, K. C. Pevey, B. L. Gunkel, T. O. McAlpin, N. C. Nadal-Caraballo, J. A. Melby, J. J. Ratcliff, 2015. North Atlantic Coast Comprehensive Study (NACCS) Coastal Storm Model Simulations: Waves and Water Levels. ERDC/CHL TR-15-14. Vicksburg, MS: U.S. Army Engineer Research and Development Center.ECB 2013-33

EM 1110-2-1100. *Coastal Engineering Manual*. Department of the Army, U.S. Army Corps of Engineers, Washington, DC 20314-1000.

EM 1110-2-6056. *Standsards and Procedures for Referencing Project Elevation Grades to Nationwide Vertical Datums*. December 31, 2010. Department of the Army, USACE, Washington DC.

ER 1110-2-8160. *Policies for Referencing Project Elevation Grades to Nationwide Vertical Datums*. March 1, 2009. Department of the Army, USACE, Washington DC.

ER 1100-2-8162. *Incorporating Sea Level Change in Civil Works Programs*. December 31, 2013. Department of the Army, USACE, Washington DC.

EurOtop, 2016. *Manual on wave overtopping of sea defences and related structures. An overtopping manual largely based on European research, but for worldwide application*. Van der Meer, J.W., Allsop, N.W.H., Bruce, T., De Rouck, J., Kortenhaus, A., Pullen, T., Schüttrumpf, H., Troch, P. and Zanuttigh, B., www.overtopping-manual.com.

FEMA (2009). "Flood Insurance Study, Nassau County, NY". Federal Emergency Management Agency, Flood Insurance Study Number 36059CV000A.

Franco, C. & Franco, L. 1999 *Overtopping formulae for caisson breakwaters with non-breaking 3-d waves*. Journal of Waterway, Port, Coastal & Ocean Engineering, Vol 125, No 2, pp 98-107, ASCE, New York.

Goda, Y. (2000). *Random Seas and Design of Maritime Structures*. World Scientific: New Jersey.

Maarten van Ormondt, Hapke, C., Roelvink, D., Nelson, T, 2015. "The Effects of Geomorphic Changes During Hurricane Sandy on Water Levels in Great South Bay"

Nadal-Caraballo, Norberto C. and Melby Jeffrey A. (2014). *North Atlantic Coast Comprehensive Study Phase I: Statistical Analysis of Historical Extreme Water Levels with Sea Level Change.* ERDC/CEHL TR-14-7, Coastal and Hydraulics Laboratory, U.S. Army Engineer and Development Center, 3090 Halls Ferry Road, Vicksburg, MS.

Nadal-Caraballo, N. C., J. A. Melby, V. M. Gonzalez, and A. T. Cox, 2015. *North Atlantic Coast Comprehensive Study (NACCS) Coastal Storm Hazards from Virginia to Maine*. ERDC/CHL TR-15-5. Vicksburg, MS: U.S. Army Engineer Research and Development Center.

Nadal-Caraballo N. C, Slusarcyzk G., Cialone M. A., and Hampson R. W., 2021. *DRAFT: Storm Surge Comparison for Proposed Nassau County Back Bays Inlet Closures*. ERDC/CHL TR-21-X. Vicksburg, MS: U.S. Army Engineer Research and Development Center.

NOAA VDATUM, https://vdatum.noaa.gov/about.html

NWS Flood Stages, https://water.weather.gov/ahps/region.php?state=nj

Sweet, W. V., Dusek, G., Obeysekera, J., Marra, J. J., 2018. Patterns and Projections of High Tide Flooding Along the U.S. Coastline Using a Common Impact Threshold. NOAA Technical Report NOS CO-OPS 086. Silver Spring, Maryland.

USACE (2016) "Fire Island Inlet to Montauk Point, New York, Draft General Reevaluation Report". U.S. Army Corps of Engineers, New York District.

USACE-NAO, 2017. *City of Norfolk Coastal Storm Risk Management Study, Hydraulics, Hydrology, & Coastal Sub-Appendix*. Norfolk Virginia, October 2017.

Ward., D. L., Ahrens, J. P., 1992. Overtopping Rates for Seawalls. Miscellaneous Paper CERC-92-3. Department of the Army. Waterways Experiment Stations, Corps of Engineers, 3909 Halls Ferry Road, Vicksburg, Mississippi 39180-6199.

Yang Z., Myers E. P., and Wong A. M, 2010. *VDATUM for Great South Bay, New York Bight, and New York Harbor: Tidal Datums and Sea Surface Topography*. NOAA Technical Memorandum NOS CS 15, Silver Spring, Maryland.

ERDC/CHL TR-21-XX

Coastal and Hydraulics Laboratory

**US Army Corps
of Engineers**®
Engineer Research and
Development Center

Storm Surge Comparison for Proposed Nassau County Back Bays Inlet Closures

Norberto C. Nadal-Caraballo, Gregory Slusarczyk, Mary A. Cialone, Robert W. Hampson, and Madison C. Yawn

August 2021

DRAFT

The U.S. Army Engineer Research and Development Center (ERDC) solves the nation's toughest engineering and environmental challenges. ERDC develops innovative solutions in civil and military engineering, geospatial sciences, water resources, and environmental sciences for the Army, the Department of Defense, civilian agencies, and our nation's public good. Find out more at www.erdc.usace.army.mil.

To search for other technical reports published by ERDC, visit the ERDC online library at http://acwc.sdp.sirsi.net/client/default.

Abstract

The U.S. Army Corps of Engineers (USACE) Philadelphia District (NAP) and the New York State Department of Environmental Conservation (NYSDEC) in partnership with Nassau County, NY are currently engaged in the Nassau County Back Bays (NCBB) Coastal Storm Risk Management CSRM (CSRM) Feasibility Study. The NCBB study area is one of nine focus areas identified in the North Atlantic Coast Comprehensive Study (NACCS) for additional analyses by the USACE to address coastal flood risk. The U.S. Army Engineer Research and Development Center, Coastal and Hydraulics Lab (ERDC-CHL) conducted a numerical hydrodynamic modeling and probabilistic hazard analysis study to evaluate the effectiveness of storm surge barriers in reducing water levels in the NCBBs. This effort included the simulation of water levels and a comparison of water surface elevations and corresponding annual exceedance frequency (AEF) between existing conditions and five final project alternatives. Results from the hydrodynamic simulations and probabilistic analysis are presented in this technical report.

Contents

Figures and Tables

Figures

Tables

Preface

The study summarized in this report was performed to address coastal flood risk within the Nassau County Back Bay. The study was funded by the U.S. Army Corps of Engineers (USACE) Headquarters through the USACE Philadelphia District (NAP). This study was conducted at the U.S. Army Engineer Research and Development Center (ERDC) Coastal and Hydraulics Laboratory (CHL), Vicksburg, MS, during the period of January 2018– September 2020.

This work was performed by the Harbors, Entrances, and Structures (HES) Branch of the Navigation Division at CHL, the Technical Director's Office at CHL, and the USACE NAP.

At the time of publication, Mr. Chad R. Bounds was Chief, HES Branch; Ms. Ashley E. Frey, Chief, Navigation Division. Dr. Ty V. Wamsley was Director, CHL, and Mr. Keith W. Flowers was Deputy Director, CHL.

The Commander of ERDC was COL Teresa A. Schlosser, and the Director was Dr. David W. Pittman.

Unit Conversion Factors

Most measurements and calculations for this study were done in SI units. The following table can be used to convert SI units to English customary units.

Multiply	By	To Obtain
m	3.28084	ft
km	0.621371	mi
km	0.539957	nmi
km/h	0.621371	mph
km/h	0.539957	kn
hPa	1.0	mb

Notation

Δp central pressure deficit of tropical cyclone, computed as the difference between a far-field atmospheric pressure of 1,013 hPa and central pressure (hPa)

θ heading direction of tropical cyclone (deg)

R_{max} radius of maximum winds of tropical cyclone (km)

V_t translational speed of tropical cyclone (km/h)

x_0 tropical cyclone reference location

AEF   annual exceedance frequency (yr^{-1})

CC   combined cyclone

CHS   Coastal Hazards System

CSRM   Coastal Storm Risk Management

CSTORM-MS   Coastal Storm Modeling System

DoE   Design of Experiments

ERDC   U.S. Army Engineer Research and Development Center

EVA   extreme value analysis

FSS   full storm suite

GPM   Gaussian process metamodeling

JPA   joint probability analysis

NACCS   North Atlantic Coast Comprehensive Study

NAP   U.S. Army Corps of Engineers Philadelphia District

NAN U.S. Army Corps of Engineers New York District

NCBB Nassau County Back Bay

NNBF Natural and Nature Based Features

NYSDEC New York State Department of Environmental Conservation

PCHA Probabilistic Coastal Hazard Analysis

RSS reduced storm suite

SLC sea level change (m)

SWL still water elevation

TC tropical cyclone

T_s peak period

XC extratropical cyclone

1 Background

The U.S. Army Corps of Engineers (USACE) Philadelphia District (NAP) and the non-federal sponsor, New York State Department of Environmental Conservation (NYSDEC) in partnership with Nassau County, NY, are currently engaged in the Nassau County Back Bay (NCBB) Coastal Storm Risk Management (CSRM) Feasibility Study. The NCBB study area is one of nine focus areas identified in the North Atlantic Coast Comprehensive Study (NACCS) (Nadal-Caraballo et al. 2015; Cialone et al. 2015) for additional analyses by the USACE to address coastal flood risk.

The NACCS was authorized under the Disaster Relief Appropriations Act, PL 113-2, in response to Hurricane Sandy. The Act provided the USACE up to $20 million to conduct a study with the goal to (1) reduce flood risk to vulnerable coastal populations, and (2) promote resilient coastal communities to ensure a sustainable and robust coastal landscape system, considering future sea level change (SLC) and climate change scenarios.

As part of the NACCS, the U.S. Army Engineer Research and Development Center (ERDC) completed a coastal storm wave and water level numerical modeling and probabilistic hazard analysis effort for the U.S. North Atlantic Coast. The NACCS provides nearshore wind, wave, and water level estimates and the associated marginal and joint probabilities critical for effective CSRM. This effort involved the application of the Coastal Hazards System (CHS) Probabilistic Coastal Hazard Analysis (PCHA) framework (Nadal-Caraballo et al. 2020) and corresponding storm suite consisting of 1050 synthetic tropical cyclones (TCs) and 100 historical extratropical cyclones (XCs). Hydrodynamic simulations of these storms were conducted using the suite of high-fidelity numerical models within the Coastal Storm Modeling System (CSTORM-MS). Documentation of the numerical modeling effort is provided in Cialone et al. 2015 and documentation of the probabilistic analysis is proved in Nadal Caraballo et al. 2015. Products of the study are available for viewing and download on the CHS website: https://chs.erdc.dren.mil/.

The NCBB study area is located on Long Island, NY, between Queens County to the west and Suffolk County to the east. Nassau County has a population of 1.3 million people, a land area of 287 square miles, and 166

square miles of water. Southern Nassau County is typified by dense, low elevation mixed-use development (residential and commercial), a highly developed shoreline, and many roads, rail roads, and critical facilities that serve Long Island and parts of New York City. Coastal flooding has caused significant economic, environmental, and community impacts in Nassau County. The study area is affected by flooding due to relatively more frequent high tides as well as less frequent but major coastal storms. Flood impacts can range from street closures to massive destruction from hurricane surge inundation, as occurred during Hurricane Sandy in 2012. The storm flooded homes, businesses, and critical infrastructure, rendered roads and Long Island Rail Road stations and infrastructure unusable, and caused school and business closures and gasoline shortages.

The objective of the NCBB CSRM Study is to investigate CSRM problems and solutions to reduce damages from coastal flooding that affects population, critical infrastructure, critical facilities, property, and ecosystems. CSRM measures under consideration include Non Structural, Structural, and Natural and Nature Based Features (NNBF). One Structural measure under consideration is inlet closures, constructed at one or more inlets in the study area. Due to the complex network of inlets and bays that control the flow of water between the ocean and back bays, NAP requested assistance from ERDC-CHL in evaluating the effectiveness of inlet closures in reducing water levels in the NCBB study area. To answer these questions, ERDC-CHL leveraged the existing NACCS CSTORM-MS.

1.1   Project Objectives

The objective of this numerical modeling study is to evaluate the effectiveness of inlet closures in reducing water levels in the NCBB study area. The Project Delivery Team (PDT) identified five closure alternatives with different combinations of inlet and bay closures and floodwalls to evaluate. The CSTORM-MS model simulations were performed for the five alternatives and baseline conditions using a subset of 25 tropical cyclones and three historical storms. Model results were used to develop frequency distributions of peak water levels that may be applied in economic analyses of flood damages and benefits.

To achieve the project objectives, the NACCS CSTORM-MS model was applied with modifications to ADCRIC mesh, ADCIRC bathymetry, and storm suite as presented herein.

2 Storm Selection

The NCBB CSRM feasibility study sought the evaluation of various with-project alternatives that include individual and multiple inlet closures, as discussed in Section 3 -- ADCIRC Mesh Details. The NCBB study made use of existing still water level (SWL) data, hydrodynamic modeling setup, and probabilistic analysis tools developed for the NACCS (Nadal-Caraballo et al. 2015; Cialone et al. 2015). Updating SWL hazard statistics for NCBB, both without- and with-project, the CHS PCHA framework for the North Atlantic region requires the simulation of both TC and XC induced SWL. The NACCS Full Storm Suite (FSS) consists of 1,050 synthetic TCs and 100 historical XCs. SWL hazard curves are initially developed for TCs and XCs independently, and are subsequently integrated to compute Combined Cyclone (CC) SWL hazard curves. The next section discusses the design of experiments (DoE) approach employed in the selection of the Reduced Storm Suite (RSS) applied in the numerical modeling for this study.

2.1 Selection of Reduced Storm Suite (RSS)

For the initial phase of the NCBB CSRM study, an RSS of 25 TCs was identified. The goal of the storm selection was to find the optimal combination of storms, given a predetermined number of events to be sampled out of the 1,050-TC FSS, to obtain a reasonable estimation of the SWL hazard. The number of storms sampled for each RSS was limited by budget and/or schedule constraints and informed by previous studies where DoE had been applied (*e.g.*, Melby et al. 2020). The storm selection process was performed using the DoE approach documented in Taflanidis et al. (2017), and Zhang et al. (2018). The DoE compares the RSS SWL hazard curves to benchmark hazards curves corresponding to the FSS at a given number of specific locations or save points. The difference between the RSS hazard curves and FSS benchmark curves is minimized by initially sampling a small subset of TCs, and then iteratively adding additional TCs (*e.g.*, 5 by 5) until the difference between the two curves is significantly reduced or becomes negligible. The save points where the hazard curve optimization takes place correspond to critical locations within the study area. A total of 65 save points were considered in this study.

Following are the general steps in the DoE approach used for the selection of the TC RSS:

1. Identify a set of save points within the study area where the DoE optimization is to be performed.
2. Develop or use existing TC SWL hazard curves for the FSS.
3. Determine the number of TCs to be sampled.
4. Develop new hazard curves for the RSS.
5. Select the annual exceedance frequency (AEF) range at which the RSS and FSS hazard curves will be compared. Differences can be computed along the entire hazard curve, segment of the hazard curve, or at specific AEFs (*e.g.*, 0.02 to 0.002 storms/year, equivalent to 50 to 500 years).
6. Calculate errors between the RSS and FSS hazard curves at predetermined AEFs.
7. Conduct an iterative optimization analysis, described in Melby et al. (2020), Appendix C, to evaluate the benefit of increased RSS size; (*e.g.*, 5 by 5, from 10 to 25 TCs).
8. Once the sought number of storms is reached (*e.g.*, 25), in order to evaluate the overall RSS performance, the RSS selected through optimization indicated in Step 7 is compared to multiple RSS where TCs are sampled in a single batch.
9. Complete storm selection by choosing the optimal RSS from Step 8.
10. The selected storms are simulated in ADCIRC and the results used to reconstruct hazard curves for NCBB without- and with-project conditions.

For this study, an RSS of 25 TCs was selected for simulating in the hydrodynamic models. The methodology for reconstruction of the NCBB SWL and the development of updated hazard curves is described in Section 2.2 and 2.3.

2.2 Overview of Water Lever Reconstruction and Development of Hazard Curves

The process of reconstructing the SWL hazard curves for the NCBB began with the selection of the RSS using the DoE approach (Zhang et al. 2018; Melby et al. 2020). For the NCBB study, two RSS of 10 and 60 TCs, respectively, were identified. The 10-TC RSS was used as part of a sensitivity analysis for initial screening of with-project alternatives (Iteration 1 and 2). For Iteration 3, ADCIRC simulations of SWL without-waves were conducted for the 25-TC RSS in order to perform a comprehensive evaluation of select with-project alternatives. Relying only on RSS simulations would result in increased uncertainty relative to the FSS. Therefore, a key component of the methodology used in this study for

the reconstruction of hazard curves is the application of surrogate modeling, or metamodeling, (*e.g.*, Taflanidis et al. 2014; Kim et al. 2015) for the estimation of the FSS with-project SWL.

More specifically, results from new NCBB hydrodynamic simulations corresponding to the 25-TC RSS were used to determine SWL ratios and absolute differences between, first, NACCS and NCBB base condition and, second, between NCBB base condition and with-project alternatives. A machine-learning method known as Gaussian process metamodeling (GPM) (Jia et al. 2015) was trained on these SWL ratios and differences. The use of GPM within the context of a PCHA study is summarized in Nadal-Caraballo et al. (2020). GPM leverages the TC parametrization scheme that allows for TCs to be described in terms of climatological characteristics and atmospheric forcing including intensity (central pressure deficit), size (radius of maximum winds), track path (translational speed and track reference location), and angle of approach (heading).

In a typical PCHA application, the GPM is used to generate the response (*e.g.*, surge, wave height) of augmented tropical cyclone suites consisting of thousands to millions of synthetic TCs. In the present study, GPM was used to predict the SWL attenuation or amplification of the FSS (i.e., 1,050 TCs) based on the SWL results of the RSS (i.e., 25 TCs) employed in NCBB. This is achieved by using the GPM output to adjust existing NACCS results, as discussed in this section. Following the methodology discussed in Slusarczyk et al. 2021, the main steps in the reconstruction of NCBB TC SWL hazard curves at individual save points are:

1. Conduct hydrodynamic surge-only simulations of the 25-TC RSS.

2. Since the NCBB simulations excluded waves, in order to estimate the contribution of wave setup, a regression model was fit to previous NACCS SWL results with and without waves (see Section 2.3.1 Estimation of Wave Setup).

3. Add wave setup by correcting the NCBB SWL without-waves results through the application of the regression model established in the previous step.

4. Compute both the ratio (K_R) between NACCS and NCBB base condition. Since the NCBB simulations also excluded astronomical tide, these results were directly compared in this step to NACCS results that also excluded tides. The base condition average ratio ($K_{R,base}$) of the NACCS to NCBB SWL was computed as follows:

$$K_{R,base} = \frac{1}{n}\sum_{i=1}^{n}\left(\frac{SWL_{RSS,NCBB,base}}{SWL_{RSS,NACCS,base}}\right)_i \qquad \text{Eq. (1-a)}$$

where: SWL = still water level; RSS = reduced storm set; $base$ = base condition; n is the RSS size.

5. For the assessment of with-project alternatives, $K_{R,alt}$ was computed as follows:

$$K_{R,alt} = \frac{1}{n}\sum_{i=1}^{n}\left(\frac{SWL_{RSS,NCBB,alt}}{SWL_{RSS,NCBB,base}}\right)_i \qquad \text{Eq. (1-b)}$$

where: alt = with-project alternatives.

6. For base condition, compute the absolute difference ($K_{A,base}$) between the NCBB SWL to NACCS SWL for the RSS:

$$K_{A,base} = \frac{1}{n}\sum_{i=1}^{n}\left(SWL_{RSS,NCBB,base} - SWL_{RSS,NACCS,base}\right)_i$$
$$\text{Eq. (2-a)}$$

7. For the assessment of with-project alternatives, $K_{A,alt}$ is computed as follows:

$$K_{A,alt} = \frac{1}{n}\sum_{i=1}^{n}\left(SWL_{RSS,NCBB,alt} - SWL_{RSS,NCBB,base}\right)_i$$
$$\text{Eq. (2-b)}$$

8. Train and validate GPM using the TC SWL ratios and absolute differences computed for the 25-TC RSS.

9. Use GPM results to estimate the TC SWL ratios and differences for the remaining of FSS (i.e., 1,050 TCs − 25 TCs = 1,025 TCs).

10. The ratios and differences computed up to the previous step are used to estimate NCBB SWL (i.e., surge + waves + tide) by correcting existing NACCS SWL. Therefore, the reconstructed NCBB SWL and SWL hazard curves account for the astronomical tide component. For base condition, estimate the NCBB TC SWL for the FSS by correcting the NACCS SWL:

$$SWL_{FSS,NCBB,base} = [(SWL_{FSS,NACCS,base} \cdot K_{R,base}) + (SWL_{FSS,NACCS,base} + K_{A,base})]/2 \qquad \text{Eq. (3-a)}$$

11. This approach, consisting of assigning equal weighting to the ratio- and difference-base adjustments, reduces the average error over the range of adjusted SWL relative to using either of the adjustments alone. Alternatively, an optimization process could also be conducted to determine the weights (i.e., w and w-1) that minimize the average error over the range of SWL specific to this study.

12. For with-project alternatives, estimate the NCBB TC SWL for the FSS by correcting the NACCS SWL:

$$SWL_{FSS,NCBB,alt} = [(SWL_{FSS,NACC,base} \cdot K_{R,alt}) + (SWL_{FSS,NACCS,base} + K_{A,alt})]/2 \qquad \text{Eq. (3-b)}$$

13. Compute TC SWL hazard curves using the joint probability analysis (JPA) previously developed for NACCS (Nadal-Caraballo et al. 2015).

The hydrodynamic simulations of SWL conducted for the NCBB did not account for the occurrence of XCs. While it is possible to identify an RSS of synthetic TC events to inform a joint probability model, given that XCs lack the well-defined vortex that characterizes TCs, the standard of practice for XCs is to sample historical events based on water level observations instead of relying on specific atmospheric forcing parameters. The following are the general steps for reconstructing the NCBB XC SWL hazard curves on a per-save point basis:

1. Using the new NCBB and previous NACCS hydrodynamic results, develop a regression model to establish the likely NCBB TC SWL attenuation or amplification (*i.e.*, response variable) as a function of

the NACCS TC SWL (*i.e.*, predictor variable) at each evaluated save point.

2. Apply the regression model to estimate the NCBB XC SWL from the SWL results corresponding to the original 100 XCs simulated for NACCS.

3. Compute XC SWL hazard curves using extreme value analysis (EVA).

Finally, the CC SWL hazard curves are computed by integrating the individual TC and XC hazard curves at each NCBB save point.

2.3 Reconstruction of Still Water Levels for Without-Project (Base) Conditions

The primary goal of the 25-TC RSS is to determine the change in storm surge and SWL hazards for the different NCBB alternatives under consideration, leveraging from existing NACCS results for 1,050 TCs and 100 XCs. However, it is necessary to first reconstruct the base condition SWL to properly account for any changes arising from updated bathymetry and topography within the study area, and from modifications to the ADCIRC grid. Also, the new NCBB hydrodynamic simulations were conducted without the presence of waves. Therefore, the NCBB SWL must be corrected for the lack of wave effects, such as wave setup. The processes of estimating wave setup and adding this component to the NCBB SWL simulations is presented in Section 2.3.1 -- Estimation of Wave Setup. The reconstruction of TC and XC base condition SWL are discussed in Section 2.3.2 -- Tropical Cyclones and Section 2.3.3 -- Extratropical Cyclones, respectively.

2.3.1 Estimation of Wave Setup

Since the ADCIRC hydrodynamic simulations of the 25 TCs selected for NCBB were performed without waves, wave setup must be estimated and added to the TC SWL. The first step in the SWL reconstruction was to estimate the wave setup at each the 65 NCBB save points by first comparing NACCS TC SWL results with and without waves. Wave setup was estimated by comparing NACCS TC SWL results with and without wave setup and developing a linear regression model for each NCBB save point of the form:

$$Y = \beta_0 + \beta_1 X + \varepsilon \qquad\qquad\qquad \text{Eq. (4)}$$

where: Y = NACCS TC SWL with wave setup (i.e., response variable); X = NACCS TC SWL without wave setup (i.e., predictor variable); β_0= intercept; β_1= slope; and ε = aleatory error.

The regression models were then used to correct the NCBB simulations by adding wave setup to the TC SWL without-waves results. The aleatory error (ε) component in Eq. (4) was not accounted for in the wave-setup correction process.

2.3.2 Tropical Cyclones

After the NCBB simulations are corrected by adding wave setup, the next step in the SWL reconstruction process is the computation of NCBB TC SWL to NACCS TC SWL ratios ($K_{R,base}$) and absolute differences ($K_{A,base}$) for the different with-project alternatives. $K_{R,base}$ and $K_{A,base}$ are computed for the 25-TC RSS in order to estimate the SWL change (i.e., attenuation or amplification) resulting from these alternatives. The relationship between the NCBB to NACCS TC SWL ratios (y-axis) and the NACCS TC SWL (x-axis) is not exclusively linear and the relationship can exhibit significant spread at some locations. Consequently, instead of relying on linear regression models, GPMs were trained for both $K_{R,base}$ and $K_{A,base}$, so SWL changes could be estimated for the 1,050-TC FSS used in the development of updated SWL hazard curves for the NCBB study.

GPM is a mathematical approximation for the input/output (x/z) relationship of a complex numerical model. It is formulated based on a database of simulations for complex processes such as hurricane storm surge. This database is frequently referenced as experiments or support points, as shown in Figure 2-1. The basis for the GPM framework used in this study is the TC parametrization in the NACCS JPA (Nadal-Caraballo et al. 2015). The synthetic TCs are the GPM input (x), while the output (z) are the CSTORM-MS water level simulation results. Each input/output pair constitutes a support point. Figure 2-1 shows a generalized input/output relationship, where support points are used to train a GPM and construct a 3-dimensional (3D) surface. Herein, the reconstruction of the NCBB SWL is a 7-dimensional hyper-space, with six TC parameters as inputs and either $K_{R,base}$ or $K_{A,base}$ as a single output.

Figure 2-1. GPM input/output relationship.
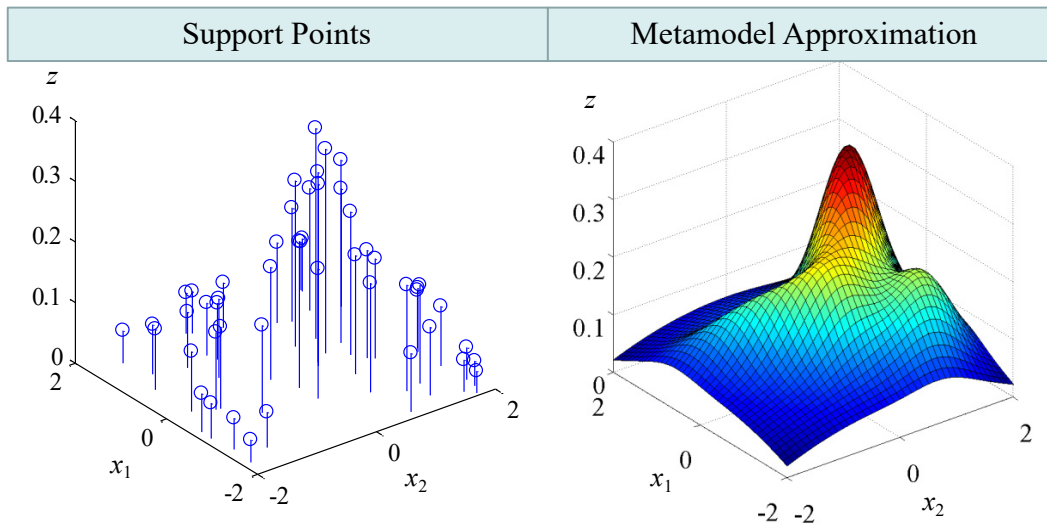
As discussed in Nadal-Caraballo et al. (2015; 2020), synthetic TCs are developed considering the historical climatology and characteristic storms of a specific region, and reflect likely combinations of storm intensity and size, track and landfalling location. The input vector (x) used in the training of GPM consists of the following TC parameters:

- Latitude of landfalling or bypassing reference location, x_{lat}
- Longitude of landfalling or bypassing reference location, x_{lon}
- Heading direction, θ
- Central pressure deficit, Δp
- Radius of maximum winds, R_{max}
- Translational speed, V_t

Training and validation of the GPM is discussed in detail in Taflanidis et al. (2014); Jia et al. (2015); Taflanidis et al. (2017); and Zhang et al. (2018).

2.3.3 Extratropical Cyclones

The standard of practice for the assessment of XC storm surge and other coastal hazards does not require this storm population to be parameterized. Without a parameterization scheme, training of a GPM is unfeasible. Therefore, a regression model is used to estimate the general relationship between the NCBB and NACCS SWL and, thus, the expected value of SWL attenuation or amplification, regardless of storm forcing. This allows the estimation of XC SWL for NCBB using a linear regression

model as a function of the previous NACCS results for 100 XCs. SWL hazard curves for XCs and CC hazard curves were developed as described in Nadal-Caraballo et al. (2015).

2.4   Reconstruction of Water Levels for With-Project Alternatives

This section discusses the reconstruction of SWL for the different NCBB with-project alternatives. The processes of reconstructing TC and XC with-project SWL are discussed in Section 2.4.1 -- Tropical Cyclones and Section 2.4.2 -- Extratropical Cyclones, respectively.

2.4.1   Tropical Cyclones

The methodology for training of GPM and reconstructing TC SWL for the with-project alternatives follows steps similar to the methodology previously discussed in Section 2.3.2 -- Tropical Cyclones for reconstruction of the base condition TC SWL. However, wave setup estimation only needs to be done once for the base condition, as discussed in Section 2.3.1 -- Estimation of Wave Setup, and the same per-save point regression models can be applied to correct the without-waves TC SWL values from the with-project alternatives. After the NCBB TC SWL is corrected for wave setup, the NCBB alternative to base TC SWL ratios ($K_{R,alt}$) and absolute differences ($K_{A,alt}$) for the 25-TC RSS are computed. Then, $K_{R,alt}$ and $K_{A,alt}$ are used as input in the training of the GPM for the different alternatives.

2.4.2   Extratropical Cyclones

As discussed in Section 2.3.3 -- Extratropical Cyclones, XCs are not parameterized. Therefore, instead of employing GPM, which requires a set of input parameters to develop the input/output relationship, the reconstruction of XC SWL relies on regression models to: 1) add wave setup to the NCBB surge-only water levels for both base condition (as discussed in Section 2.3.3 -- Extratropical Cyclones) and the different with-project alternatives; and 2) to establish the relationship between each NCBB with-project alternative TC SWL and the NCBB base condition TC SWL in order to estimate XC SWL. The with-project XC SWL hazard curves were developed as described in Nadal-Caraballo et al. (2015). The reconstructed CC SWL hazard curves for the with-project alternatives considered in NCBB and the discussion of these results are presented in Section 5 -- SWL Hazard Curves.

3   ADCIRC Mesh Details

The ADCIRC mesh developed for the NACCS (Cialone et al. 2015) was modified, providing detailed representation of the NCBB study area. There were two major changes implemented in the NACCS grid, that is, refinement of the study area and de-refining of the remote area (Chesapeake Bay) while the original boundary of the domain (Figure 3-1) was not altered.

Figure 3-1. Outline plot showing the boundary of the ADCIRC computational domain.
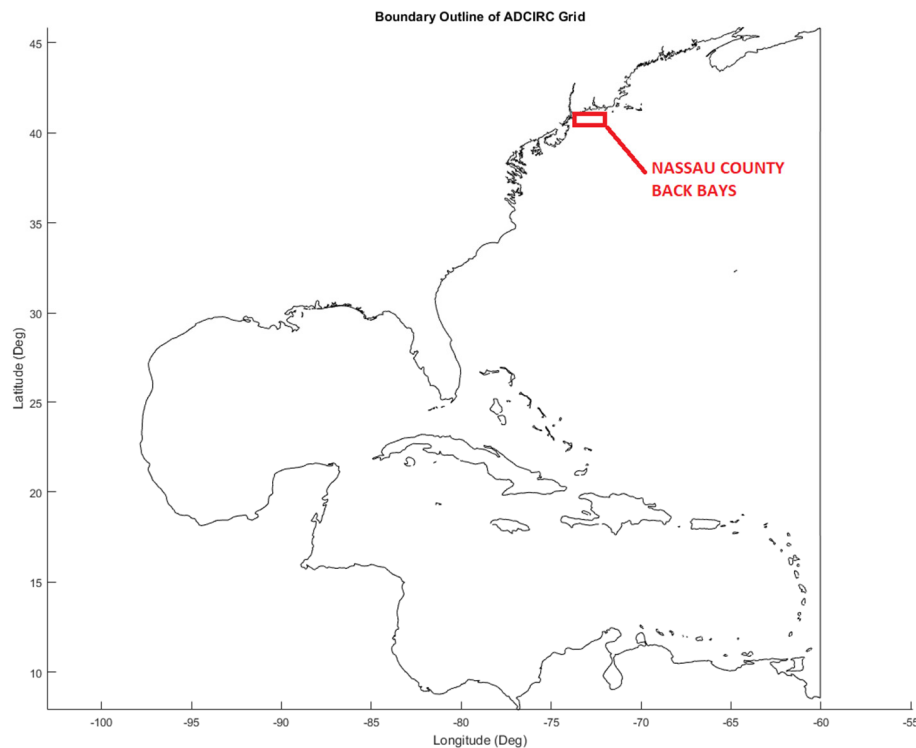
Refinement of the grid in the study area was necessary to fully capture and analyze the hydrodynamic processes in the area of interest. Moreover, this procedure facilitated the implementation of the complex configurations of the storm surge barriers at the specific location required by the study sponsor. The purpose of grid de-refining is to reduce the mesh resolution in areas remote from the area of interest in order to decrease model simulation times without significantly affecting the flow volume exchange between de-resolved and the study areas. The total number of 3.12 million nodes in the NACCS grid was reduced to 2.51 million (approximately a 20% reduction) in the NCBB grid due to the Chesapeake Bay region de-

refining. Figure 3-2 shows the grid resolution before (a) and after (b) de-refining in the Chesapeake Bay area.

Figure 3-2. Chesapeake Bay area (a) before and (b) after de-refining.
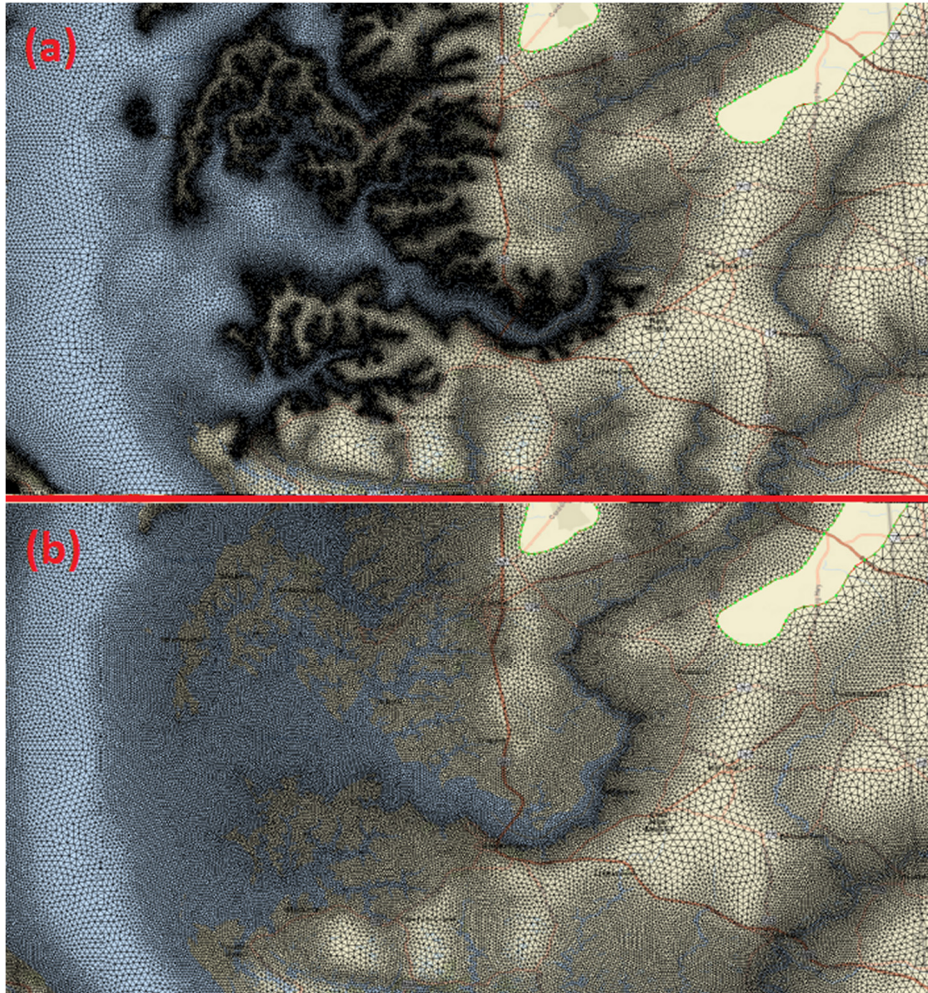
In order to show that the de-refining procedure did not significantly alter the model results in the region of interest, a comparison of water surface elevation time series from Hurricane Sandy simulations made with the without-project condition NCBB (also referenced in this text as the "Base Grid" or "Base Condition") and the NACCS grid was made at 5 save points (the locations of the save points are displayed in Figure 3-3). Moreover, since the comparison was made for a historical event (Hurricane Sandy) and the selected save point locations coincide with U.S. Geological Survey (USGS) tide gauges (Table 3-1), it was possible to compare the simulated results with the data obtained from the gauges for this event. Finally, besides the grid refinement in the study area, the topographic and bathymetric data were updated in the study region with data from Lidar

surveys provided by the project sponsor (USACE New York District: NAN). Also the elevation of the Long Beach dunes (Figure 3-4) was raised to +14 ft NAVD88 in accordance with the Federal CSRM project. Figures 3-5 through 3-9 show water surface elevation time series at selected save point locations for Hurricane Sandy, where the red line represents the hydrographic signal obtained from the NCBB Base condition (NCBB_Base_pg05) model simulation (modified NACCS grid: refined, de-refined, and updated topo/bathy) and the green line represents the hydrographic signal from the USGS gauge.

Figure 1-3. Save point locations.

Figure 3-2. Long Beach: restored dunes.
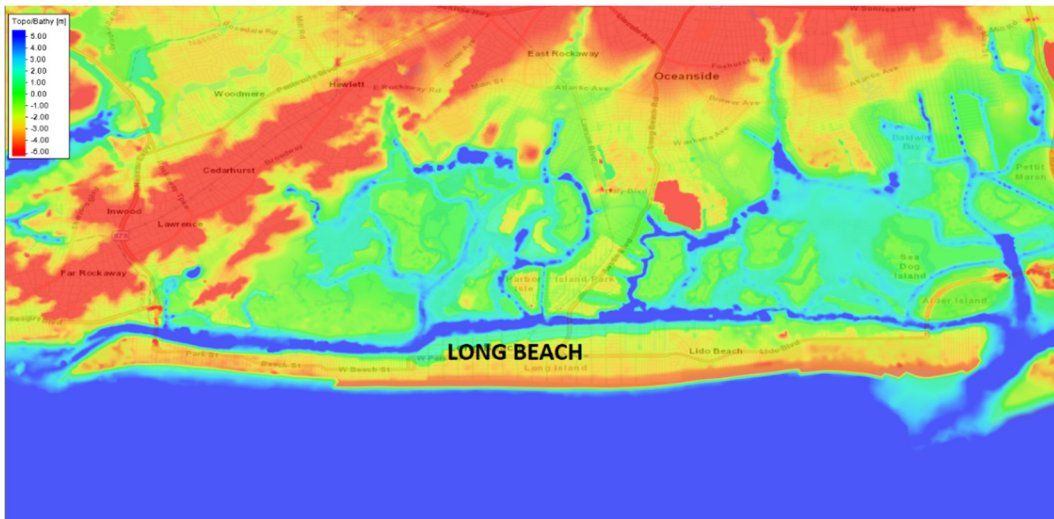
Figure 3-3. Tidal signal for GREAT SOUTH BAY AT LINDENHURST NY gauge.
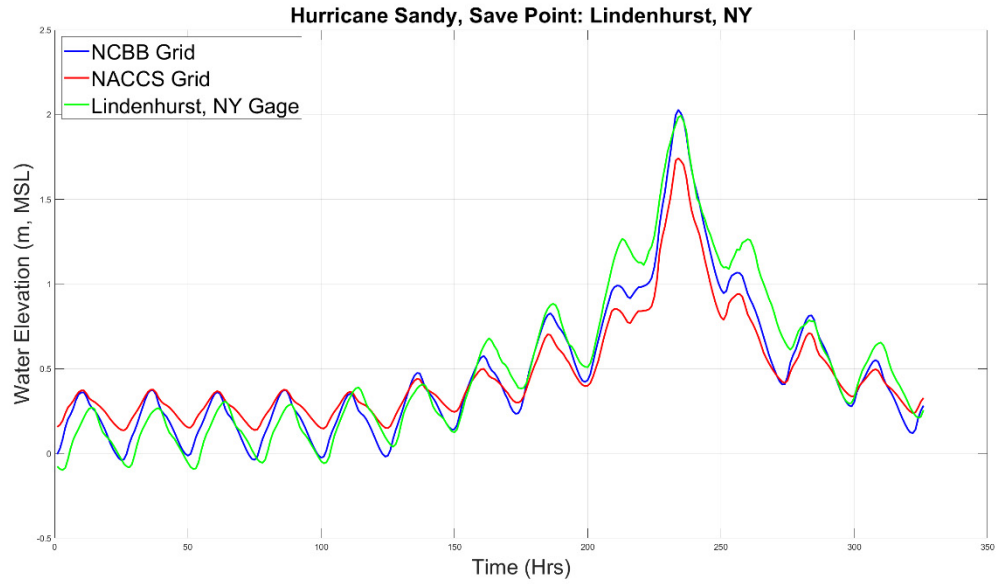
Figure 3-4. Tidal signal for HOG ISLAND CHANNEL AT ISLAND PARK NY gauge.
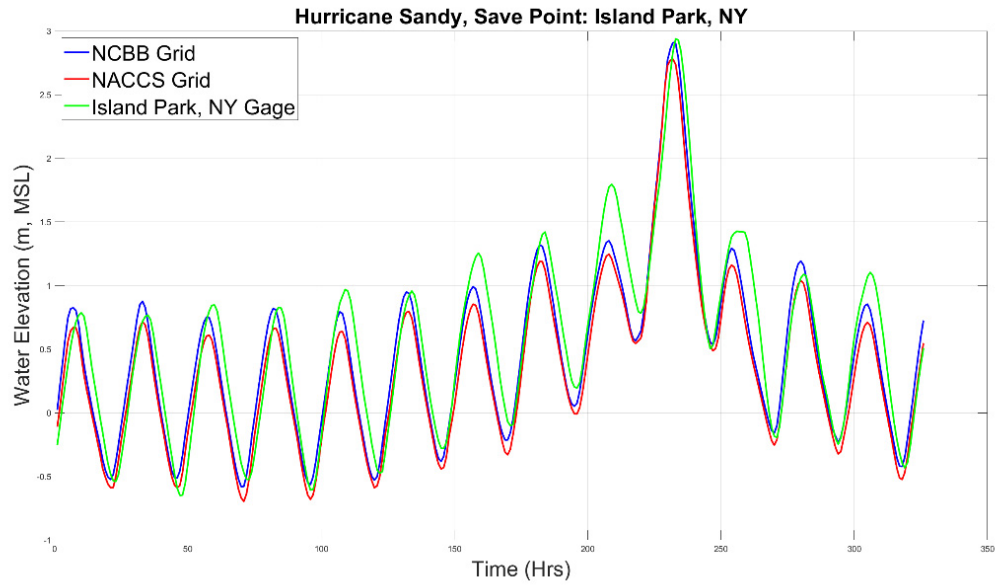
Figure 3-5. Tidal signal for EAST ROCKAWAY INLET AT ATLANTIC BEACH NY gauge.
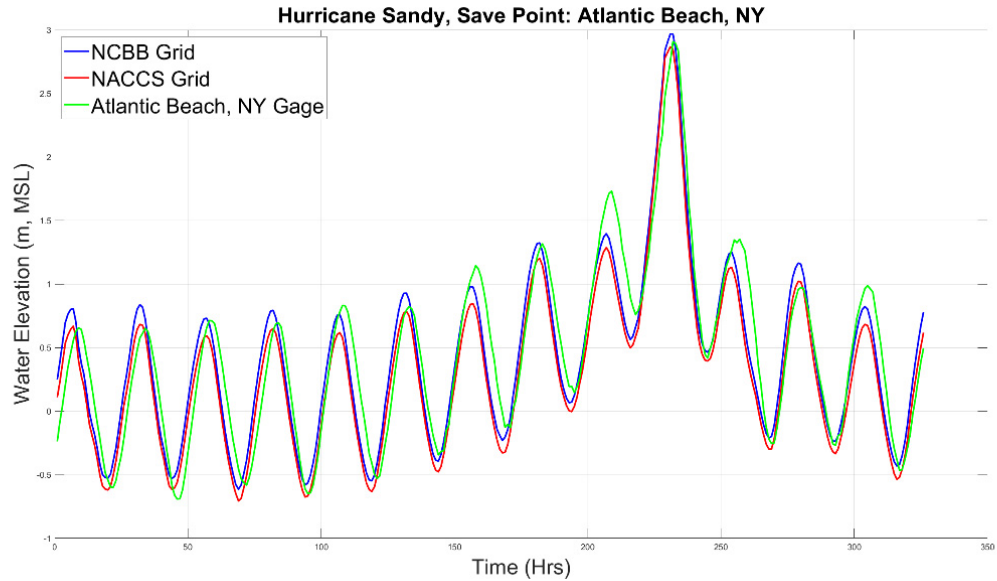
Figure 3-6. Tidal signal for REYNOLDS CHANNEL AT POINT LOOKOUT NY gauge.
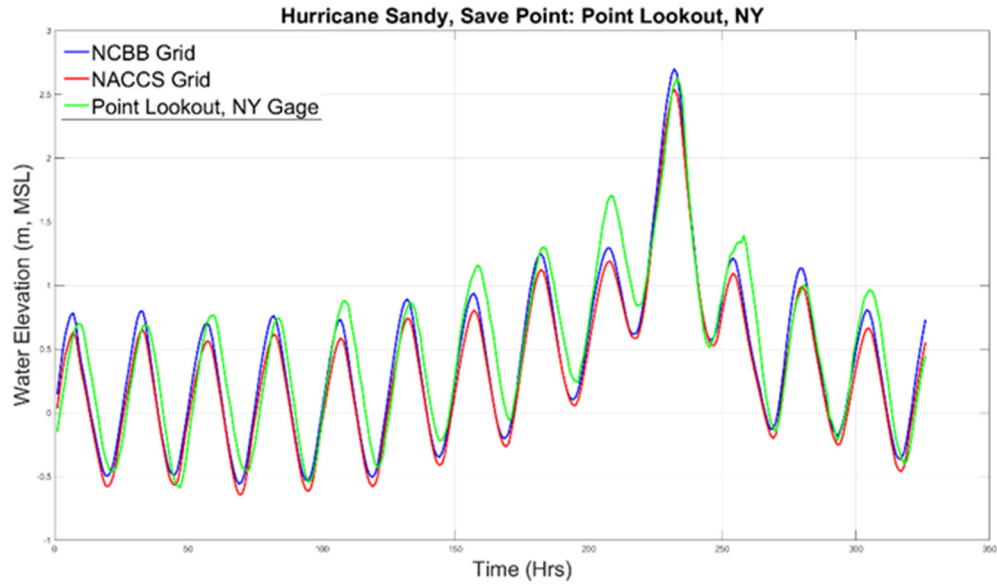
Figure 3-7. Tidal signal for HUDSON BAY AT FREEPORT NY gauge.
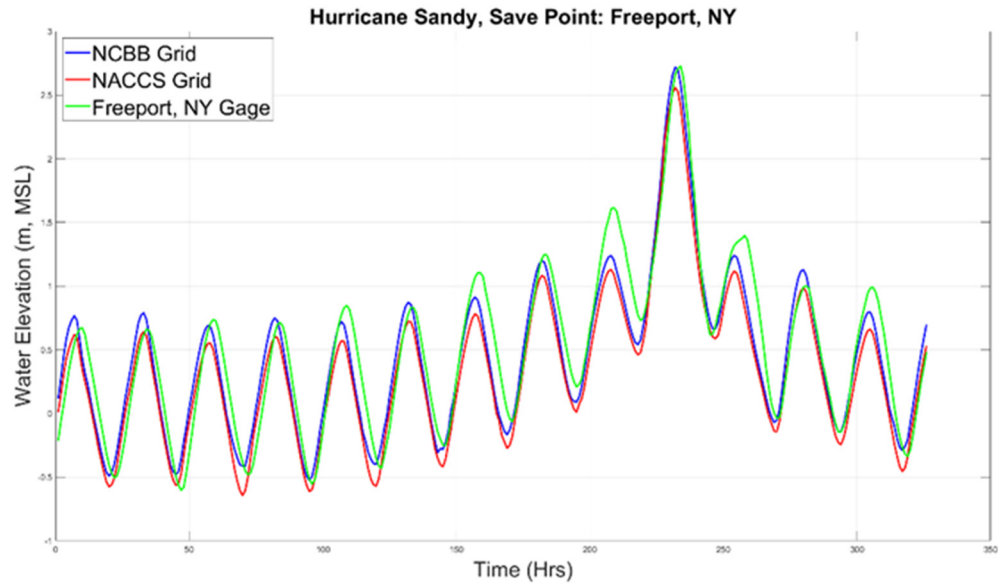
The USGS gauge IDs and locations, the maximum water elevation at each of the gauges obtained from the ADCIRC simulation (NCBB_Base_pg05) and historical records (USGS), and the absolute and the relative differences of maximum water level between water surface elevation from NCBB-Base-pg05 save points and the USGS gauges are shown in Table 3-1.

Table 3-1. Comparison between simulated (NCBB_Base_pg05) and historical (USGS) water surface elevations for selected USGS gauges during Hurricane Sandy.

USGS Gauges		NCBB_Base_pg05	USGS	NCBB_Base_pg05 - USGS	
ID	Location	The peak surge (m)	The peak surge (m)	Max diff for the peak surge (m)	Max diff for the peak surge (%)
01309225	GREAT SOUTH BAY AT LINDENHURST NY	2.09	1.99	0.10	4.77
01311143	HOG ISLAND CHANNEL AT ISLAND PARK NY	2.97	2.95	0.02	0.56
01311145	EAST ROCKAWAY INLET AT ATLANTIC BEACH NY	3.03	2.93	0.10	3.49
01310740	REYNOLDS CHANNEL AT POINT LOOKOUT NY	2.76	2.65	0.10	3.91
01310521	HUDSON BAY AT FREEPORT NY	2.78	2.73	0.06	2.03

The average absolute difference for maximum water level elevation was ~0.07 meters and the corresponding average relative difference was 2.95%. The greatest percent difference in maximum water levels was observed at Lindenhurst save point #01309225 (0.09 m, 4.77%). These results provide assurance that the NCBB model: 1) compares well to measurements in the region of interest; and 2) compares well to the NACCS model results, indicating that the NCBB grid refinements and de-refinements did not change the quality of the NACCS grid validation.

Once the Base Grid (NCBB_Base_pg05) was created and validated, the subsequent "surge barrier alternative" grids were derived from the Base Grid by implementing storm surge barriers as weir-pairs sub-grid features (Figure 3-10). Implementing weir-pairs in the ADCIRC mesh helps to maintain model stability. This is because the sub-grid scale formulation for weir-pairs prevents the model from transitioning from sub to supercritical flows during the course of the simulation in the event that the water elevation is high enough to overtop the structure. The NCBB Base Grid has a spatial resolution (element size) ranging from approximately 10 to 1000 m and MSL as a vertical datum.

Five proposed alternative grids, described in the remaining of Section 3, were modeled in addition to the existing condition (Base Condition). Each of the alternative grids contains multiple inlet and/or bay closures. All weir-pair structures were set to a +18.28 m (+60 ft) MSL elevation. Simulations were initiated with the surge barriers in place and the surge barriers remained closed for the entire simulation. In addition to the inlet and/or bay closures the alternatives included elevated dunes along the ocean shoreline located in-between closures to eliminate overwash along the barrier islands. The simulation results are discussed in Section 4.

Figure 3-8. Point Lookout (a) before and (b) after weir-pair implementation.
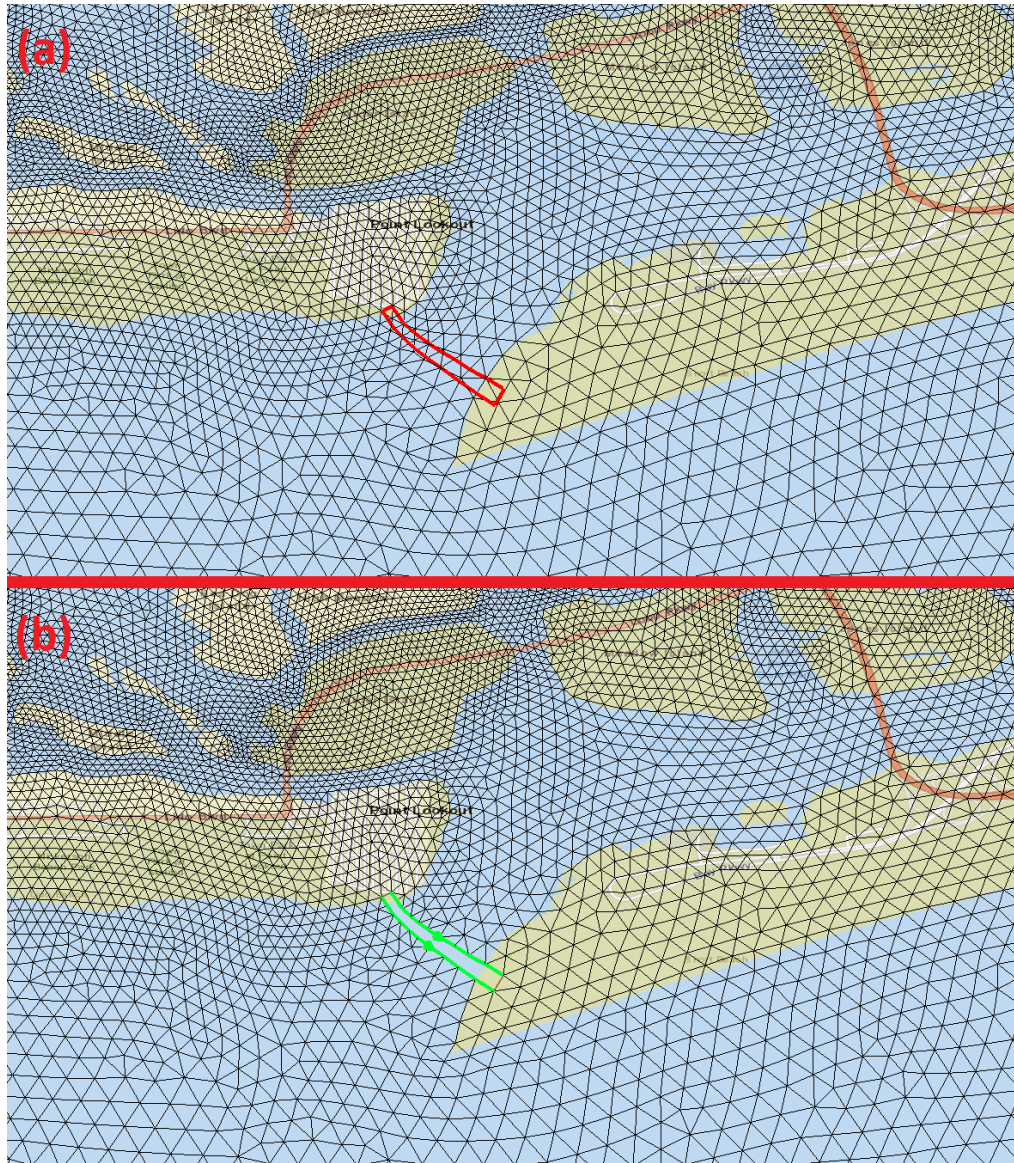
## 3.1   Alternative 1A

The Alternative 1A included the following closures (shown in Figure 3-11):

1. East Rockaway Inlet
2. Jones Inlet
3. Fire Island Inlet

Figure 3-9. Alternative 1A.

3.2   Alternative 1B

The Alternative 1B included the following closures (shown in Figure 3-12) as well as elevated dunes along the ocean shoreline in-between closures to prevent overwash along the barrier islands:

1. Head of Bay Closure
2. East Rockaway Inlet
3. Jones Inlet
4. Wantagh State PKWY

Figure 3-10. Alternative 1B.

3.3 Alternative 1C

The Alternative 1C included the following closures (shown in Figure 3-13) :

1. East Rockaway Inlet
2. Meadowbrook State PKWY

Figure 3-11. Alternative 1C.
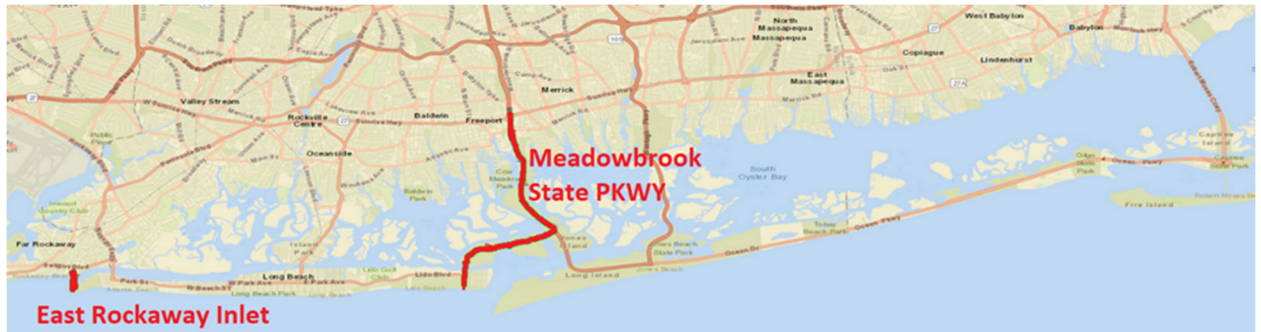
3.4 Alternative 1D

The Alternative 1D included the following closures (shown in Figure 3-14):

1. East Rockaway Inlet
2. Jones Inlet
3. Robert Moses Causeway

Figure 3-12. Alternative 1D.

3.5 Alternative 2

The Alternative 2 included floodwalls along the perimeter of the bay shoreline and along Long Beach (shown in Figure 3-15).

Figure 3-15. Alternative 2.

4   Simulation Results

The numerical modeling task consisted of evaluating the impact of combinations of inlet and bay closures on water levels in the NCBB for a suite of 25 storm events. The storm selection process was described in Section 2 and the grid alternatives were described in Sections 3.1 – 3.5. The following section describes the effect of closure configurations on maximum water level in the Nassau County back bays. First, the analysis was based on comparing differences in the maximum water level for combination of closures (with project) condition relative to the base (without project) condition in the study area. Secondly, maximum water levels for the base condition at specific points in a hydraulic reach were compared to maximum water levels with closures in place. As expected, each of the proposed alternatives generated unique responses to each simulated storm, but generally those responses for a given alternative was similar for all storms. Therefore, for the brevity of this document, only one representative storm (433) will be discussed for each alternative in the subsequent sections. This storm is characterized by its size (Rmax of 55 km), central pressure deficit (88 mb), forward speed (62 km/hr), and storm track (landfall near 39,38°N, 74.51°W), resulting in one of the most intense water level responses of the 25 storms simulated for this study. The complete set of maximum water level plots, difference plots, and dot plots can be found in the Appendix.

4.1   Maximum Storm Surge Results – Alternative 1A

Figure 4-1, Figure 4-2, and Figure 4-3 show maximum water elevation for the Base Grid, maximum water elevation with Alternative 1A (East Rockaway, Jones, and Fire Island Inlets closed), and the difference in maximum water elevations between Alternative 1A and the Base Grid for synthetic tropical storm 433, respectively.

Figure 4-1. Maximum water elevation: Storm 433, Base grid.
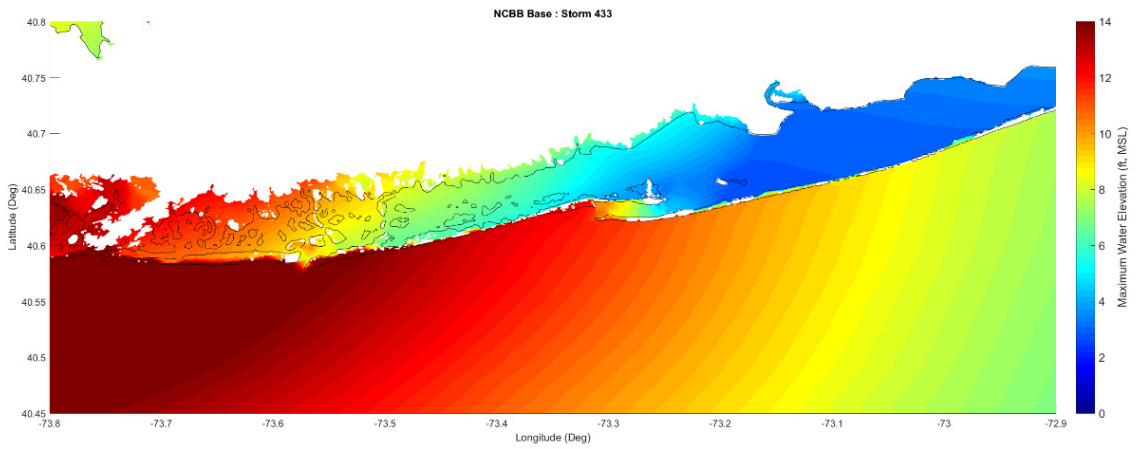
Figure 4-2. Maximum water elevation: Storm 433, Alternative 1A.
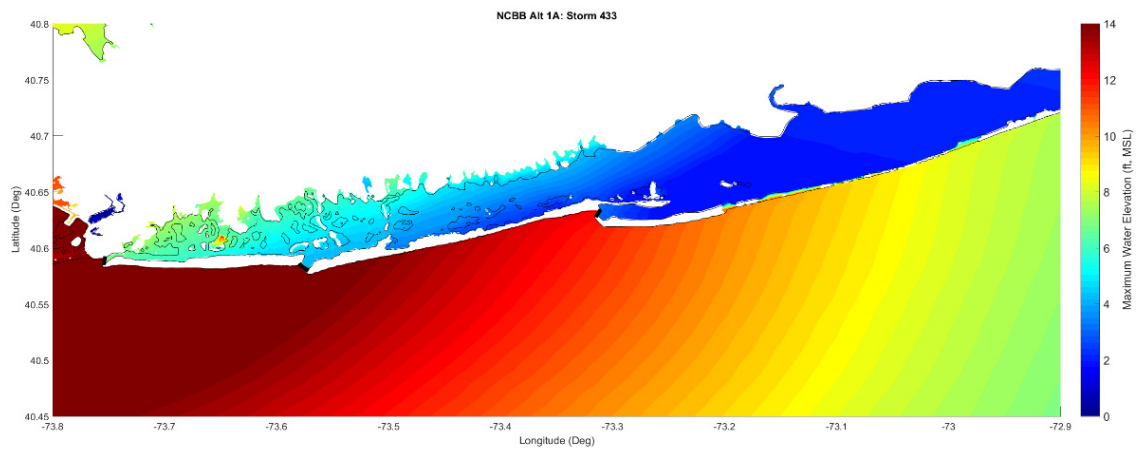
Figure 4-3. Difference in maximum water elevation (storm 433): Alternative 1A – Base.

A close investigation of the impact of Alternative 1A on water levels in NCBB study area shows a similar pattern for all 25 simulated storms. That

is, the greatest reduction in water level occurs in the section between East Rockaway Inlet and Meadowbrook State PKWY of approximately 1.5 m for Storm 433. Moving to the east, the reduction in water level with the Alternative in place gradually decreases (approximately 1.2 m between Meadowbrook State PKWY and Wantagh State PKWY, then 0.95 m in the westernmost part of South Oyster Bay (to the east of Wantagh State PKWY), and 0.5 m in the easternmost of the South Oyster Bay (to the west of Robert Moses Causeway). This behavior continues in Great South Bay (to the east of Robert Moses Causeway) with 0.5 m of the water level reduction in the westernmost part of the Great South Bay and 0.4 m in the easternmost part of Great South Bay. The overtopping that occurred along the barrier island separating South Great Bay from the Atlantic Ocean minimized the benefit of the Alternative on reducing water level in the east and west most endpoints of the bay (Storm 433). However, the analysis of a less intense storm (184: Figure 4-4 and Figure4-5) reveals a slightly different pattern in Great South Bay due to the fact that there is no overtopping for this event. That is, the easternmost part of the bay experiences the greatest reduction in water level (0.38 m), while the westernmost region only experiences a reduction of 0.24 m. The other sections of the NCBB study area follow the same pattern as in case of the storm 433. The magnitude of this reduction is in the other sections is correlated to the magnitude of the storm. Therefore, for storm 184, the average reduction of water level in the section between East Rockaway Inlet and Meadowbrook State PKWY is 0.8 m, between 0.65 m and 0.55 m from Meadowbrook State PKWY to Wantagh State PKWY, and 0.55 m and 0.25 m in western and easternmost part of South Oyster Bay, respectively.

Figure 4-4. Maximum water elevation: Storm 184, Alternative 1A.
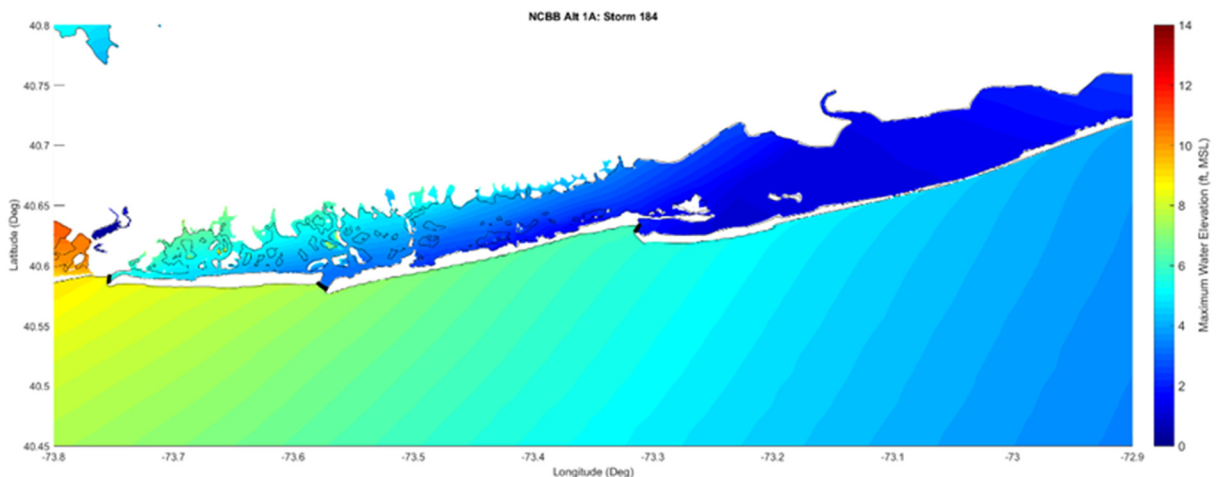
Figure 4-5. Difference in maximum water elevation (storm 184): Alternative 1A – Base.
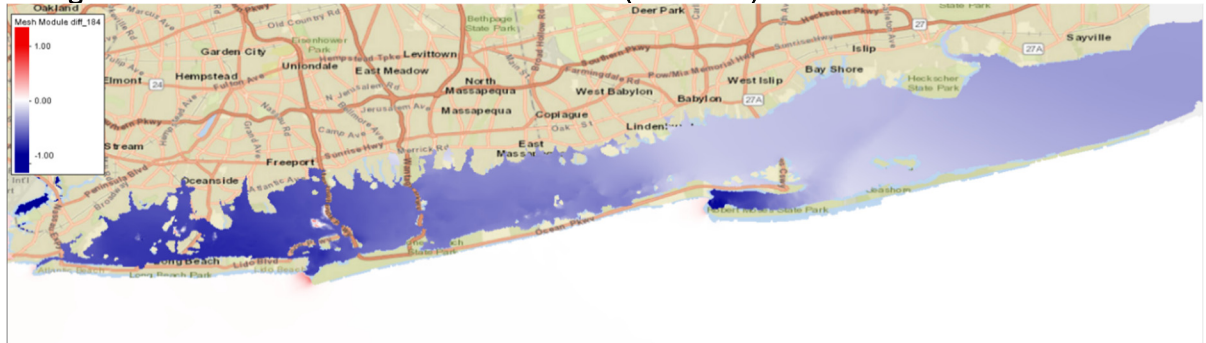
4.2   Maximum Storm Surge Results – Alternative 1B

Figure 4-6, Figure 4-7, and Figure 4-8 show maximum water elevation for the Base Grid, maximum water elevation with Alternative 1B (Head of Bay, East Rockaway, Jones, and Wantagh State PKWY closures), and the difference in maximum water elevations between Alternative 1B and the Base Grid for synthetic tropical storm 433, respectively.

Figure 4-6. Maximum water elevation: Storm 433, Base grid.
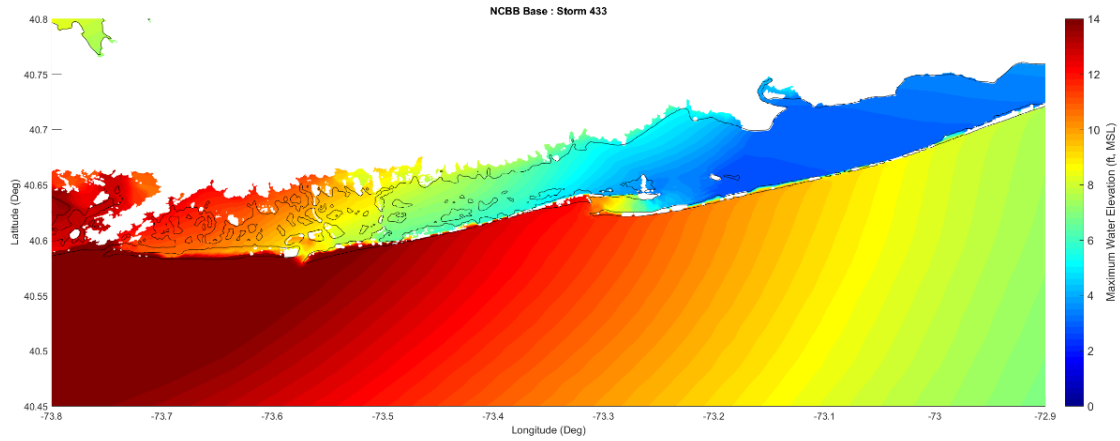
Figure 4-7. Maximum water elevation: Storm 433, Alternative 1B.
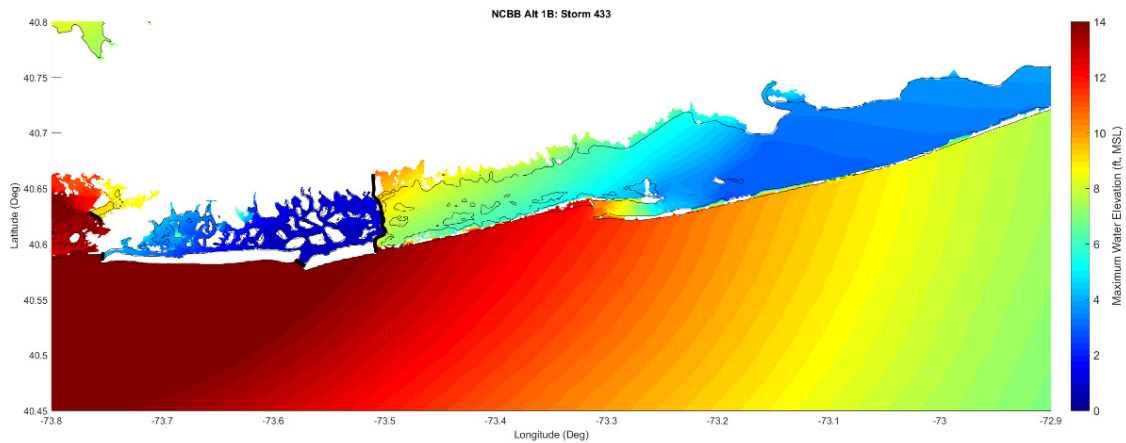
Figure 4-8. Difference in maximum water elevation (storm 433): Alternative 1B – Base.

Alternative 1B shows the greatest reduction (~2.85 m) in water level in the central part of the section between East Rockaway Inlet and Wantagh State PKWY (storm 433). The reduction in the westernmost as well as the easternmost part of this section is approximately 2.3 m (Figure 4-9) due to the seiching of the trapped water behind the closures. This general pattern

of reduced/increased water levels with Alternative 1B in place is identical for all 25 storms, but with somewhat different intensity and extent of reduction within the protected area and somewhat different increase in water level external to the protected area. As was observed with Alternative 1A, the reduction in water level depends on storm intensity (for storm 184 the reduction in the central part is ~1.9 m and ~1.5 at the endpoints of the section).

Figure 4-9. Zoom: Difference in maximum water elevation (storm 433): Alternative 1B – Base.
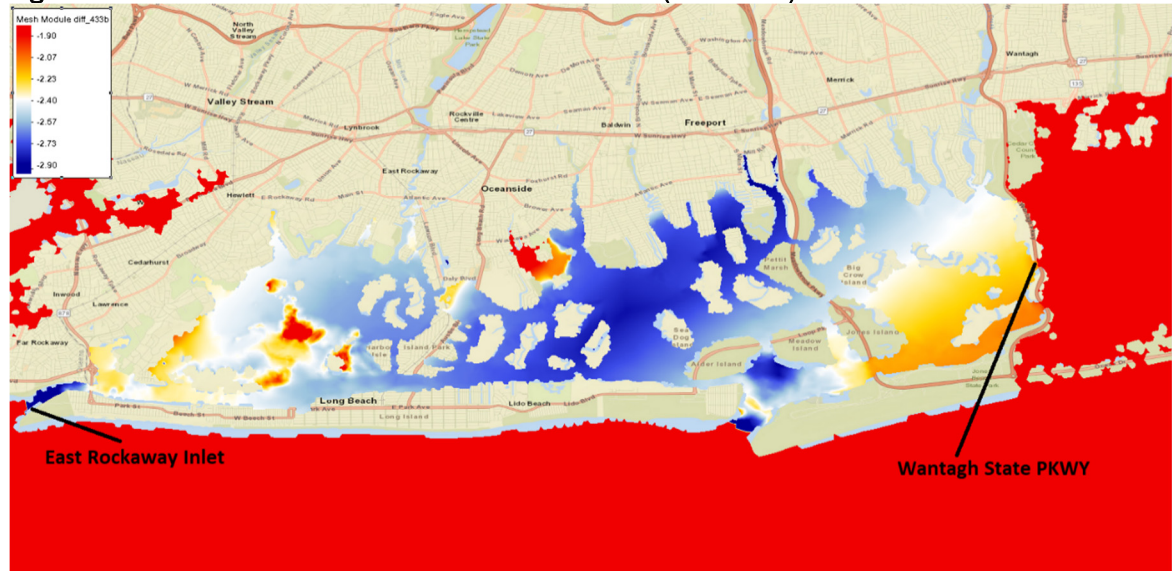
However, for this alternative (1B), a slight increase in water level in South Oyster Bay (eastward to Wantagh State PKWY) is observed (Figure 4-10). This increase is most pronounced in the vicinity of Wantagh State PKWY (~0.27 m for both of the storm) and Robert Moses Causeway (~0.23 for storm 433 and ~0.15 for storm 184) with a minimum increase in the central part of South Oyster Bay (~0.04 for storm 433). Storm 184, on the other hand, shows the same increase of ~0.15 m throughout the rest of South Oyster Bay due to lower intensity and less seiching.

Figure 4-10. Zoom of South Oyster Bay: Difference in maximum water elevation (storm 433): Alternative 1B – Base.
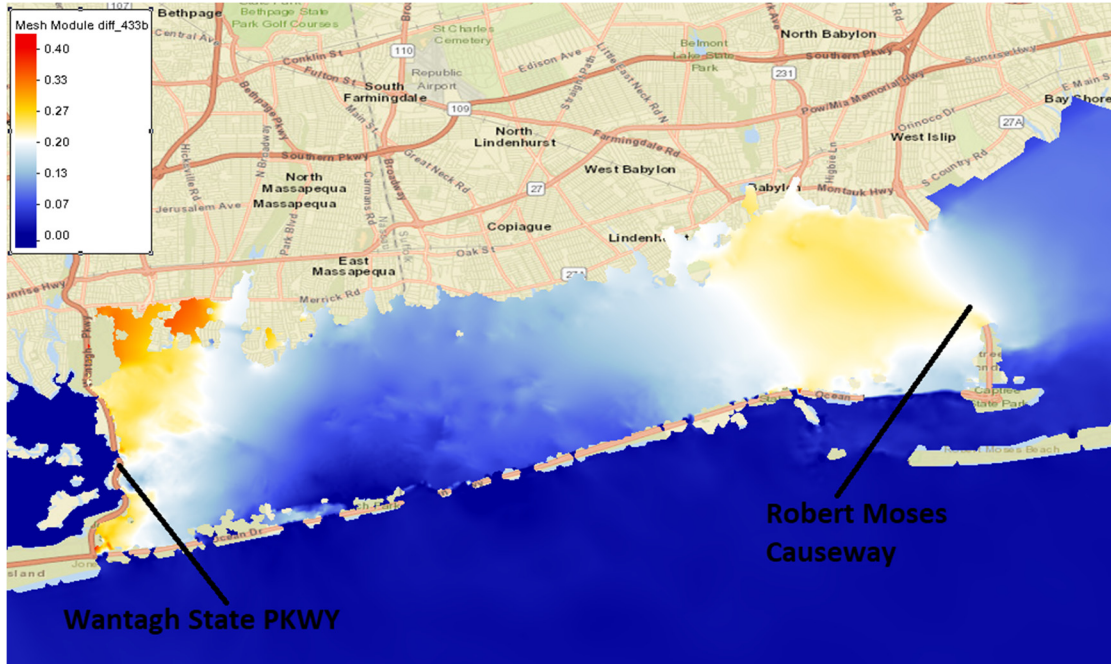
4.3 Maximum Storm Surge Results – Alternative 1C

Figure 4-11, Figure 4-12, and Figure 4-13 show maximum water elevation for the Base Grid, maximum water elevation with Alternative 1C (East Rockaway and Meadowbrook State PKWY closures), and the difference in maximum water elevations between Alternative 1C and the Base Grid for synthetic tropical storm 433, respectively.

Figure 4-11. Maximum water elevation: Storm 433, Base grid.
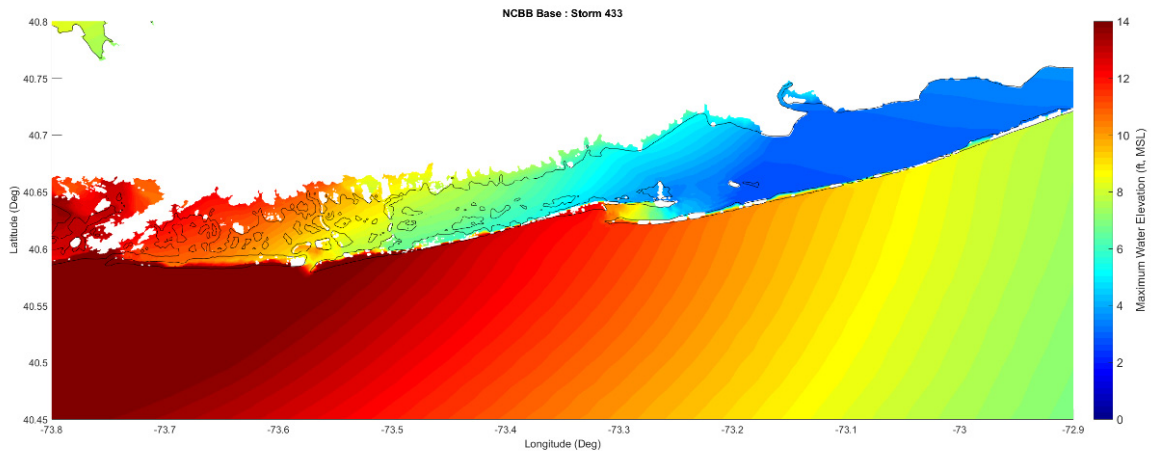
Figure 4-12. Maximum water elevation: Storm 433, Alternative 1C.
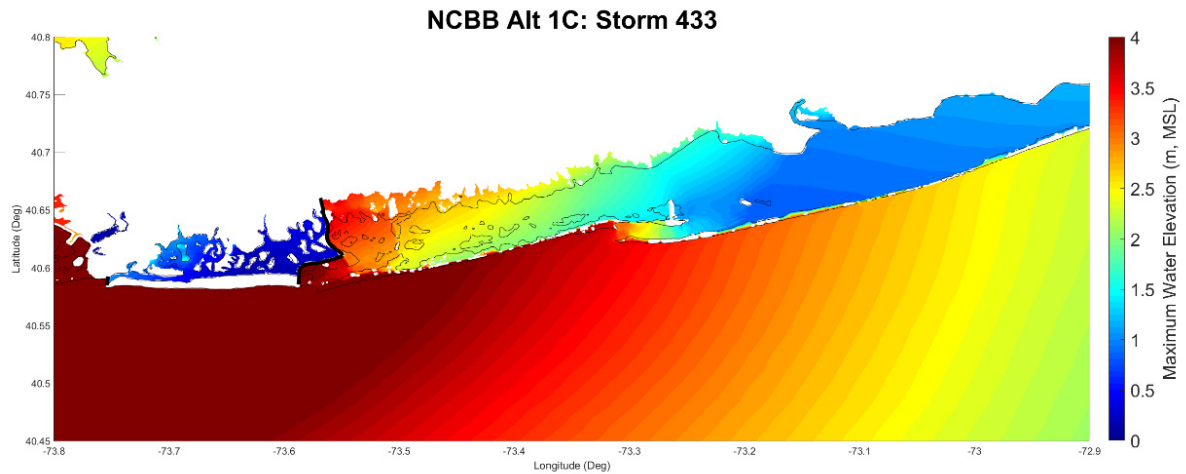

Figure 4-13. Difference in maximum water elevation (storm 433): Alternative 1C – Base.
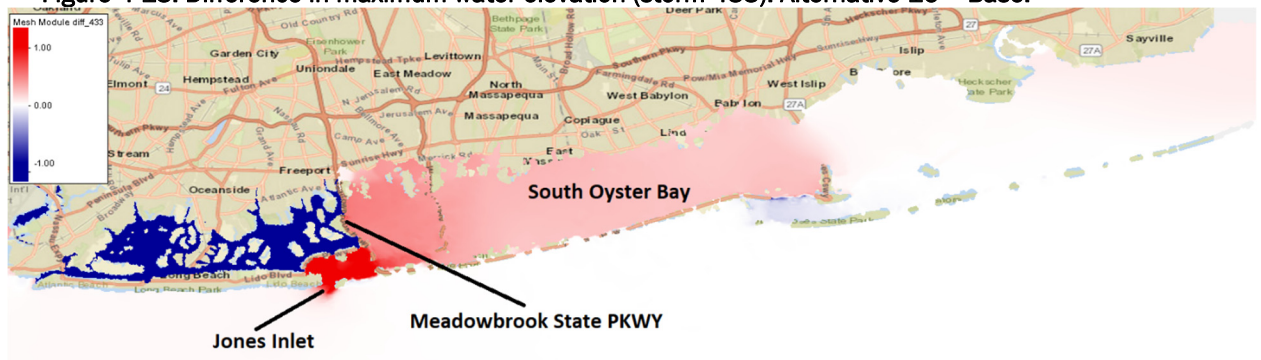

Figure 4-12 shows that the typical response for Alternative 1C is very similar to the Alternative 1B response; with the greatest reduction in water level in the central part of the protected region (~3.00 m for storm 433 and ~2.08 m for storm 184) and symmetrical lower reduction at the eastern and western parts of the region (~1.7 m for storm 433 and ~ 1.75 m for storm 184). As it was for Alternative 1B, there is an increase in water level to the east of the protected area (to the right of Meadowbrook State PKWY), where the elevated water is ~0.45 m for Storm 433 and ~xxx m for Storm 184. The elevated water level gradually dissipates moving eastward through South Oyster Bay to a minimum value of ~0.23 m for storm 433 and ~0.11 m for storm 184 at the east most part of the bay. Another increase in water elevation is observed southward of the Meadowbrook State PKWY closure at Jones Inlet. The accumulation of water in this area is ~1.14 m and ~0.42 m for storm 433 and storm 184, respectively.

4.4 Maximum Storm Surge Results – Alternative 1D

Figure 4-14, Figure 4-15, and Figure 4-16 show maximum water elevation for the Base Grid, maximum water elevation with Alternative 1D (East Rockaway, Jones, and Robert Moses Causeway closures), and the difference in maximum water elevations between Alternative 1D and the Base Grid for synthetic tropical storm 433, respectively.

Figure 4-14. Maximum water elevation: Storm 433, Base grid.
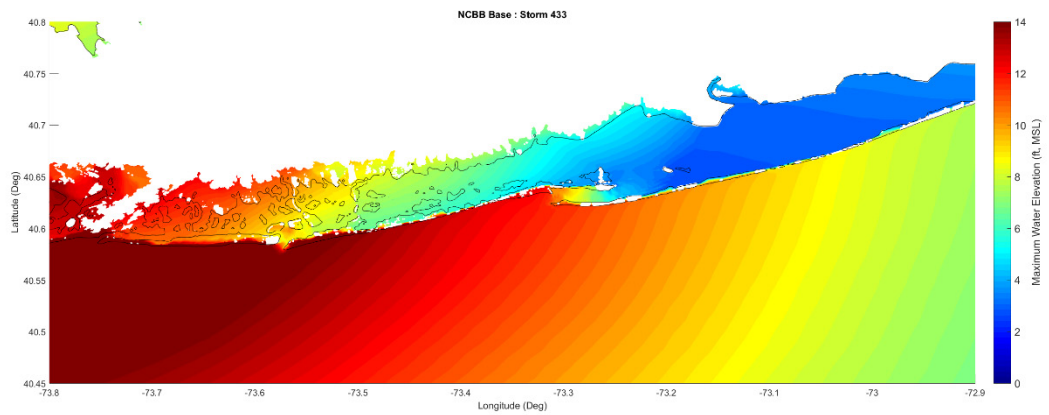
Figure 4-15. Maximum water elevation: Storm 433, Alternative 1D.

Figure 4-16. Difference in maximum water elevation (storm 433): Alternative 1D – Base.
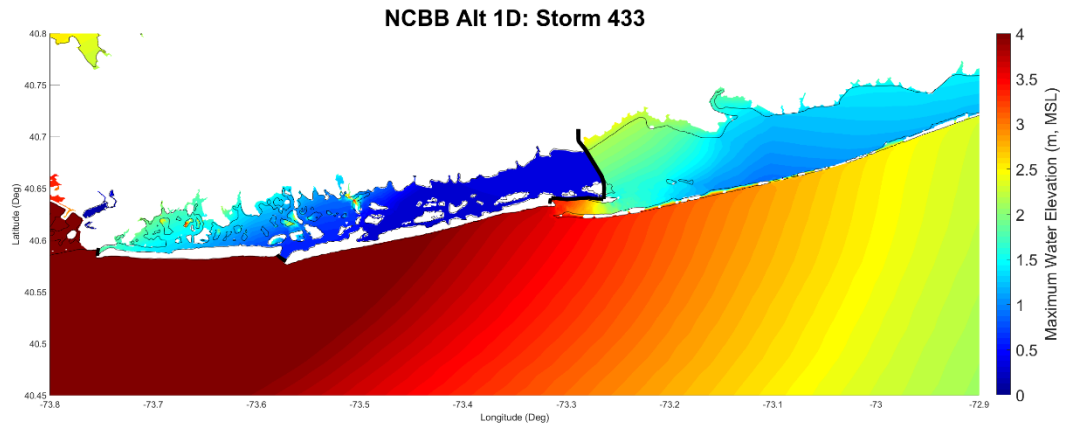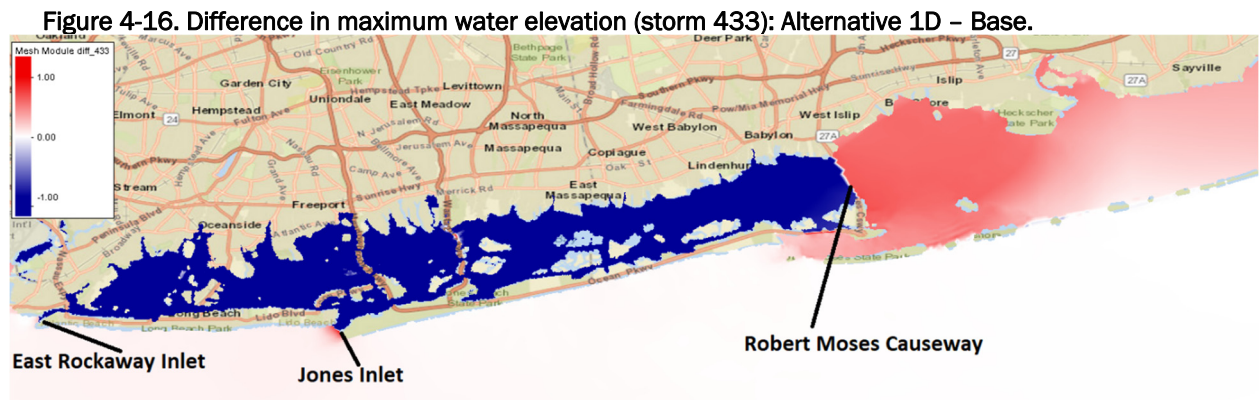
Figure 4-16 demonstrates the effectiveness of Alternative 1D in reducing water levels in the NCBB sub-region enclosed by inlet and bay closures. The pattern reduction for Alternative 1D is slightly different than Alternative 1B or 1C due to the extended length of the protected sub-region (the west-to-east length of the protected area). For storm 433, the water elevation is reduced by ~1.8 m in the vicinity of East Rockaway Inlet and Wantagh State PKWY whereas the central part of this sub-region shows a reduction of ~2.0 m (the same symmetric pattern as in 1B and 1C). However, beyond that point, that is eastward of Wantagh State PKWY, the gradual decrease in the reduced water level with the alternative in place is observed, with a minimum value of ~0.8 m at the Robert Moses Causeway (Figure4-17). Because the base condition has the greatest water levels on the western end of Long Island Sound (the long fetch allows water to pile up near East Rockaway Inlet) and the protection from Alternative 1D prevents propagation into this area; these two factors result in the greatest differential/reduction in water level in this region. Furthermore, eastward of the Robert Moses Causeway, the increase in water elevation with the alternative in place is observed with a maximum of approximately 0.65 m at the causeway and a minimum increase of approximately 0.25 m at the eastern end of Great South Bay. The same pattern of response to Alternative 1D inside the protected sub-region and outside in Great South Bay is observed for all 25 storms, with varying magnitudes of decrease or increase of water levels.

Figure 4-17. Zoom: Difference in maximum water elevation (storm 433): Alternative 1D – Base.

4.5 Maximum Storm Surge Results – Alternative 2

Figure 4-18, Figure 4-19, and Figure 4-20 show maximum water elevation for the Base Grid, maximum water elevation with Alternative 2 (referred to as the floodwall), and the difference in maximum water elevations between Alternative 2 and the Base Grid for synthetic tropical storm 433, respectively.

Figure 4-18. Maximum water elevation: Storm 433, Base grid.
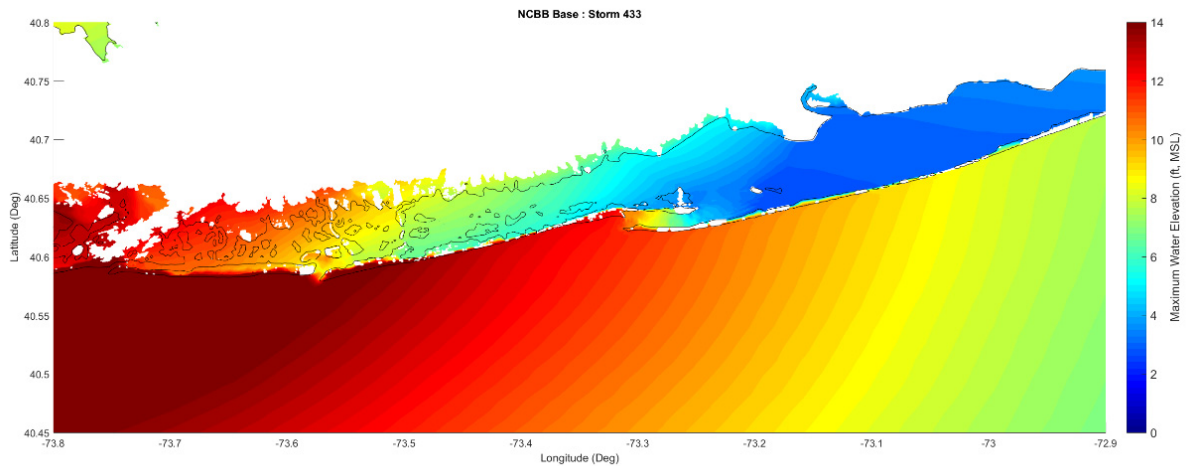
Figure 4-19. Maximum water elevation: Storm 433, Alternative 2.
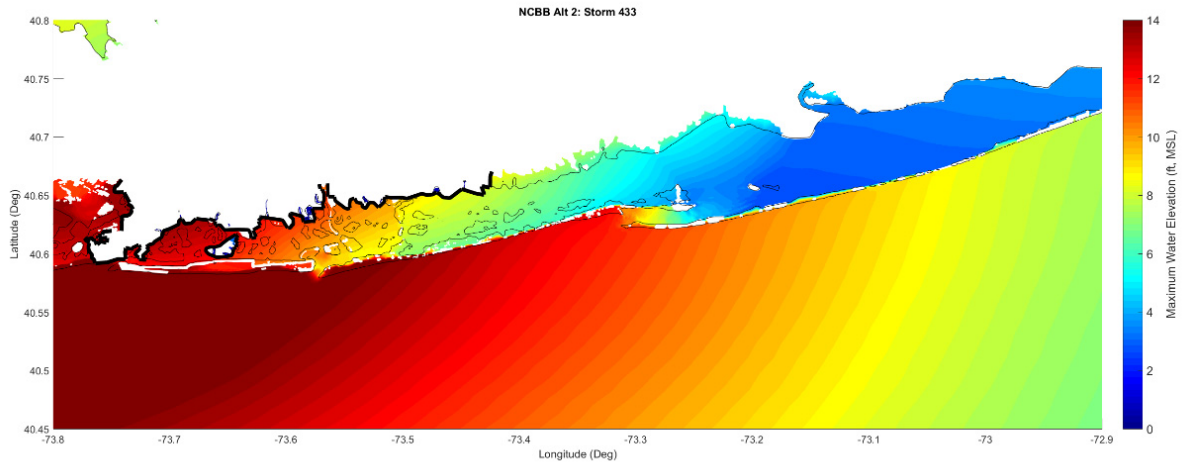
Figure 4-20. Difference in maximum water elevation (storm 433): Alternative 2 – Base.

Alternative 2 shows local reductions in water level landward of the floodwall and an increase in water level in the area of NCBB between East rockaway Inlet and Robert Moses Causeway. For storm 433, this increase is the greatest (~0.44 m) in the westernmost part of the area and diminishes towards the eastern part of the area with a minimum value (~0.05) at the Robert Moses Causeway.

5   SWL Hazard Curves

Five alternatives, shown again in Figure 5-1, plus the baseline configuration are evaluated in this section by presenting the SWL hazard curves (Figure 5-3) at nine locations throughout the study area (Figure 5-2). The nine locations selected capture effectiveness and impacts of the closure structures throughout the study area and outside the study area in Great South Bay.

Alternative 1A, with closures at the three inlets, has no significant reduction in the SWL hazard curves at Long Beach and Bay Park, the westernmost save points (Figure 5-3). Farther east at Lido Beach, Freeport, and Seaford there is a reduction of 0.5 m to 1 m in the SWL hazard curve relative to the baseline condition at the 100-year return period. Moving even farther east into Great South Bay (Lindenhurst to Patchogue), the reduction in the SWL hazard curve decreases to 0 m and 0.5 m at the 100-year return period. The trends in the SWL hazard curves are consistent with the description of the model results in Section 4, where the greatest reductions in water levels occurred in the middle of the study area. Even with the three inlets closed, winds push water in Great South Bay westward into the study area limiting the effectiveness of Alternative 1A, especially at the western end of the study area in the vicinity of Long Beach and Bay Park.

Alternative 1B, with closures at East Rockaway Inlet, Jones Inlet, and along the Wantagh State Parkway greatly reduces SWL hazard curves at all save points located "inside" the closure structures (Figure 5-3). Unfortunately, east of the Wantagh State Parkway, the SWL hazard curves increase by over 1 m at Seaford and nearly 1 m at Lindenhurst relative to the baseline conditions at the 100-year return period. Farther east in the Great South Bay (Great Cove, Ocean Beach, and Patchogue), increases in the SWL hazard curve are between 0 m and 0.5 m at the 100-year return period. Alternative 1B and the remaining alternatives with closure structures across the interior of the bay show that observations in Section 4 of local wind-driven storm surge "piling up" at these bay closures ultimately increases the SWL hazard curves east of the structures. It is of note that the increases in the SWL hazard curves are not limited to immediately east of the structure and extend well into Great South Bay.

Alternative 1C, with closures at East Rockaway Inlet and along the Meadowbrook State Parkway, greatly reduces SWL hazard curves at all save points located "inside" the closure structures (Figure 5-3). Like Alternative 1B, Alternative 1C greatly increases the SWL hazard curves east of the Meadowbrook State Parkway by more than 0.5 m at Seaford relative to the baseline conditions at the 100-year return period. Increases in the SWL hazard curve farther east are not as great as Alternative 1B, indicating that leaving Jones Inlet open reduces the potential "piling up" of local wind-driven storm surge at the interior bay closure. However, increases of 0 to 0.25 m in the SWL hazard curve remain throughout Great South Bay (Lindenhurst, Great Cove, Ocean Beach, and Patchogue) at the 100-year return period.

Alternative 1D, with closures at East Rockaway Inlet, Jones Inlet, and along the Robert Moses Causeway greatly reduces SWL hazard curves at all save points located "inside" the closure structures (Figure 5-3). However, the SWL hazard curve for Alternative 1D is up to 1 m higher than Alternatives 1B and 1C, which indicates the potential for local wind-driven storm surge inside the closures. East of the Robert Moses closure structure, SWL hazard curves in Great South Bay (Great Cove, Ocean Beach, and Patchogue) are between 0.5 m and 1 m greater than the baseline conditions.

Alternative 2, with floodwalls along the Nassau County bay shoreline show a slight increase in the SWL hazard curves throughout the study area, with increases of up to 0.25 m relative to the baseline condition at the 100-year return period.

Figure 5-1. Alternatives.
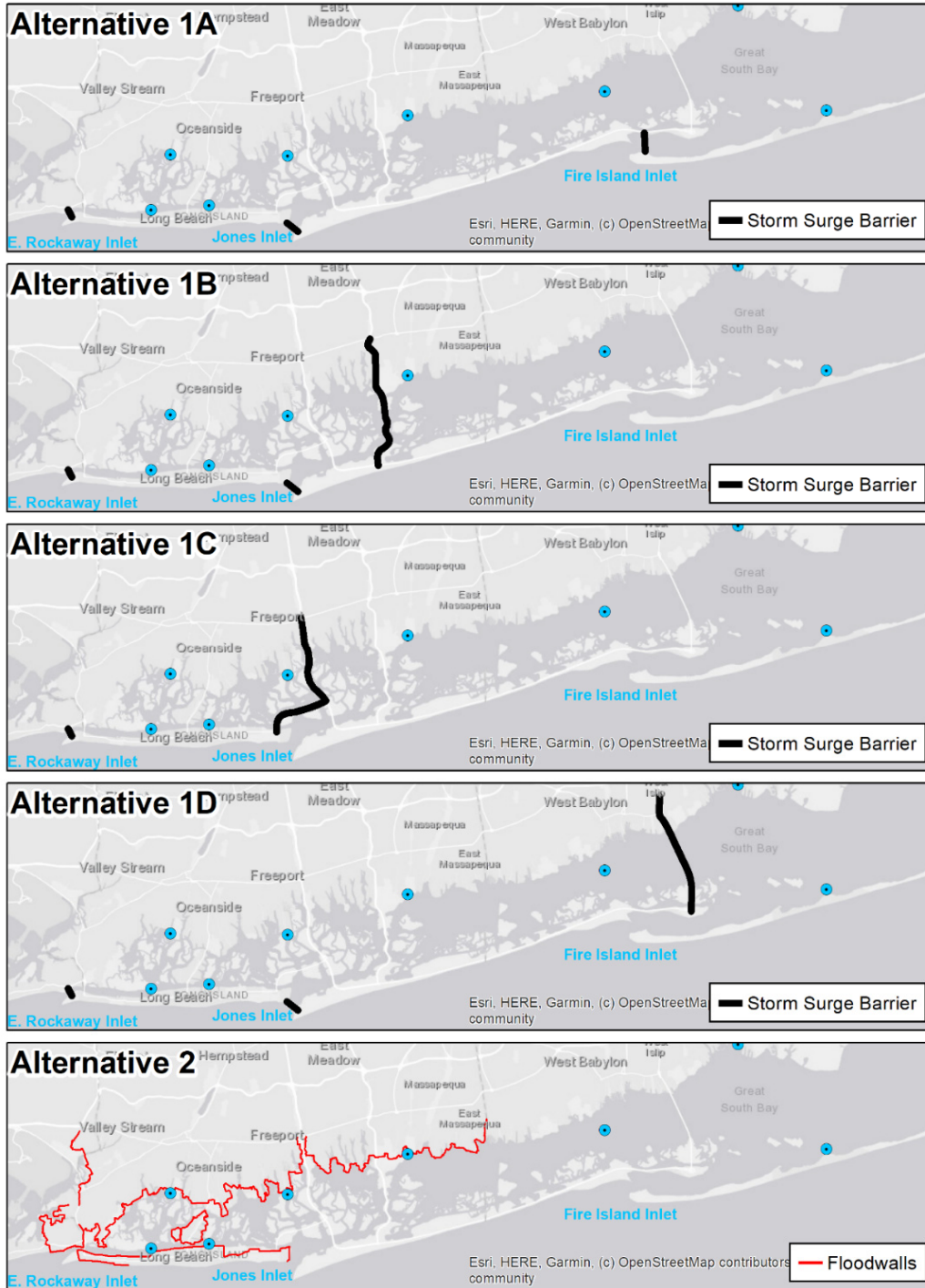
Figure 5-2. Save points.

Figure 5-3. SWL hazard curves produced from modeling results of each Alternative.
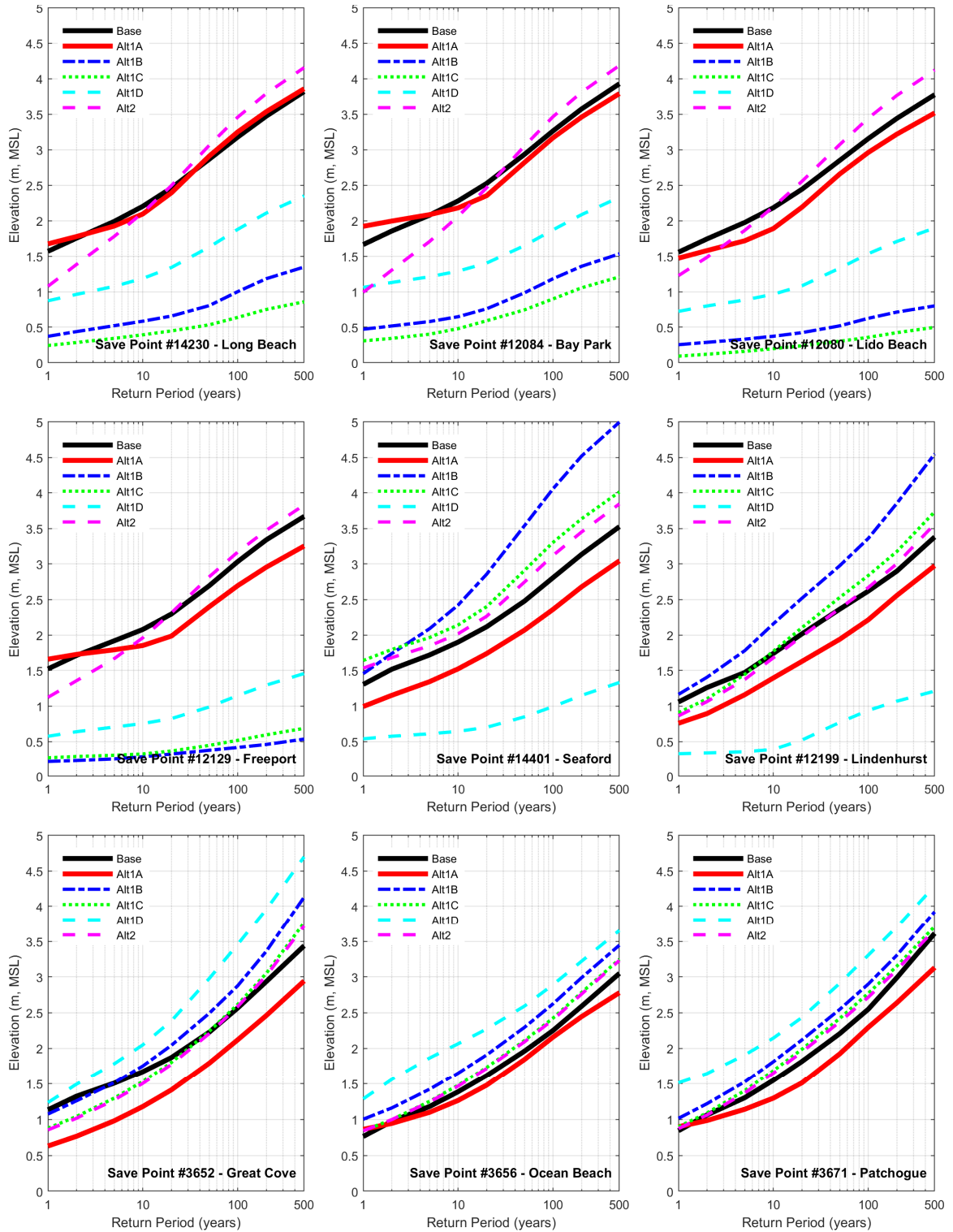
6 Conclusions

Analysis of the maximum surge envelopes for the simulated storm suite shows that each alternative provides a fairly consistent pattern of response to storms, with the magnitude of protection being a function of the storm intensity and track. The results show that two principal processes are responsible for flooding in the NCBB study area: (1) storm surge propagation through tidal inlets and (2) local wind-driven storm surge along the east-west bay axis. Effective closure alternatives must address both of these processes.

6.1 Alternative 1A

As storms are prevented from propagating surge into the bays with Alternative 1A (inlet closures) in place, the region experiences a reduction in the total volume of water in the bay. Unfortunately, local wind-driven storm surge along the east-west bay axis limits the effectiveness of Alternative 1A with almost no reduction in flooding in the western portion of the study area near Long Beach.

6.2 Alternatives 1B through 1D

In addition to inlet closures and raised barrier islands, Alternatives 1B through 1D all include a cross-bay closure at different locations in the bay. The result of these alternatives is a similar pattern of reduction within the enclosed area and increased water levels east of the cross-bay closure. Increased water levels are not limited to immediately east of the cross-bay closure location and extend well into Great South Bay. Within the enclosed area, seiching is observed, with the more pronounced oscillations for the fast-moving/intense storms. Alternative 1D protects the largest back bay areas and shows the most consistent response to storms, but it had the greatest increase in water levels in Great South Bay. Alternative 1C protects the smallest back bay area but leaving Jones Inlet open reduced the "piling up" of local wind-driven surge relative to the other alternatives.

6.3 Alternative 2

As Alternative 2 consists of a floodwall along the perimeter of the bays and along Long Beach storm surge still propagates into the bay through the inlets and along the long axis of Long Island Sound, but this alternative protects the area landward of the floodwall.

References

Cialone M. A., T. C. Massey, M. E. Anderson, A. S. Grzegorzewski, R. E. Jensen, A. Cialone, D. J. Mark, K. C. Peavey, B. L. Gunkel, T. O. McAlpin, N. C. Nadal-Caraballo, J. A. Melby, and J. J. Ratcliff. 2015. North Atlantic Coast Comprehensive Study (NACCS) coastal storm model simulations: Waves and water levels. ERDC/CHL TR-15-14. Vicksburg, MS: U.S. Army Engineer Research and Development Center.

Jia, G., and A. A. Taflanidis. 2013. Kriging metamodeling for approximation of high-dimensional wave and surge responses in real-time storm/hurricane risk assessment. Computer Methods in Applied Mechanics and Engineering 261-262:24-38.

Jia, G., A. A. Taflanidis, N. C. Nadal-Caraballo, J. A. Melby, A. B. Kennedy, and J. M. Smith. 2016. Surrogate modeling for peak or time-dependent storm surge prediction over an extended coastal region using an existing database of synthetic storms. Natural Hazards 81:909-938.

Kim, S. W., J. A. Melby, N. C. Nadal-Caraballo, and J. Ratcliff. 2015. A time- dependent surrogate model for storm surge prediction based on an artificial neural network using high-fidelity synthetic hurricane modeling. Natural Hazards 76:565-585.

Luettich, R. A., R. H. Birkhahn, and J. J. Westerink. 1991. Application of ADCIRC-2DDI to Masonboro Inlet, North Carolina: A brief numerical modeling study. Contractors Report. Vicksburg, MS: US Army Engineer Waterways Experiment Station.

Melby, J. A., T. C. Massey, A. L. Stehno, N. C. Nadal-Caraballo, S. Misra, V. M. Gonzalez. 2020. Sabine Pass to Galveston Bay, TX Pre-Construction, Engineering and Design (PED) Hurricane Coastal Storm Surge and Wave Hazard Assessment Report 1- Background and Approach. ERDC/CHL Technical Report. Vicksburg, MS: U.S. Army Engineer Research and Development Center.

Nadal-Caraballo, N. C., M. O. Campbell, V. Gonzalez, M. J. Torres, J. A. Melby, and A. A. Taflanidis. 2020. Coastal Hazards System: A

Probabilistic Coastal Hazard Analysis Framework. Proceedings from the International Coastal Symposium (ICS) 2020. Journal of Coastal Research 95:1211-1216.

Nadal-Caraballo, N. C., J. A. Melby, V. M. Gonzalez, and A. T. Cox. 2015. North Atlantic Coast Comprehensive Study – Coastal Storm Hazards from Virginia to Maine. ERDC/CHL TR-15-5. Vicksburg, MS: U.S. Army Engineer Research and Development Center.

Slusarczyk, G., M. A. Cialone, N.C. Nadal-Caraballo, and R. W. Hampson. 2021. Numerical Storm Surge Modeling and Probabilistic Analysis for Evaluating Proposed New Jersey Back Bays Inlet Closures. ERDC/CHL TR-21-XX. Vicksburg, MS: U.S. Army Engineer Research and Development Center.

Taflanidis, A. A., G. Jia, N. Nadal-Caraballo, A. Kennedy, J. Melby, and J. Smith. 2014. Development of Real-Time Tools for Hurricane Risk Assessment. In proceedings of 2nd International Conference on Vulnerability, Uncertainty, and Risk, July 13-16, Liverpool, UK.

Taflanidis, A.A., J. Zhang, N. C. Nadal-Caraballo, and J. A. Melby. 2017. Advances in surrogate modeling for hurricane risk assessment: storm selection and climate change impact. In proceedings of 12th International Conference on Structural Safety & Reliability, August 6-10, Vienna, Austria.

Zhang, J., A. A. Taflanidis, N. C. Nadal-Caraballo, J. A. Melby, and F. Diop. 2018. Advances in surrogate modeling for storm surge prediction: storm selection and addressing characteristics related to climate change. Natural Hazards 94:1225-1253.